The Dissertation Committee for Shawn Monique Castro Certifies that this is the approved version of the following dissertation

THE ROLE OF REACTIVE OXYGEN SPECIES AS MEDIATORS OF RESPIRATORY SYNCYTIAL VIRUS INDUCED PULMONARY INFLAMMATION

Committee:

Roberto P. Garofalo, M.D., Supervisor

Antonella Casola, M.D.

Kent Pinkerton, Ph.D.

Istvan Boldogh, Ph.D.

Xiaodong Cheng, Ph.D.

Mary Moslen-Treinen, Ph.D.

Dean, Graduate School

THE ROLE OF REACTIVE OXYGEN SPECIES AS MEDIATORS OF RESPIRATORY SYNCYTIAL VIRUS INDUCED PULMONARY INFLAMMATION

by

Shawn Monique Castro, B.S., M.S.

Dissertation

Presented to the Faculty of the Graduate School of

The University of Texas Medical Branch

in Partial Fulfillment

of the Requirements

for the Degree of

Doctor of Philosophy

The University of Texas Medical Branch

June, 2008

DEDICATION

To my dearest family, friends, sisters *Kaitlyn*, *Kristyn*, and *Karalyne Mary Elizabeth* and all the children of Galveston, Island may your hearts burn for the investigation of truth, and the pursuit of higher education.

"Regard man as a mine rich in gems of inestimable value. Education can alone cause them to reveal its treasures and enable mankind to benefit therefrom."

Baha'u'llah

ACKNOWLEDGEMENTS

Noteworthy endeavors are rarely completed in isolation, even if the weight of the task is confined within a few pages of a book. Consequently, the following dissertation could not have been accomplished without a few massive bouts of nudging and pulling and the generous outpourings of financial, intellectual, and emotional support from an infinite number of souls too numerous to name. With the utmost respect, I thank and bless my friends, family, grandparents, teachers, and mentors who have walked with me on my path towards a higher education. I have advanced throughout my graduate career with perseverance and by riding on waves of hope held by parental professors wiser than myself. In the wake of my predecessors, I too actively choose to serve as an agent of change in bringing forth an ever advancing society by pursuing a vocation in environmental stewardship.

My deepest gratitude to mentors who have left this earthly world of existence: Dr. Jose Miguel Cimadevilla, of St. Mary's University for his support and encouragement in pursuing a career in biomedical research, Dr. Michelle Trankina for her sharing her zest for life and passion for development biology, and Dr. Lynn Wiley University of California, Davis for being such a magnificent example of the divine art of living in science.

With earnest appreciation I thank Dr. Roberto Garofalo and Dr. Antonella Casola for providing me with the opportunity to complete my graduate studies and for all their support in facilitating the great movement from conducting experimental research to reaching publication status. A process that although painfully slow might not have ever gathered momentum without their assistance. Dr. Mary Moslen, my scientific fairy godmother, thank you for providing me with numerous opportunities of professional growth and for cultivating a can do attitude, when many times I though I couldn't. Many thanks to Dr. Istvan Boldogh and Dr. Xiaodong Cheng for the time and patience you've shown by renewing your commitment to serve as dissertation committee members. I would also like to thank Dr. Kent Pinkerton, quite possibly the world's most gracious inhalation/pulmonary toxicologist. Since my first rotation in your laboratory, investigating perturbations of the respiratory system has been a mainstay, thanks for providing such a grounding foundation! Lastly, I would like to thank the Pharmacology and Toxicology graduate program especially, Dr. Kenneth Johnson for allowing me to complete all graduate requirements for conferring the doctoral degree.

This dissertation work was funded by predoctoral fellowships from the NIEHS sponsored Environmental Toxicology Training Grant T32-07254 and the Ruth L. Kirschstein NSRA F31 GM072231-01.

THE ROLE OF REACTIVE OXYGEN SPECIES AS MEDIATORS OF RESPIRATORY SYNCYTIAL VIRUS INDUCED PULMONARY INFLAMMATION

Publication No._____

Shawn Monique Castro, Ph.D.

The University of Texas Medical Branch, 2008

Supervisor: Roberto P. Garofalo, M.D.

ABSTRACT

Respiratory Syncytial Virus (RSV) is the leading cause of epidemic respiratory tract illness in children worldwide. Although the mechanisms of RSV-induced airway disease are unknown, experimental evidence suggests that early local inflammatory processes serve as major initiating events in the pathogenesis of RSV-induced lung disease. RSV induced inflammation is mediated in part by small inflammatory chemokines. We investigated the mechanism of RSV-induced chemokine RANTES gene expression in epithelial cells and identified reactive oxygen species as critical signaling molecules involved in STAT and IRF transcription factor activation and the IKKε pathway, two activated pathways involved in the regulation of pro-inflammatory gene expression. We showed that RSV induced oxidative stress in vivo and that antioxidant therapy with butylated hydroxyanisole (BHA) attenuated RSV induced oxidative stress, pulmonary inflammation and airway hyper-responsiveness. The one caveat to anti-

inflammatory antioxidant therapy was the slight increase in RSV viral load observed following antioxidant administration. To eliminate the undesired outcome of increased viral load, a combination therapy approach was utilized employing BHA and the potent anti-viral IFN-α. Combination therapy yielded similar results of diminishing RSV-induced pulmonary inflammation while also decreasing RSV viral load in the lungs. Another key mediator regulated by oxidative stress and involved in inflammation is Poly (ADP)-Ribose Polymerase (PARP). We demonstrated that RSV is a potent inducer of PARP activity and that pharmacological inhibition of PARP with INO-1001 abolished RSV-induced PARP activity. INO-1001 also significantly reduced RSV-induced release of inflammation and lung pathology. Of environmental significance, cigarette smoke is also a potent oxidant mixture and important risk factor for the severity of RSV-induced disease. The mechanism(s) causing a worsening of RSV-induced lung disease by environmental tobacco exposure are unclear. Therefore, we investigated the effect of co-exposure of airway epithelial cells to cigarette smoke condensate (CSC) and RSV on inflammatory chemokine gene expression. We demonstrated that CSC and RSV synergistically increased MCP-1 and IL-8 chemokine expression through NF-κB and IRF transcription activation. Overall, the modulation of RSV-induced oxidative processes, either by dampening ROS production through pharmacological intervention or by heightening it by toxicant exposure, identify ROS as major signaling molecules involved in regulating RSV-induced inflammation.

TABLE OF CONTENTS

LIST OF FIGURES

CHAPTER 1: INTRODUCTION

Respiratory Syncytial Virus

Respiratory syncytial virus (RSV) is the single most important pathogen causing epidemic respiratory tract illness in children worldwide. RSV, an enveloped negative-sense single-stranded RNA virus, is sufficiently distinct in its protein products to be placed within a separate genus (*Pneumonvirus)* of the *Paramyxoviridae* family. In infants and children, RSV is the most common etiological agent of bronchiolitis and is also responsible for 50% of pneumonia cases in children up to two years of age (1). RSV is so ubiquitous that it will infect 100% of children by the age of 3. Each year, approximately 100,000 children are hospitalized with RSV disease with an estimated annual cost close to $300 million in the USA alone (2-3). Recent data from the US also indicate that hospitalization rates caused by RSV infections are increasing which suggests that unknown environmental co-factors could be contributing to the severity of RSV infection. For example, several epidemiologic reports have found that environmental tobacco smoke (ETS) exposure has been associated with more severe RSV infection (4-6). A vaccine for RSV has yet to be developed and immunity to natural infection is incomplete, thus repeated attacks of acute respiratory tract illness, ranging from common colds to pneumonia, affect every individual through adulthood. In addition to acute morbidity associated with RSV infection, there are long term consequences of RSV infection. For instance, RSV bronchiolitis has been linked to the development and

severity of asthma (7) and RSV infection triggers recurrent episodes of wheezing in asthmatic children (8).

Pathogenesis of RSV Lower Respiratory Tract Infection (LRTI)

As previously mentioned, RSV infection can develop into significant lower respiratory tract disease, mainly bronchiolitis, which is a clinical syndrome characterized by wheezing, dyspnea, and various degrees of respiratory distress. The pathology included mononuclear cell infiltration of the bronchiolar submucosa, edema, and necrosis of the bronchiolar epithelium, which result in the formation of mucus plugs and air trapping (9). However, analysis of autopsy samples from patients diagnosed with severe bronchiolitis revealed only small amounts of viral antigen present in patchy distribution throughout the lung (10). These findings as well as numerous other studies suggest that early inflammatory and immune events characteristic of the "innate" host response are crucially responsible for the damage of the airway mucosa observed in RSV bronchiolitis.

RSV Induced Pulmonary Inflammation

RSV infection in the lung is characterized by profound inflammation of the airway mucosa. The mechanisms involved in the pathogenesis of acute RSV-induced airway disease are largely unknown. However, experimental evidence generated in our laboratory (11-13) and others (14-15) support the hypothesis that a major component in the pathogenesis of RSV-induced disease is a shift from immune defense to immunopathology due to an exuberant inflammatory response, orchestrated primarily by RSV-infected epithelial cells.

Role of Epithelial Cells as Initiators of Inflammation

The airway epithelial cell is the major target of RSV infection. Under normal conditions, the respiratory epithelium represents the principal cellular barrier between the environment and the internal milieu of the airways and is also responsible for particulate clearance and surfactant secretion. However, after exposure to infection agents such as RSV or environmental exposures to cigarette smoke, chemical pollutants and particulate matter, airway epithelial cells secrete a variety of pro-inflammatory molecules including cytokines and chemokines small cytokines, which initiate and sustain immune and inflammatory responses in the airway mucosa (16-19). Chemokines regulate the migration and activation of leukocytes into the lung and therefore play a key role in the inflammatory and infectious processes of the lung (20). Several reports have identified epithelial cells as major sources of chemokines in the lung (21-22). We and others have demonstrated that RSV infection is a strong inducer of chemokine production both in vitro, in animal models and in children (13, 23-25). Recent clinical studies have detected elevated chemokine concentration in nasal washes of children infected with RSV (26-27) and found that the severity of disease is associated with the atypical presence and elevated levels of chemokines in the bronchoalveolar lavage of hospitalized children (25). In mouse model of RSV infection, our laboratory found that modulation of viral-induced chemokine production correlated with the level of pulmonary inflammation (28). Since the onset of inflammation is thought to be a key initiating component of RSV-induced lung disease, a major research objective in this dissertation was to define the mechanisms of RSV-induced chemokine gene expression in the airway epithelium.

ROS as Signaling Mediators of Chemokine Gene Expression

The mechanism by which RSV activated signaling pathways stimulate chemokine gene expression, have not been fully elucidated. We previously found that RSV infection of airway epithelial cells induces reactive oxygen species (ROS) production (29). ROS are ubiquitous, highly diffusible and reactive molecules produced as a result of the incomplete reduction of molecular oxygen. ROS damage lipids, proteins, DNA, and other cellular components. However, in the past few years, there has been an increased recognition of their role as intracellular signaling molecules. Inducible ROS generation has been shown following stimulation with a variety of molecules, including cytokines, growth factors, and infections with certain viruses such as HIV, Hepatitis B, and influenza (30) and intracellular redox changes in response various stimuli, have been shown to modulate gene expression (31). However prior to when I started this dissertation project little was known regarding the role of ROS in RSV-induced gene expression, and there were no published studies describing the role of ROS in RSV-induced lung inflammation. My project addressed the main hypothesis that:

The two roles for ROS in the pathogenesis of RSV-induced lung injury are the induction of inflammatory gene expression and the production of oxidative stress in the airway mucosa.

Experimental Objectives

In a previous study, our laboratory showed that treatment of airway epithelial cells with the antioxidant butylated hydroxyanisol (BHA) inhibited RSV-induced

RANTES chemokine production and activation of the interferon regulatory factor (IRF), transcription factors (29) which are key regulators of inflammatory and antiviral genes such as interferons (32). BHA treatment inhibited RSV induced IRF-1 and -7 gene expression and protein synthesis and the nuclear translocation of IRF-3, indicating that a redox –sensitive pathway was involved in RSV-induced IRF activation (29). The IRF-3 gene is constitutively expressed, while expression of the IRF-1 and IRF-7 genes is RSV inducible (29). Expression of both IRF-1 and IRF-7 is regulated by RSV-induced signal transducers and activators of transcription (STAT) transcription factors. STAT proteins are also detected in the airway epithelium in patients with asthma, a disease characterized by acute conditions of oxidative stress and inflammation. Chapter 2, describes our investigations about whether the mechanisms of RSV-induced IRF-1 and -7 activation were redox sensitive and further examines the involvement of ROS in RSV-induced STAT activation.

A broad range of antioxidants including BHA and NAD(P)H oxidase inhibitors exhibited same effects but chose to use BHA because it consistently blocked RSV induced effects. BHA is a phenolic antioxidant and this class of antioxidants serve to induce AOE, scavenge ROS, and block cellular signaling effects such as transcription factor activation (33-34). The prior finding that BHA antioxidant treatment blocked RSV-induced IRF-3 nuclear translocation (29) indicated that the signaling pathway leading to IRF-3 activation was also redox sensitive. Chapter 3 describes experiments which tested the hypothesis that the upstream signaling pathway leading to IRF-3 activation was mediated by RSV-induced intracellular ROS. IRF-3 phosphorylation is an initial activating step following viral infection. Therefore, we investigated the potential

involvement of kinase IKKε in phosphorylating IRF-3 following RSV infection and examined the role of ROS in mediating IKKε activity.

Although, our laboratory had previously shown that RSV-induced ROS production in airway epithelial cells and that treatment with antioxidants and NAD(P)H oxidase inhibitors ultimately attenuated RSV-induced chemokine secretion, no reports were found indicting that RSV infection produced ROS or led to the condition of oxidative stress in the airway mucosa of the lung. Therefore, experiments in Chapter 4 used the Balb/c mouse model of RSV infection to test the hypothesis that RSV infection induces oxidative stress in the lung and that ROS are involved the pathogenesis of RSV-induced pulmonary inflammation. We evaluated the therapeutic potential of the antioxidant BHA in alleviating the clinical symptoms of disease and airway hyperreactivity along with a panel of RSV-induced inflammatory modulators such as cytokines and chemokines.

Antioxidants scavenge ROS. Therefore, the experimental use of antioxidants in Chapters 2-4 further substantiated the role of ROS in mediating RSV-induced chemokine expression and inflammation both in airway epithelial cells and in the lung. Since antioxidants also indirectly function as anti-inflammatory agents, one important concern involving the use of anti-inflammatory compounds in treating infectious agents such as RSV involves the potential for inhibiting innate immune responses. Preventing such protective immune responses could delay viral clearance and lead to viral persistence in the lung; both of these negative consequences could support re-infection or prolong clinical symptoms of respiratory distress. Therefore, experiments in Chapter 5 explored

the efficacy of combination therapy with the antioxidant/anti-inflammatory agent BHA and the antiviral IFN-α. We selected IFN-α since our laboratory had identified IFN-α as a powerful antiviral agent that significantly lowered RSV viral replication even when given 3 days RSV-postinfection (35). However, post-infection treatment with IFN-α did not significantly affect the acute clinical symptoms of disease (personal communication). Since it is plausible for a harboring residual virus to negatively modulate the host response upon subsequent re-infection, we investigated the therapeutic potential of combination therapy on decreasing RSV viral replication and the severity of disease.

Experiments from Chapters 4 evaluated the role of ROS in producing RSV-induced oxidative stress in airway epithelial cells as well as the bronchoalveolar airspace of the lung. The condition of oxidative stress has been investigated in various inflammatory lung diseases, primarily because inflammation involves the migration and activation of leukocytes which in addition to airway epithelial cells are powerful producers of ROS themselves. Based on experimental evidence in Chapter 4 that antioxidant therapy reduced RSV-induced pulmonary inflammation we attempted to identify unifying modulators of oxidative stress and inflammation by investigating the role of nuclear enzyme Poly (ADP) Ribose-Polymerase (PARP). Oxidative stress is an obligatory event required for the activation of PARP (36). Recent investigations using various model systems of acute lung diseases suggest that PARP inhibition protects against oxidative stress and inflammation (37-38). However, no reports document a role of PARP in viral-induced inflammation. Therefore, experiments for Chapter 6 used the

mouse model of RSV infection to investigate whether pharmacological inhibition of PARP attenuated RSV-induced pulmonary inflammation.

Environmental tobacco smoke (ETS) which consists mainly of passive second hand tobacco smoke has been identified as a risk factor associated with the severity of RSV disease (39), indicating that factors other than those of the innate immune response may be involved in the pathogenesis of RSV disease. Exposure to ETS is associated with an increased frequency of lower respiratory tract illness during infancy, particularly RSV bronchiolitis (40). However, the pathogenic mechanism(s) underlying the epidemiologic association between exposure to ETS and severity of RSV infections is currently unknown.

To examine the association between cigarette smoke exposure and RSV infection, experiments in Chapter 7, were designed to test the hypothesis that exposure to cigarette smoke exacerbates airway disease by enhancing RSV-induced chemokine secretion in airway epithelial cells. For ease of experimental design, cigarette smoke condensate (CSC) as a surrogate of cigarette smoke exposure. The CSC used in this study contained the particulate component of mainstream cigarette smoke however, side stream smoke also contains a particulate phase (41). Therefore the CSC modeled stimulation from components of the tar phase irrespective of the exposure route. Both CSC and RSV have been shown to induce chemokine interleukin-8 (IL-8) gene expression (16,42). Therefore, we investigated whether co-exposure to these two inflammatory stimuli produced a synergistic induction of chemokine release and the potential mechanism by which cigarette smoke could enhance the severity of RSV-induced disease.

RSV is pervasive and infection of the respiratory track is a global concern. There is no effective vaccine available against RSV and immunotherapy prevention is costly and with a highly limited therapeutic window at best. Mounting experimental evidence indicates that pulmonary inflammation is a key process involved in the pathogenesis of RSV induced lung disease and that RSV-induced cytokines and chemokines are important mediators of the inflammatory process. Therefore, identification of the molecular mechanisms leading to RSV-induced inflammatory gene expression and lung injury is fundamental for developing therapeutic strategies to reduce the morbidity and mortality associated with RSV infection.

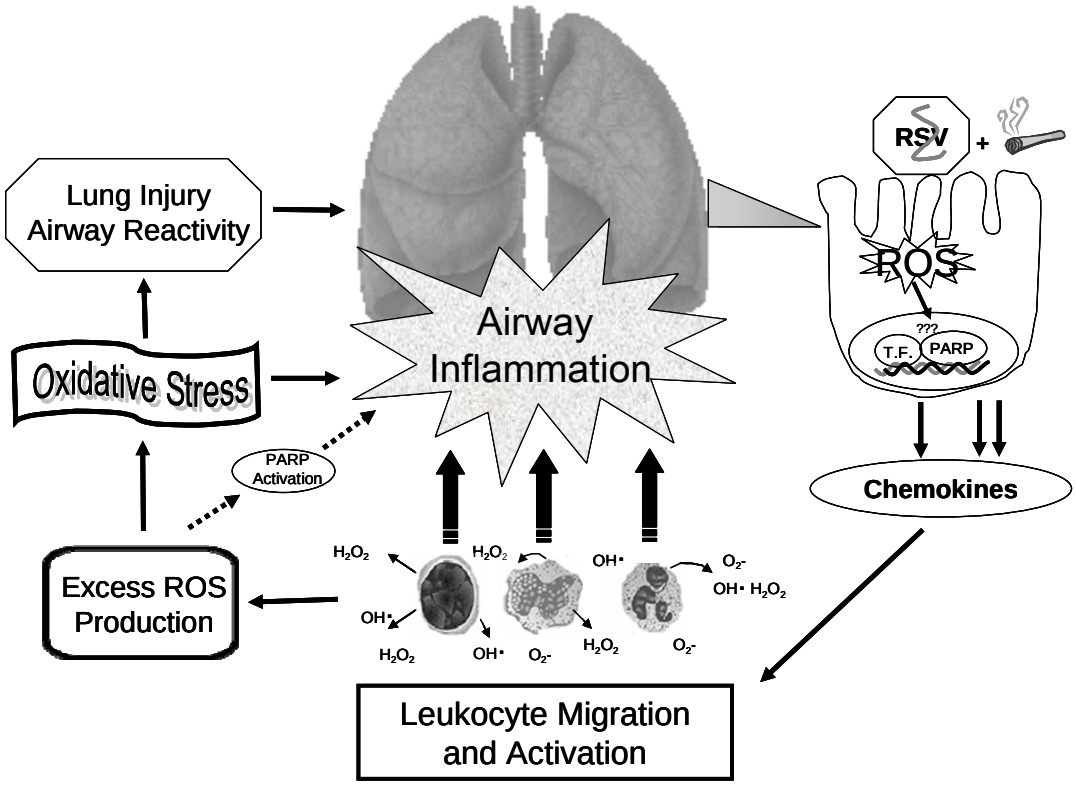

FIGURE 1.1 OVERALL DIGRAM OF RSV-INDUCED AIRWAY INFLAMMATION ADDRESSED IN DISSERTATION. The respiratory epithelial cell is the primary target of RSV infection. RSV-induced ROS production signals transcription factor (T.F.) activation and enhanceosome proteins such as PARP leading to chemokine gene expression and protein release. Stimulation of alveolar epithelial cells with CSC synergistically increases RSV- induced transcription factor activation and chemokine expression. The secretion of inflammatory chemokines signal rapid leukocyte migration to the airspace of the lung. Activated leukocytes produce excess ROS and activate PARP. Attenuation of RSV–induced oxidative stress and PARP activation block RSV-induced airway inflammation and the associated long term consequences of airway reactivity.

CHAPTER 2: REACTIVE OXYGEN SPECIES MEDIATE VIRUS-INDUCED STAT ACTIVATION ROLE OF TYROSINE PHOSPHATASES*

ABSTRACT

Respiratory syncytial virus (RSV) is the leading cause of epidemic respiratory tract illness in children in the United States and worldwide. RSV infection of airway epithelial cells induces formation of reactive oxygen species (ROS), whose production mediates the expression of cytokines and chemokines involved the immune/inflammatory responses of the lung. In this study, we have investigated the role of ROS in RSV-induced signal transducers and activators of transcription (STAT) activation and interferon regulatory factor (IRF) gene expression in human airway epithelial cells. Our results indicate that RSV replication induces IRF-1 and -7 gene transcription, a response abrogated by antioxidants. RSV infection induces binding of STAT to the IRF-1 γ-interferon-activated sequence (GAS) and IRF-7 interferon-stimulated responsive element (ISRE). STAT1 and STAT3 bind IRF-1 GAS, whereas STAT1, STAT2, IRF-1, and IRF-9 bind IRF-7 ISRE. Antioxidant treatment blocks RSV-induced STAT binding to both the IRF-1 GAS and IRF-7 ISRE by inhibition of inducible STAT1 and STAT3 tyrosine phosphorylation, suggesting that RSV-induced ROS formation is required for STAT activation and IRF gene expression. Although protein tyrosine phosphorylation is necessary for RSV-induced STAT activation, Janus kinase and Src kinase activation do not mediate this effect. Instead, RSV infection inhibits intracellular tyrosine phosphatase activity, which is restored by antioxidant treatment. Pharmacological inhibition of

*"Reprinted from Journal of Biological Chemistry, Vol. 279 No. 4 Pages 2461-2469, Liu T., Castro S., Brasier A. R., Jamaluddin M., Garofalo R. P., and Casola A., Reactive Oxygen Species Mediate Virus-Induced STAT Activation: Role of Tyrosine Phosphotases, Copyright (2004), with permission from the American Society for Biochemistry and Molecular Biology"

tyrosine phosphatases induces STAT activation. Together, these results suggest that modulation of phosphatases could be an important mechanism of virus-induced STAT activation. Treatment of alveolar epithelial cells with the NAD(P)H oxidase inhibitor diphenylene iodonium abolishes RSV-induced STAT activation, indicating that NAD(P)H oxidase-produced ROS are required for downstream activation of the transcription factors IRF and STAT in virus-infected airway epithelial cells.

INTRODUCTION

Respiratory syncytial virus (RSV) is an enveloped, negative-sense single-stranded RNA virus (43). Since its isolation, RSV has been identified as a leading cause of epidemic respiratory tract illness in children in the United States and worldwide. In fact, RSV is so ubiquitous that it will infect 100% of children before the age of 3. It is estimated that 40–50% of children hospitalized with bronchiolitis and 25% of children with pneumonia are infected with RSV, resulting in 100,000 hospital admissions annually in the United States alone (43). Although the mechanisms of RSV-induced airway disease and the associated long term consequences are largely unknown, the local inflammatory response is thought to play a fundamental role. Airway epithelial cells are the target of RSV infection, and they respond to the infection producing a variety of mediators involved in lung immune/inflammatory responses, such as cytokines, chemokines, interferons, and up-regulating adhesion molecules and major histocompatibility complex antigens on the cell surface (44). Regulation of cellular responses to extracellular stimuli is a central aspect of host defense, and it is coordinated by intracellular networks in which different subsets of transcription factors are involved in the expression of diverse set of target genes, depending on the nature of the extracellular stimulus. RSV induces gene expression through the coordinate induction of multiple transcription factors that assemble in nucleoprotein complexes, defined

"enhanceosomes," as we demonstrated for the chemokines interleukin-8 and RANTES (regulated upon activation, normal T-cells expressed and secreted) (45).

The cellular signaling events leading to RSV-induced transcription factor activation are mostly unknown. Reactive oxygen species (ROS) are ubiquitous, highly diffusible and reactive molecules, produced as a result of reduction of molecular oxygen, including species such as hydrogen peroxide, superoxide anion, and hydroxyl radical, and they have been implicated in damaging cellular components such as lipids, proteins, and DNA. In the past few years, there has been increased recognition of their role as redox regulators of cellular signaling (31,46). We have shown recently that RSV infection of airway epithelial cells rapidly induces ROS production (29). Pretreatment of airway epithelial cells with the antioxidant butylated hydroxyanisole (BHA), as well a panel of chemically unrelated antioxidants, blocked RSV-induced chemokine gene expression and protein secretion, through inhibition of interferon regulatory factor (IRF) activation. Antioxidant treatment inhibited de novo IRF-1 and -7 gene expression, protein synthesis, and IRF-3 nuclear translocation, indicating that a redox-sensitive pathway was involved in RSV-induced IRF activation (29).

The IRF proteins belong to a family of transcription factors involved in the regulation of important immune/inflammatory genes, including RANTES and interleukin-15, as well as of genes necessary to mount an effective antiviral response, such as interferons (32). IRF-3 is constitutively expressed, but IRF-1 and -7 are virus-inducible (32). Here we investigated the unknown mechanism of antioxidant inhibition of virus-induced IRF-1 and -7 activation. Our results indicate that RSV infection of alveolar epithelial cells induces IRF-1 and -7 gene transcription, an effect abrogated by BHA treatment. RSV infection induces members of the signal transducers and activators of transcription (STAT) family to bind the IRF-1 γ-interferon-activated sequence (GAS)

and the IRF-7 interferon-stimulated responsive element (ISRE) of transcription factors belonging to the STAT1 and STAT3 bind IRF-1 GAS, whereas STAT1, STAT2, IRF-1, and IRF-9 bind IRF-7 ISRE. Antioxidant treatment blocks RSV-induced binding to both IRF-1 GAS and IRF-7 ISRE and inhibits RSV-induced STAT1 and -3 phosphorylation and nuclear translocation. These data suggest that RSV-induced ROS formation is involved in STAT activation and IRF gene expression, following RSV infection. Although protein tyrosine phosphorylation is necessary for RSV-induced STAT activation and induction of IRF promoter, Janus kinase (JAK) and Src kinase activation do not mediate this effect. Interestingly, RSV infection induces a significant decrease in intracellular tyrosine phosphatase activity, which is restored by antioxidant treatment, and pharmacological inhibition of tyrosine phosphatases in airway epithelial cells induces STAT activation. Together, these results suggest that modulation of phosphatases could be an important mechanism of virus-induced STAT activation. Finally, treatment of alveolar epithelial cells with the NADPH oxidase inhibitor diphenylene iodonium (DPI) abolishes STAT activation, indicating that NAD(P)H oxidase system is an important enzyme for the generation of ROS and the subsequent activation of STAT, following RSV infection. This study provides novel insights into the role of ROS in virus-induced IRF and STAT protein activation.

MATERIALS AND METHODS

Reagents

Antibodies anti-STAT1 (sc-592X), anti-STAT2 (sc-476X), anti-STAT3 (sc-482X), anti-STAT5 (sc-1656X), anti-tyrosine-phosphorylated STAT1 (sc-8394), anti-tyrosine-phosphorylated STAT3 (sc-8059), anti-IRF-1 (sc-497X), and anti-IRF-9 (sc-496X) were purchased from Santa Cruz Biotechnology. The chemical inhibitors AG490, AG82, protein phosphatase (PP)1, PP2, and DPI were purchased from Calbiochem.

RSV Preparation

The A2 strain of RSV was grown in Hep-2 cells and purified by centrifugation on discontinuous sucrose gradients as described elsewhere (47). The virus titer was determined by a methyl-cellulose plaque assay. No contaminating cytokines were found in these sucrose-purified viral preparations (48). Viral pools were routinely tested for mycoplasma contamination by PCR analysis and were used if they had <0.125 EU/ml endotoxin (by Limulus assay). Virus pools were aliquoted, quick frozen on dry ice/alcohol, and stored at –70 °C until used.

Cell Culture and Infection of Epithelial Cells with RSV

A549, human alveolar type II-like epithelial cells (ATCC), were maintained in F12K medium containing 10% (v/v) fetal bovine serum, 10 mM glutamine, 100 IU/ml penicillin, and 100 μg/ml streptomycin. Cell monolayers were infected with RSV at a multiplicity of infection of 1 (unless otherwise stated), as described previously (23). An equivalent amount of a 20% sucrose solution was added to uninfected A549 cells, as a control. When BHA or other inhibitors were used, cells were pretreated with the compound for 1 h and then infected in the presence of that compound. Because BHA was diluted in ethanol and the other inhibitors in dimethyl sulfoxide, equal amounts of either ethanol or dimethyl sulfoxide were added to untreated cells, as a control. The total number of cells and cell viability, following treatment, was measured by trypan blue exclusion.

Northern Blot

Total RNA was extracted from control and infected A549 cells by the acid guanidinium thiocyanate-phenol chloroform method. 20 μg of RNA was fractionated on a 1.2% agarose-formaldehyde gel, transferred to nylon membranes, and hybridized to a radio-labeled IRF-1, IRF-7, and RSV N protein cDNAs as described previously (29,49).

The hybridization temperature for all probes was 60 °C. After washing, membranes were exposed for autoradiography with Kodak XAR film at –70 °C, using intensifying screens. After exposure, membranes were stripped and rehybridized with a β-actin probe.

Cell Transfection

To investigate IRF-1 and -7 gene transcription, we transiently transfected A549 cells with the IRF-1 or -7 promoter, linked to the luciferase reporter gene (generous gifts from Dr. A. B. Deisserot, Yale University, New Haven, and Dr. P. M. Pitha, Johns Hopkins, Baltimore, respectively) (50-51). Logarithmically growing A549 cells were transfected in triplicate in 60-mm Petri dishes by DEAE-dextran, as described previously (11). Cells were incubated in 2 ml of HEPES-buffered Dulbecco's modified Eagle's medium (10 mM HEPES, pH 7.4) containing 20 μl of 60 mg/ml DEAE-dextran (Amersham Biosciences) premixed with 6 μg of either IRF-1 or -7 plasmids and 1 μg of cytomegalovirus β-galactosidase internal control plasmid. After 3 h, the medium was removed, and 0.5 ml of 10% (v/v) dimethyl sulfoxide in phosphate-buffered saline was added to the cells for 2 min. Cells were washed with phosphate-buffered saline and cultured overnight in 10% fetal bovine serum and Dulbecco's modified Eagle's medium. The next morning, cells were infected with RSV, and cells were lysed at different times postinfection to measure independently luciferase and β-galactosidase reporter activity, as described previously (11). Luciferase was normalized to the internal control β-galactosidase activity. All experiments were performed in duplicate or triplicate.

Electrophoretic Mobility Shift Assay (EMSA)

Nuclear extracts of uninfected and infected A549 cells were prepared using hypotonic/nonionic detergent lysis, as described previously (11). Proteins were normalized by protein assay (Protein Reagent, Bio-Rad) and used to bind to a duplex

oligonucleotide corresponding to the IRF-1 GAS and IRF-7 ISRE, whose sequences are as follows:

IRF-1 GAS, 5'-GATCCAGCCTGATTT CCCCGAAATGACGGC-3'

3'-CGGACTAAAGGGGCTTTACT GCCGCTCTAG-5'

IRF-7 ISRE, 5'-TTTAGGTTT CGCTTT CCCGGG-3'

3'-TCCAAAGCGAAAGGGCCCTCG-5'

DNA binding reactions contained 10–15 μg of nuclear proteins, 5% glycerol, 12 mM HEPES, 80 mM NaCl, 5 mM dithiothreitol, 5 mM Mg_2Cl, 0.5 mM EDTA, 1 μg of poly(dI-dC), and 40,000 cpm of ^{32}P-labeled double-stranded oligonucleotide in a total volume of 20 μl. The nuclear proteins were incubated with the probe for 15 min at room temperature and then fractionated by 4% nondenaturing PAGE in 0.5x TBE buffer (22 mM Tris-HCl, 22 mM boric acid, 0.25 mM EDTA, pH 8) at 120 volts. After electrophoretic separation, gels were dried and exposed for autoradiography with Kodak XAR film at –70 °C using intensifying screens. In the gel mobility supershift, commercial antibodies against specific transcription factors were added to the binding reactions and incubated on ice for 1 h prior to fractionation on 4% PAGE.

Western Immunoblot

Nuclear proteins were prepared as described previously, fractionated by SDS-PAGE, and transferred to polyvinylidene difluoride membrane (11). Membranes were blocked with 5% albumin in TBS-Tween and incubated overnight with antibody recognizing the tyrosine-phosphorylated form of STAT1 and STAT3. Membranes were stripped and reprobed with antibodies to STAT1 and STAT3. For secondary detection,

we used a horseradish-coupled anti-rabbit or anti-mouse antibody, in the enhanced chemiluminescence assay (Amersham Biosciences).

Intracellular Tyrosine Phosphatase Assay

Total intracellular tyrosine phosphatase activity was performed using the tyrosine assay kit from Promega, according to manufacturer's protocol. This is a colorimetric assay that determines the amount of free phosphate generated in a reaction, which includes the source of phosphatase plus a tyrosine phosphopeptide, by measuring the absorbance of a molybdate-malachite green-phosphate complex. Briefly, total cell lysates from A549 cells, control and infected with RSV, in the absence or presence of 400 M BHA, were prepared using radioimmune precipitation assay buffer, as described previously (29). Excess free phosphate was removed from cell lysates using the provided spin columns and 3 μg of samples were mixed with 100 μM tyrosine phosphopeptide substrate and incubated at 30°C for 20–60 minutes. Reactions were stopped adding a molybdate dye solution, color was allowed to develop for 15–20 minutes, and absorbance was read at 600 nm with a plate reader. Phosphatase activity was expressed as generation of pmol of free phosphate/min/μg of protein.

RESULTS

BHA Inhibits RSV-induced IRF Transcription

We have recently shown that RSV infection of A549 cells, type II-like alveolar epithelial cells, induced IRF-1 and -7 gene expression, and antioxidant treatment greatly diminished RSV-induced steady-state IRF mRNA levels (29). Treatment of A549 cells with 400 μM BHA almost completely abolished the expression of IRF-1 and IRF-7 genes following RSV infection, without significantly affecting viral replication, as determined by levels of RSV N protein expression (Figure 2.1).

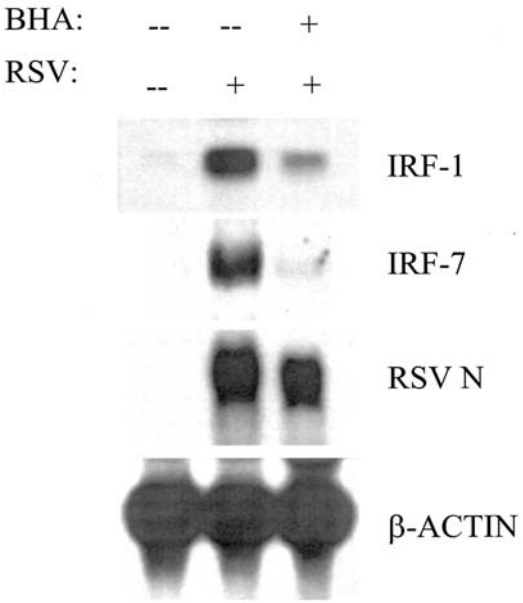

FIGURE 2.1 NORTHERN BLOT OF IRF mRNA IN RSV-INFECTED EPITHELIAL CELLS. A549 cells were infected with RSV for 15 h in the absence or presence of 400 μM BHA. 20 μg of RNA extracted from control and infected cells were fractionated on a 1.2% agarose-formaldehyde gel, transferred to nylon membrane, and hybridized to radiolabeled IRF-1, IRF-7, and RSV N protein cDNA probes. Membranes were stripped and hybridized with a radiolabeled β-actin probe to show equal loading of the samples.

Antioxidant treatment slightly reduced cell viability (a decrease of ~10% in BHA-treated cells versus untreated, data not shown) without reducing the amount of virus released by infected cells, as shown previously (29). Previous studies, investigating interferon-β and -γ stimulation of IRF-1 and -7 gene induction, have demonstrated that IRF gene expression is controlled at the transcription level (51-54). To determine whether IRF-1 gene transcription was increased after RSV infection, A549 cells were transiently transfected with a construct containing 1.3 kb of the human IRF-1 promoter linked to the luciferase reporter gene (50). The day after, cells were infected with RSV for various lengths of time and harvested to measure luciferase activity. As shown in Figure 2.2A, RSV infection induced a time-dependent increase in IRF-1 promoter activation, which started between 3 and 6 h postinfection, peaked at 12 h, and started to decrease at 24 h. To determine whether the antioxidant effect of BHA influenced IRF gene transcription, A549 cells were transfected with the IRF-1 promoter, infected with RSV in the absence or presence of 400 μM BHA, and harvested 12 h later to measure luciferase activity. We have shown previously that a 400 μM concentration of

BHA is able to block ~90% of RSV-induced ROS production without interfering with cell viability (29). As shown in Figure 2.2B, treatment with BHA completely abolished RSV-induced luciferase activity, suggesting that the antioxidant inhibits IRF-1 gene expression, at least partially, by interfering with gene transcription.

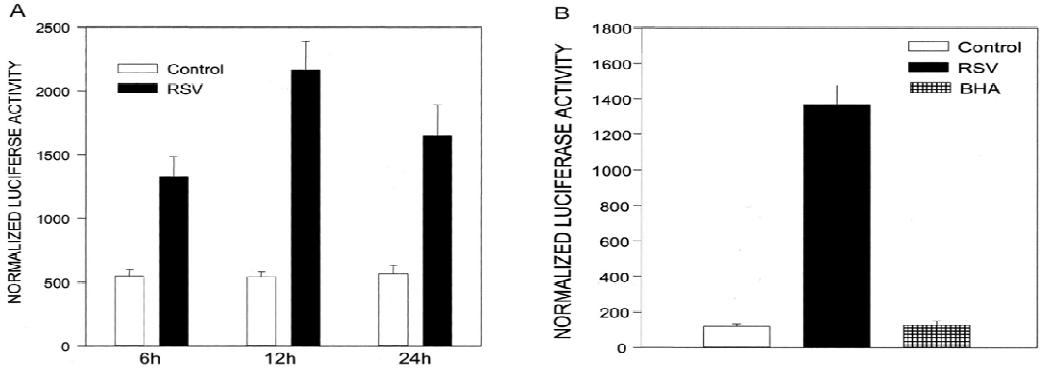

FIGURE 2.2 IRF-1 PROMOTER ACTIVATION AFTER RSV INFECTION A) time course. A549 cells were transiently transfected with the IRF-1 promoter plasmid and infected with RSV, multiplicity of infection of 1. At different times postinfection, cells were harvested to measure luciferase activity. Uninfected plates served as controls. B) effect of BHA. A549 cells were transfected with the IRF-1 promoter plasmid, infected with RSV for 12 h, in the absence or presence of 400 μM BHA, and harvested to measure luciferase activity. For each plate luciferase was normalized to the β-galactosidase reporter activity. Data are expressed as the mean ± S.D. of normalized luciferase activity.

To investigate IRF-7 gene transcription following RSV infection, we performed similar studies using A549 cells transiently transfected with a construct containing 1.7 kb of the human IRF-7 promoter linked to the luciferase reporter gene (52). As with IRF-1, RSV infection induced a time-dependent increase in luciferase activity, which started around 3 h postinfection, peaked at 6 h, and then declined after 12 h Figure 2.3A. Similarly, BHA treatment completely abolished RSV-induced luciferase activity, indicating that antioxidant treatment also inhibits IRF-7 gene transcription Figure 2.3B. It is important to notice that, although BHA treatment inhibited RSV-induced IRF-1 and -7

promoter activation, it did not affect the basal level of transcription of both genes, indicating that BHA affects only the inducible component of gene transcription. We have also shown previously that BHA does not affect expression of constitutively transcribed cellular genes, such as β-actin (29).

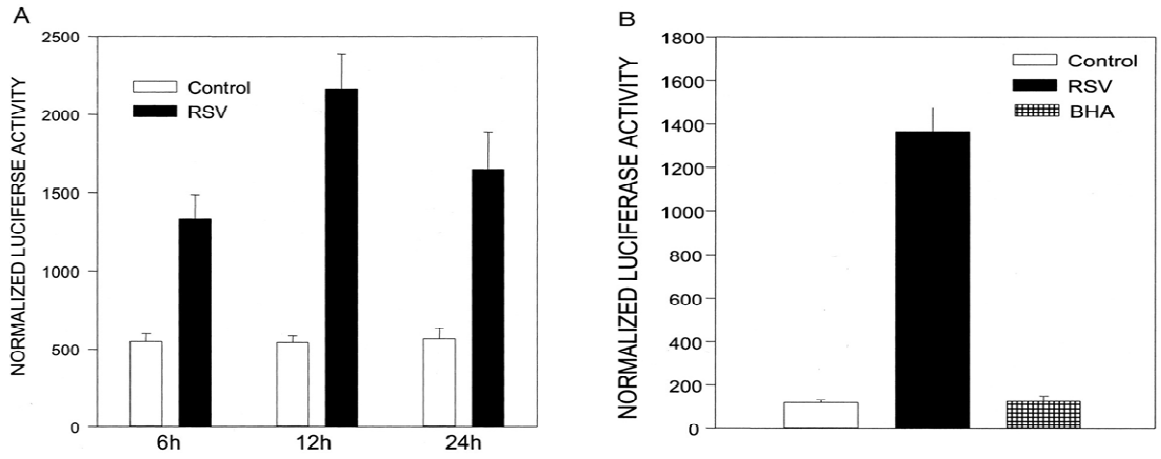

FIGURE 2.3 IRF-7 PROMOTER ACTIVATION AFTER RSV INFECTION A) Time course. A549 cells were transiently transfected with the IRF-7 promoter plasmid and infected with RSV, multiplicity of infection of 1. At different times postinfection, cells were harvested to measure luciferase activity. Uninfected plates served as controls. B) Effect of BHA. A549 cells were transfected with the IRF-7 promoter plasmid, infected with RSV for 6 h, in the absence or presence of 400 μM BHA, and harvested to measure luciferase activity. For each plate luciferase was normalized to the β-galactosidase reporter activity. Data are expressed as the mean ± S.D. of normalized luciferase activity.

RSV-Induced STAT Activation Is Redox-Sensitive

Several studies have investigated the promoter elements involved in the regulation of IRF-1 gene expression and have identified the GAS as a major site necessary for inducible transcription (52). To determine whether RSV infection produced changes in the abundance of DNA-binding proteins recognizing the IRF-1 GAS, EMSAs were performed with nuclear extracts prepared from A549 cells, control and infected with RSV

for various lengths of time. As shown in Figure 2.4A, a single nucleoprotein complex (C3) was formed from nuclear extracts of control cells on the IRF-1 GAS probe. RSV infection induced the appearance of two other complexes, C1 and C2 (better resolved on longer electrophoresis as in Figure 2.4C, starting between 1 and 3 h postinfection, peaking around 3–6 h, and declining after 12 h of infection. The sequence specificity of the different complexes was examined by competition with unlabeled oligonucleotides in EMSA Fig. 4B. C1 and C2 were competed by the wild type but not by the mutated oligonucleotide, indicating GAS-specific binding. IRF-1 GAS has been shown to bind transcription factors of the STAT family (55). To determine the composition of the RSV-inducible complexes, we performed supershift assays using a panel of antibodies reacting with the different members of STAT family of transcription factors. The anti-STAT1 antibody induced the disappearance of C2 and the appearance of a supershifted band, whereas the anti-STAT3 antibody caused a reduction of C1 and the appearance of a supershifted band (supershifted complexes are indicated by the arrows), as shown in Figure 2.4C. Antibodies recognizing STAT2, STAT5, and IRF-9 did not induce changes in binding or mobility shifts. These data indicate that STAT1 and -3 are the major components of the RSV-inducible IRF-1 GAS complexes.

To determine whether BHA-induced inhibition of IRF-1 gene transcription was the result of changes in STAT binding to the IRF-1 GAS, we performed EMSAs using nuclear extracts prepared from A549 cells, control or infected with RSV for 3 h, in the absence or presence of BHA. As shown in Figure 2.5, RSV infection induced a significant increase in STAT binding, which was completely abolished by treatment with BHA.

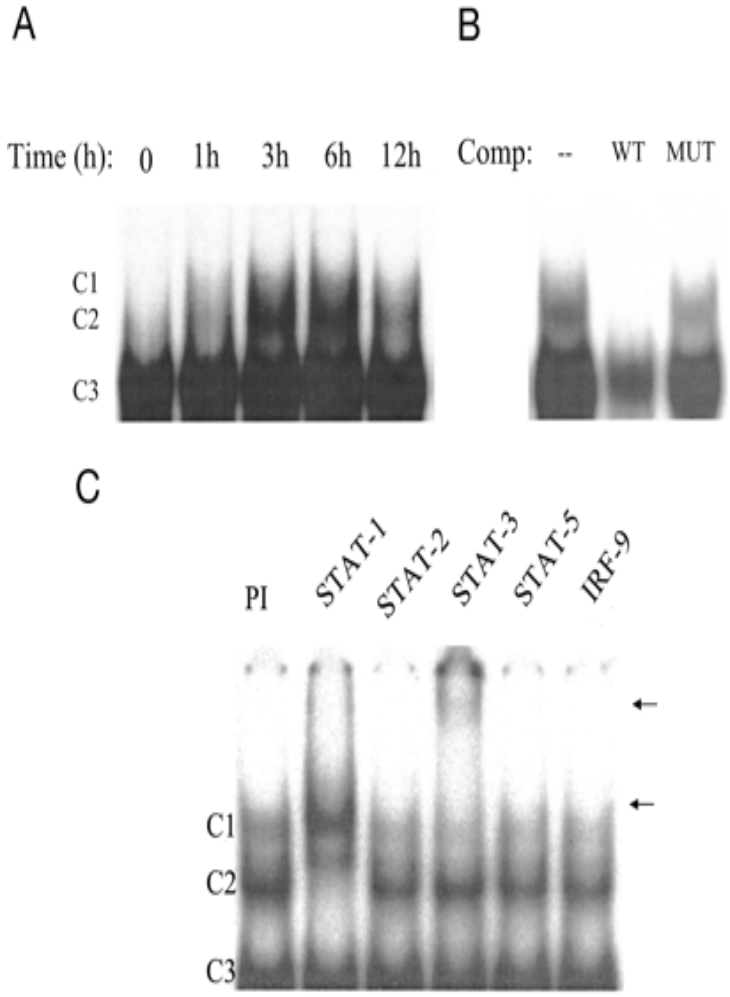

FIGURE 2.4 EMSA OF IRF-1 GAS BINDING COMPLEXES IN RESPONSE TO RSV INFECTION A) Autoradiogram of time course. Nuclear extracts were prepared from control and RSV-infected A549 cells at the indicated times and used for EMSA. The time (in h) following RSV infection is indicated at the top. B) Competition assay. Nuclear extracts of A549 cells infected for 6 h were used in the EMSA. 2 pM unlabeled wild type (WT) or mutated (MUT) competitors were included in the binding reaction as indicated at the top. C) Supershift interference assay. Nuclear extracts of A549 cells infected for 6 h were used in the EMSA in the presence of preimmune serum (PI), anti-STAT1, -2, -3, -5, and anti-IRF-9 antibodies. Arrows indicate supershifted complexes.

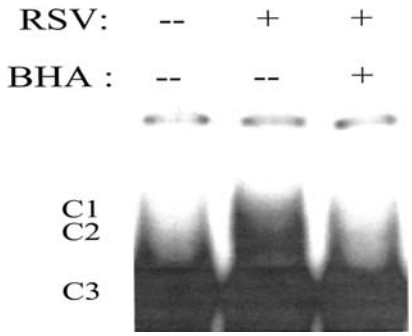

FIGURE 2.5 EMSA OF IEF-1 GAS BINDING COMPLEXES IN RESPONSE TO ANTIOXIDANT TREATMENT Nuclear extracts were prepared from A549 cells, control and infected with RSV for 3 h, in the absence or presence of 400 μM BHA, and used for binding to the IRF-1 GAS in EMSA. Shown are the inducible complexes formed on the probe in response to RSV infection.

IRF-7 gene transcription is controlled mainly through activation of the promoter ISRE site, which binds transcription factors of the STAT and IRF families (51). To determine whether inhibition of RSV-induced IRF-7 transcription by antioxidant treatment was also the result of changes in abundance of proteins binding to the IRF-7 ISRE, we performed EMSAs using nuclear extracts of A549 cells, control and infected with RSV for various lengths of time, in the presence or absence of BHA. As shown in Figure 2.6A, a single nucleoprotein complex (C3) was formed from nuclear extracts of control cells on the IRF-7 ISRE probe. RSV infection induced the appearance of three other complexes, C1, C2, and C4, starting around 3 h postinfection, with a progressive increase in binding intensity at 6 h and a decline after 12 h of infection. Antioxidant treatment greatly reduced binding of the RSV-inducible complexes to the ISRE probe at all time points. The sequence specificity of the different complexes was examined by competition with unlabeled oligonucleotides in EMSA (Figure 2.6B). C1, C2, and C4 were competed by the wild type but not by the mutated oligonucleotide, indicating binding specificity. Supershift assays showed that anti-IRF-1 antibody induced a reduction of C4 and appearance of supershifted bands (indicated by the arrows), whereas the anti-STAT1, -2, and IRF-9 antibodies caused the disappearance or reduction of C1 and, in case of anti-STAT2, the appearance of a faint supershifted band (Figure 2.6C). These data indicate that IRF-1 is the major component of the RSV-inducible C4, and STAT1, STAT2, and IRF-9, which together form the ISGF3 complex, are the major components of C1. We were not able to identify the composition of C2.

STAT proteins are constitutively expressed and, in unstimulated cells, are located in the cytoplasm. Upon activation, they are phosphorylated on specific tyrosine residues, a post-translational modification necessary for dimerization and nuclear translocation, both of which are required for DNA binding (56). To determine whether RSV infection

of A549 cells induced STAT1 tyrosine phosphorylation, we performed Western blot analysis of nuclear proteins extracted from A549 cells uninfected or infected for various lengths of time. As shown in Figure 2.7A, RSV infection induced a time-dependent increase in tyrosine phosphorylation and nuclear translocation of STAT1, starting between 1 and 3 h postinfection. To determine whether BHA inhibition of RSV-induced STAT binding to the IRF-1 GAS was the result of inhibition of STAT phosphorylation, we performed Western blot analysis of nuclear proteins extracted from A549 cells uninfected or infected for various lengths of time, in the presence or absence of BHA, using anti-STAT1 phosphotyrosine-specific antibodies.

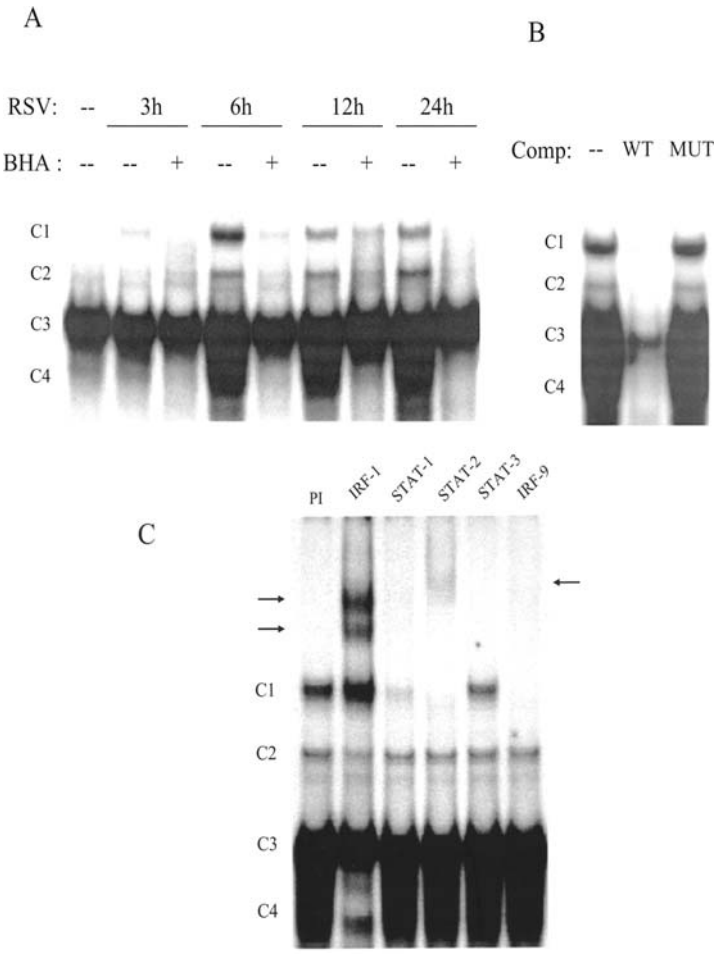

FIGURE 2.6 EMSA OF IRF-7 ISRE-BINDING COMPLEXES IN RESPONSE TO RSV INFECTION A) Effect of antioxidant treatment. Nuclear extracts were prepared from A549 cells, control and infected with RSV for various lengths of time, in the absence or presence of 400 μM BHA, and used for EMSA. The time (in h) after RSV infection is indicated at the top. B) Competition assay. Nuclear extracts of A549 cells infected for 6 h were used in the EMSA. 2 pM unlabeled wild type (WT) or mutated (MUT) competitors were included in the binding reaction as indicated at the top. C) Supershift interference assay. Nuclear extracts of A549 cells infected for 6 h were used in the EMSA in the presence of preimmune serum (PI), anti-STAT1, -2, -3, and anti-IRF-1 and -9 antibodies. Arrows indicate supershifted complexes.

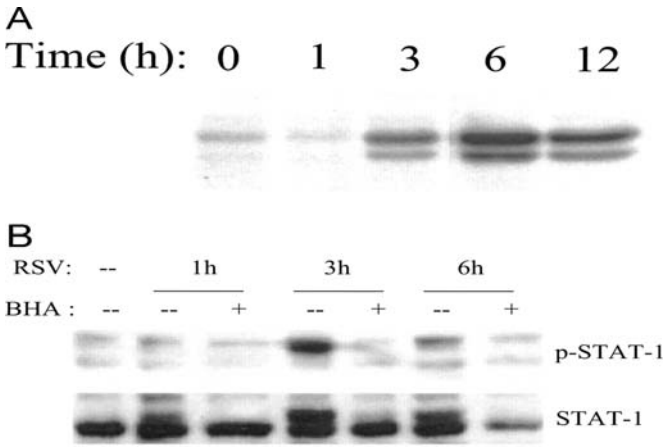

FIGURE 2.7 EFFECT OF BHA ON STAT1 PHOSPHORYLATION AND NUCLEAR ABUNDANCE A) Time course. Nuclear extracts were prepared from A549 cells, control and infected with RSV for 1, 3, 6, and 12 h and assayed for phosphorylated STAT1 by Western blot. B) Effect of BHA. A549 cells were infected with RSV for 1, 3, and 6 h in the absence or presence of 400 μM BHA. Cells were harvested to prepare nuclear extracts, and equal amounts of protein from control and infected cells were assayed for phosphorylated and total STAT1 by Western blot.

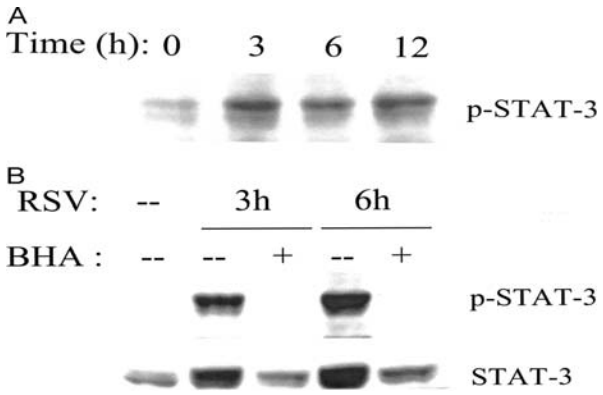

FIGURE 2.8 EFFECT OF BHA ON STAT3 PHOSPHORYLATION AND NUCLEAR ABUNDANCE A) Time course. Nuclear extracts were prepared from A549 cells, control and infected with RSV for 3, 6, and 12 h, and assayed for phosphorylated STAT3 by Western blot. B) Effect of BHA. A549 cells were infected with RSV for 3 and 6 h, in the absence or presence of 400 μM BHA. Cells were harvested to prepare nuclear extracts, and equal amounts of protein from control and infected cells were assayed for phosphorylated and total STAT3 by Western blot.

As shown in Figure 2.7B, RSV-induced STAT1 phosphorylation was completely blocked by BHA treatment. The same blot was stripped and reprobed with an anti-STAT1 antibody, showing two forms of nuclear STAT. The first form is present in uninfected and infected cells and is not affected by antioxidant treatment. The second form is RSV-inducible and disappears following BHA treatment, likely representing the tyrosine-phosphorylated STAT1. RSV infection also induced a time-dependent increase in the abundance of nuclear phosphorylated STAT3, as shown in Figure 2.8A. Antioxidant treatment completely abolished RSV-induced STAT3 phosphorylation, as shown in Figure 2.8B. The same blot was stripped and reprobed with an anti-STAT3 antibody, showing that RSV-induced STAT3 nuclear translocation was greatly reduced by BHA treatment. Together, these data indicate that RSV-induced ROS formation is involved in STAT activation and IRF gene expression.

RSV Infection Inhibits Tyrosine Phosphatase Activity, Restored by Antioxidants

A number of receptor-associated and nonreceptor-associated tyrosine kinases have been show to phosphorylate STAT proteins (56). Among them, the best characterized ones are the JAKs. JAKs are a family of tyrosine kinases which includes JAK1, 2, 3, and Tyk2. JAK1, JAK2, and Tyk2 are ubiquitously expressed, whereas JAK3 is tissue-specific. JAK1 can form heterodimers with JAK2, JAK3, or Tyk2, depending on the activating stimulus (57). To determine whether RSV infection induced JAK activation, we measured JAK2 and Tyk2 phosphorylation by Western blot. We did not detect significant levels of JAK phosphorylation at early time points of infection, from 1 to 6 h, when RSV-induced STAT activation occurs, although there was increased JAK2 and Tyk2 tyrosine phosphorylation following stimulation of A549 cells with interferon-γ and -β, respectively (data not shown). Furthermore, an inhibitor of JAK2 activation,

AG490, did not block RSV-induced STAT binding to the IRF-1 GAS or activation of the IRF-1 promoter (data not shown). We also investigated kinases belonging to the Src family, which have been shown to mediate receptor-independent STAT protein tyrosine phosphorylation (58-59), using the broad spectrum Src kinase family inhibitors PP1 and PP2 (60). Similar to the results of AG490, neither PP1 or PP2 inhibited STAT activation and IRF-1 promoter induction following RSV infection, suggesting that other molecules might be involved. However, tyrosine phosphorylation is an important event in regulating RSV-induced STAT activation because treatment of A549 cells with a generic tyrosine kinase inhibitor, AG82, significantly reduced STAT binding to the IRF-1 GAS (Fig. 9A) and IRF-1 promoter induction (Figure 2.9B), following RSV infection. Protein phosphorylation is a reversible and dynamic process, which requires not only protein kinases but also protein phosphatases (PPs). H_2O_2 treatment has been shown to induce an increase in the overall intracellular levels of protein tyrosine phosphorylation, and it has been suggested that one of the mechanisms mediating the biological effects of H_2O_2 treatment is inhibition of PPs (61). To determine whether RSV infection alters PP function, we assayed total intracellular protein-tyrosine phosphatase activity in cells uninfected or infected with RSV, in the absence or presence of antioxidant. As shown in Figure 2.10, RSV infection significantly decreased protein-tyrosine phosphatase activity in the first 12 h of infection, with maximal inhibition at 3 h postinfection, when there is significant RSV-induced STAT phosphorylation, which was completely reversed by BHA treatment. Protein-tyrosine phosphatase activity returned to control levels at 24 h postinfection. To confirm the possibility that inhibition of tyrosine phosphatase activity in airway epithelial cells can lead to STAT activation, we determined STAT1 phosphorylation, by Western blot analysis, in A549 cells treated with sodium pervanade, a derivative of the tyrosine phosphatase inhibitor sodium orthovanadate. As shown in

Figure 2.11, there was a significant induction of tyrosine-phosphorylated STAT1 shortly after cellular treatment with the inhibitor, suggesting that modulation of phosphatases can indeed be an important mechanism of virus-induced STAT activation.

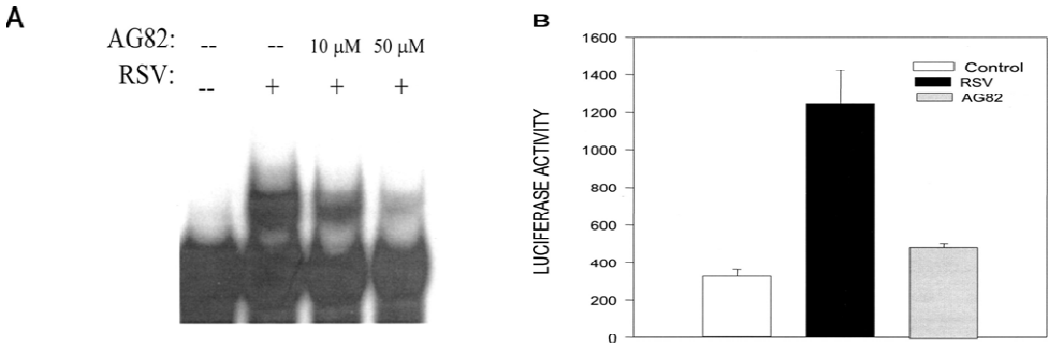

FIGURE 2.9 TYROSINE PHOSPHORYLATION IS NECESSARY FOR STAT-MEDIATED IRF PROMOTER ACTIVATION A) nuclear extracts were prepared from A549 cells, control and infected with RSV for 6 h, in the absence or presence of either 10 or 50 μM AG82, and used for binding to the IRF-1 GAS in EMSA. B) A549 cells were transiently transfected with the IRF-1 promoter plasmid, infected with RSV in the presence or absence of 50 μM AG82, and harvested at 12 h postinfection to measure luciferase activity. Uninfected plates served as controls.

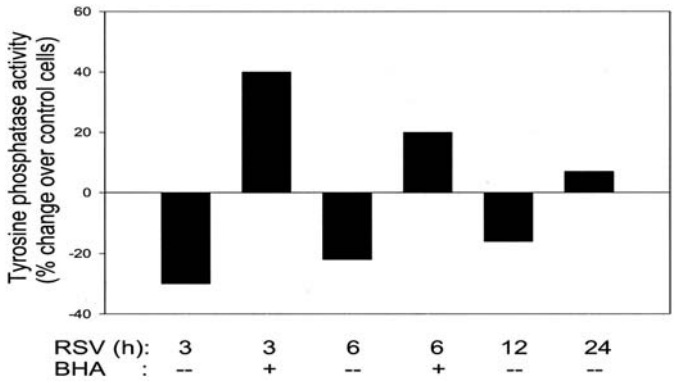

FIGURE 2.10 EFFECT OF VIRAL INFECTION AND ANTIOXIDANT TREATMENT ON INTRACELLULAR TYROSINE PHOSPHATASE ACTIVITY Total cell lysates were prepared from A549 cells, uninfected and infected with RSV, in the absence or presence of 400 μM BHA, and assayed for intracellular tyrosine phosphatase activity. Values are expressed as a percent of positive or negative change compared with uninfected cells. Bars represent the mean value of triplicate samples of one experiment, n = two experiments.

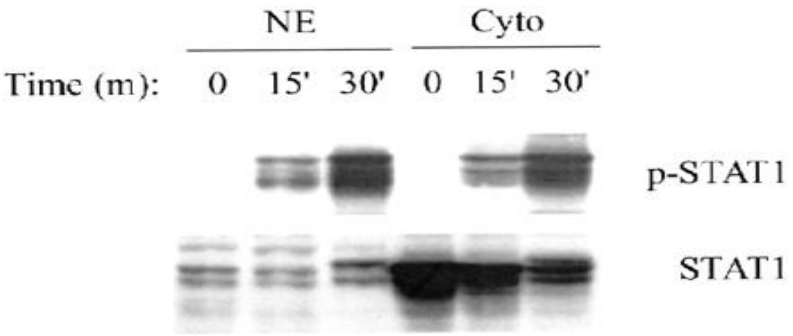

FIGURE 2.11 INHIBITION OF TYROSINE PHOSPHATASES INDUCES STAT1 PHOSPHORYLATION Cytoplasmic (Cyto) and nuclear extracts (NE) were prepared from A549 cells, control and treated with 100 μM sodium pervanadate for 15 and 30 min, and assayed for phosphorylated STAT1 by Western blot. Membrane was stripped and reprobed with an antibody recognizing total STAT1.

NAD(P)H Oxidase Is Involved in RSV-induced STAT Activation

An important source of inducible intracellular ROS, generated in response to a variety of stimuli, is the membrane-bound NAD(P)H oxidase system (62). To test whether RSV-induced STAT activation was mediated through ROS production by this enzyme complex, we treated RSV-infected A549 cells with DPI, a known NAD(P)H oxidase inhibitor. As shown in Figure 2.12, DPI completely abolished RSV-induced STAT binding to the IRF-1 GAS, indicating that the NAD(P)H oxidase system is an important enzyme for the generation of ROS and subsequent activation of STAT following RSV infection. Because DPI is not completely specific for NAD(P)H oxidase, we investigated the effect of inhibitors of nitric oxide synthase (N-nitro-L-arginine methyl ester), and mitochondrial electron transport (rotenone and antimycin A) on STAT activation. Although N-nitro-L-arginine methyl ester and rotenone did not have any effect on STAT binding to the IRF-1 GAS, antimycin A partially reduced STAT activation, probably by virtue of reducing the overall ROS intracellular load (data not shown).

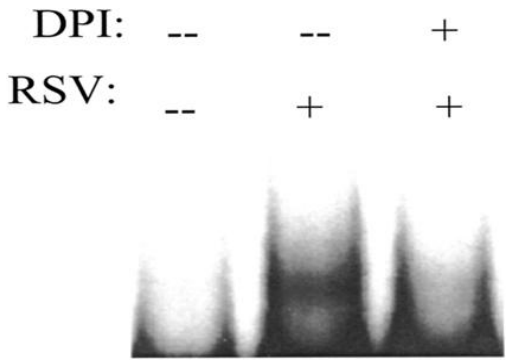

FIGURE 2.12 EFFECT OF NAD(P)H OXIDASE INHIBITION ON STAT ACTIVATION. Nuclear extracts were prepared from A549 cells, control and infected with RSV for 6 h, in the absence or presence of 50 μM DPI, and used for binding to the IRF-1 GAS in EMSA. Shown are the inducible nucleoprotein complexes formed on the probe in response to RSV infection.

DISCUSSION

Lower respiratory tract infections caused by RSV are characterized by profound cellular inflammation of the airway mucosa, which contributes to disease manifestations including air flow limitation, lung atelectasis/emphysema, and hypoxemia (1). The mechanisms that regulate airway inflammation in viral respiratory infections are not fully understood. However, airway epithelial cells represent a major initiator of pulmonary host defense and inflammatory reactions by their ability to synthesize and secrete soluble mediators, upon injury or infection, which are important for the recruitment and activation of immune/inflammatory cells. Indeed, airway epithelial cells infected with RSV produce a variety of these proinflammatory molecules, such as cytokines and chemokines (44).

The intracellular signaling events leading to RSV-induced gene expression are mostly unknown. Free radicals and ROS species have recently been shown to function as second messengers influencing a variety of molecular and biochemical processes, including expression of a number of genes (31). Virus-induced ROS generation has been

linked to NF-κB activation and gene expression in influenza virus and human immunodeficiency virus-infected cells (63). We have shown recently that antioxidant treatment of airway epithelial cells blocked RSV-induced RANTES gene expression and protein secretion, through inhibition of de novo IRF-1 and -7 gene expression and protein synthesis and IRF-3 nuclear translocation (29). In the present study we have investigated the mechanism of inhibition of IRF induction by antioxidant treatment. We show that RSV infection of alveolar epithelial cells induces IRF-1 and -7 gene transcription in a time-dependent manner, which is completely blocked following antioxidant treatment. RSV infection induces STAT protein phosphorylation, nuclear translocation, and binding to the IRF-1 and -7 promoters, an event necessary for IRF-inducible transcription, as seen with interferon stimulation (51-52) Antioxidant treatment completely abolishes RSV-induced STAT activation by blocking tyrosine phosphorylation, therefore preventing STAT translocation and DNA binding to both the IRF-1 GAS and IRF-7 ISRE promoter sequences. Oxidative stress has been traditionally linked to activation of the transcription factors NF-κB and AP-1 and the ras/rac mitogen-activated protein kinase pathway (31) and (46). However, recent studies have shown that activation of the JAK-STAT pathway is also redox-sensitive. Simon et al. (64) demonstrated that STAT1 and STAT3 are activated in response to H_2O_2 in fibroblasts, and JAK-STAT activation following stimulation with angiotensinogen II and oxidized low-density lipoprotein is inhibited by antioxidant treatment (65-66). Little is known about the role of ROS in virus-induced STAT activation. Very recently Gong et al. (67) have shown that the human hepatitis C virus NS5A protein alters intracellular calcium levels, triggering ROS formation and nuclear translocation of NF-κB and STAT3, which is completely inhibited by the use of antioxidants. Similarly, the hepatitis B virus X protein induces ROS formation through association with an outer mitochondrial anion channel, an event that leads to NF-κB and

STAT3 activation, which is sensitive to antioxidant treatment, as well as manganese superoxide dismutase overexpression (68). In this study we have shown that RSV-induced STAT activation also seems to be ROS-dependent because it is completely blocked by antioxidant treatment. The mechanism involved in ROS formation and STAT activation, following RSV infection, is not clear yet. We investigated possible tyrosine kinase signaling complexes leading to STAT activation in alveolar epithelial cells following RSV infection. The use of standard JAK2 and Src kinase inhibitors failed to block RSV-induced STAT activation, and we did not find consistent activation of Tyk2 at early time points of infection, suggesting that alternative pathways could be involved, such as the mitogen-activated protein kinase kinase kinase, MEKK1, which has been shown to regulate STAT3 activation (69). However, we found that RSV infection significantly inhibited protein-tyrosine phosphatase activity, which was restored by antioxidant treatment. Very little information is available regarding virus-induced regulation of protein-tyrosine phosphatase activity and their role in signaling pathways activated by viral infections. However, exogenous H_2O_2 treatment has been shown to induce an increase in the overall intracellular levels of protein tyrosine phosphorylation, triggering activation of multiple signaling molecule and transcription factors, ultimately leading to gene expression (61) and it has been suggested that one of the mechanisms mediating the biological effects of H_2O_2 treatment is inhibition of protein phosphatases (61). More specifically, two studies have shown that H_2O_2 inhibits specific protein-tyrosine phosphatases, whereas antioxidants can increase protein-tyrosine phosphatase activity (70-72). It is possible that virus-induced ROS activate STAT through an imbalance between cellular tyrosine kinases and phosphatases, resulting in increased net phosphorylation and therefore activation. Interestingly, we have shown that airway epithelial cell treatment with pervanade, a derivative of the tyrosine phosphatase inhibitor

orthovanadate, can induce STAT1 phosphorylation. Similar results have been reported in other cell types, and STAT activation as well as subsequent STAT-driven gene expression occurs in a ligand-independent manner, which does not require JAK1, JAK2, or Tyk2 activity (73-75).

Intracellular ROS can be generated by different systems, including the NAD(P)H oxidase system, the mitochondrial electron transport chain, and enzymes such as xanthine oxidase, and cyclooxygenase plays an important role in the regulation of intracellular signaling cascades in various cell types including fibroblasts, endothelial cells, myocytes, smooth muscle cells, etc. (76). In our study, treatment of RSV-infected alveolar epithelial cells with DPI, an inhibitor of the NAD(P)H complex, completely abolishes virus-induced STAT activation, suggesting that the NAD(P)H oxidase system is an important enzyme for the generation of ROS and subsequent activation of STAT, following RSV infection. Indeed, angiotensinogen II-induced STAT activation occurs via the NAD(P)H oxidase system (77), and Rac1, a small GTP-binding protein that is part of the NAD(P)H complex in nonphagocytic cells, has been shown to regulate STAT3 activity (78). Because DPI is not completely specific for NAD(P)H oxidase, current studies are in progress to define better the role of NAD(P)H complex in RSV-induced ROS formation and STAT activation, by looking at membrane translocation of components of the oxidase system and by interference with its activation overexpressing dominant negative mutants of Rac1.

In summary, our study indicates that RSV-induced ROS formation, occurring likely through the NAD(P)H oxidase system, is involved in STAT activation, and subsequent IRF-1 and -7 gene expression. Modulation of intracellular tyrosine phosphatase activity, following viral infection, could potentially be a very important mechanism involved in activation of molecules regulated by tyrosine phosphorylation-

like STAT proteins. Identification of the molecular mechanisms involved in RSV-induced gene expression is fundamental for developing strategies to modulate the inflammatory responses associated with RSV infection of the lung.

CHAPTER 3: IKKEPSILON REGULATES VIRAL-INDUCED INTERFERON REGULATORY FACTOR-3 ACTIVATION VIA A REDOX-SENSITIVE PATHWAY*

ABSTRACT

Respiratory syncytial virus (RSV)-induced chemokine gene expression occurs through the activation of a subset of transcription factors, including Interferon Regulatory Factor (IRF)-3. In this study, we have investigated the signaling pathway leading to RSV-induced IRF-3 activation and whether it is mediated by intracellular reactive oxygen species (ROS) generation. Our results show that RSV infection induces expression and catalytic activity of IKKε, a noncanonical IKK-like kinase. Expression of a kinase-inactive IKKε blocks RSV-induced IRF-3 serine phosphorylation, nuclear translocation and DNA-binding, leading to inhibition of RANTES gene transcription, mRNA expression and protein synthesis. Treatment of alveolar epithelial cells with antioxidants or with NAD(P)H oxidase inhibitors abrogates RSV-induced chemokine secretion, IRF-3 phosphorylation and IKKε induction, indicating that ROS generation plays a fundamental role in the signaling pathway leading to IRF-3 activation, therefore, identifying a novel molecular target for the development of strategies aimed to modify the inflammatory response associated with RSV infection of the lung.

INTRODUCTION

RSV is an enveloped, negative-sense single-stranded RNA virus, belonging to the paramyxovirus family. Since its isolation, RSV has been identified as a leading cause of epidemic respiratory tract illness in children, in the U.S. and worldwide (9). RSV induces

* "Reprinted from Virology,Vol 353, Pages 155-165 Indukuri H., Castro S.M., Liao S., Feeney L., Dorsch M., Coyle A. J., Garofalo R. P., Brasier A. R., and Casola A., Ikkepsilon Regulates Viral-Induced Interferon Regulatory Factor-3 Activation Via A Redox-Sensitive Pathway, Copyright (2006), with permission from Elsevier Limited License No. 1927820565947"

a broad spectrum of clinical diseases ranging from otitis media to mild upper respiratory infection, acute laryngeo-tracheo-bronchitis, or more severe lower respiratory tract infections. In young children (1 month–2 years old), RSV infection can develop into significant lower respiratory tract disease, histologically distinguishable into two syndromes: (1) pneumonia, with diffuse mononuclear inflammation of the bronchi, bronchioles and interalveolar walls; and (2) bronchiolitis, characterized by necrosis of the bronchiolar epithelium, edema, and mononuclear cell infiltration of the bronchiolar submucosa with mucus plugs and air trapping (79-80). Airway epithelial cells are the main targets of RSV infection. Following inhalation or self-inoculation of the virus into the nasal mucosa and infection of the local respiratory epithelium, RSV spreading along the respiratory tract occurs mainly by cell-to-cell transfer of the virus along the intracytoplasmic bridges (81). Under normal conditions, the respiratory epithelium is responsible for clearance of inhaled particulates and maintenance of alveolar patency. However, following inhalation of infectious agents, it is able to secrete a variety of molecules involved in antiviral and innate immune responses, like interferons, cytokines and chemokines, and therefore plays a major role in the initial host protective response to viral infections. A number of molecules have been described that are produced by human airway epithelial cells as a consequence of RSV infection. We, as well as others, have demonstrated that RSV is a potent stimulus for chemokine production, including interleukin (IL)-8 and RANTES, in cultured human nasal, bronchial and alveolar epithelial cells (13,24,82). In the past few years, we have characterized the mechanisms involved in RSV-induced expression of the chemokines IL-8 and RANTES, whose expression in epithelial cells require viral replication (11,23,45). RSV-induced RANTES expression is dependent on the activation of IRFs, especially IRF-3, which are absolutely necessary for RANTES promoter induction (45). We have also shown that ROS are

important mediators of RSV-induced RANTES gene expression, modulating IRF-1, -3 and -7 activation (29). Treatment of airway epithelial cells with the antioxidant butylated hydroxyanisol (BHA) inhibits RSV-induced IRF-1 and -7 gene expression and protein synthesis (29), through inhibition of Signal Transducers and Activators of Transcription (STAT)-1 and -3 activation (83). BHA treatment also inhibits IRF-3 nuclear translocation, indicating that a redox-sensitive pathway is involved in RSV-induced IRF-3 activation (29). However, the signaling pathway(s) leading to RSV-induced IRF-3 activation, and whether it is ROS-dependent, is currently not known.

IRF-3 is a constitutively expressed protein, which is phosphorylated on several serine/threonine residues present on the C-terminus of the protein, upon viral infection. This event allows dimerization, nuclear localization and DNA-binding (84). Two separate groups have identified the I kappa B kinase (IKK)-like molecule IKKε, together with Tank Binding Kinase (TBK)1, as a critical component of the virus-activated kinase (VAK) complex responsible for IRF-3 phosphorylation (85-86). Overexpression of IKKε induces IRF-3 and -7 nuclear translocation and binding to Interferon Regulated Responsive Element (ISRE) promoter sites, leading to the expression IFN-β and RANTES genes (85-86). In this study, we have investigated the role of IKKε, as well as ROS generation, in RSV-induced IRF-3 activation. RSV induces IKKε mRNA expression and protein synthesis, as well as its catalytic activity. Expression of a kinase-inactive IKKε blocks RSV-induced RANTES gene transcription, mRNA expression and protein synthesis. This occurs through inhibition of IRF-3 serine phosphorylation, an event known to be necessary for viral-induced nuclear translocation, DNA-binding and activation of chemokine gene transcription (84). Antioxidant treatment of alveolar epithelial cells inhibits RSV-induced IRF-3 serine phosphorylation and IKKε induction. Moreover, treatment of alveolar epithelial cells with various NAD(P)H oxidase

inhibitors, including diphenylene iodonium (DPI), apocyanin and aminoethyl benzene sulfonyl fluoride (AEBSF), significantly reduces RANTES secretion, IRF-3 phosphorylation and IKKε induction, indicating that NAD(P)H oxidase-produced ROS are required for induction of the signaling pathway leading to IRF-3 activation in viral-infected airway epithelial cells.

MATERIALS AND METHODS

RSV preparation

The RSV A2 strain was grown in Hep-2 cells and purified by centrifugation on discontinuous sucrose gradients as described elsewhere (47). The virus titer of the purified RSV pools, was 8–9 log10 plaque forming units (PFU)/ml using a methylcellulose plaque assay. No contaminating cytokines were found in these sucrose-purified viral preparations (48). LPS, assayed using the limulus hemocyanin agglutination assay, was not detected. Virus pools were aliquoted, quick-frozen on dry ice/alcohol and stored at −70°C until used.

Cell culture and infection of epithelial cells with RSV

A549, human alveolar type II-like epithelial cells, and 293, a human embryonic kidney epithelial cell line (ATCC), were maintained in F12K and MEM medium respectively, containing 10% (v/v) FBS, 10 mM glutamine, 100 IU/ml penicillin and 100 μg/ml streptomycin. Cell monolayers were infected with RSV at multiplicity of infection (MOI) of 3 (unless otherwise stated), as described (23). An equivalent amount of a 30% sucrose solution was added to uninfected A549 cells, as a control. When inhibitors were used, cells were pretreated for 1 h and then infected in the presence of the compound. Since inhibitors were diluted either in ethanol or in DMSO, equal amount of diluent was added to untreated cells, as a control. Total number of cells and cell viability, following

treatment, were measured by trypan blue exclusion. No cell toxicity was observed for any compound at concentrations used for the experiments.

Western Blotting

Total cell lysates were prepared by adding ice-cold lysis buffer (50mM Tris–HCl, pH 7.4, 150mM NaCl, 1 mM EGTA, 0.25% sodium deoxycholate, 1mM Na3VO4, 1 mM NaF, 1% Triton X-100 and 1μg/ml of aprotinin, leupeptin and pepstatin. After incubation on ice for 10 min, the lysates were collected and detergent insoluble materials were removed by centrifugation at 4°C at 14,000 × g. Cytoplasmic and nuclear extracts were prepared using hypotonic/nonionic detergent lysis, as previously described (11). Proteins (20 to 50 μg per sample) were then boiled in 2× Laemmli buffer for 2 min and resolved on SDS-PAGE. Proteins were transferred for 6h onto Hybond-ECL nitrocellulose membrane (Amersham Pharmacia Biotech) and nonspecific binding sites were blocked by immersing the membrane in TBST blocking solution [10 mM Tris–HCl, pH 7.6, 150 mM NaCl, 0.05% Tween-20 (v/v)] containing 5% skim milk powder or 5% bovine serum albumin for 30min. After a short wash in TBST, the membranes were incubated with the primary antibody overnight at 4°C, followed by an anti-rabbit peroxidase-conjugated secondary antibody (Santa Cruz Biotechnology), diluted 1:10,000 in TBST for 30 min at room temperature. After washing, the proteins were detected using ECL (Amersham Pharmacia Biotech) according to manufacturer's protocol. The primary antibodies used for Western blots were: rabbit anti-IKKε polyclonal (Millennium Pharmaceutical), rabbit polyclonal antibody to phospho-IRF-3, which recognize the viral-induced C-terminal phosphorylated form of the molecule (87), (a gift from Rongtuan Lin, McGill University, Montreal, Canada), rabbit polyclonal antibodies against IRF-3 (Santa Cruz Biotechnology).

RANTES ELISA

Immunoreactive RANTES was quantified using the double antibody DuoSet ELISA kit (R&D Systems) following the manufacturer's protocol.

Northern Blot and Real Time PCR

Total RNA was extracted from control and infected A549 cells by the acid guanidium thiocyanate-phenol chloroform method (88). Twenty micrograms of RNA were fractionated on a 1.2% agarose-formaldehyde gel, transferred to nylon membranes and hybridized to a radiolabeled RANTES cDNA, as previously described (45). After washing, membranes were exposed for autoradiography using Kodak XAR film at −70°C, using intensifying screens. After exposure, membranes were stripped and rehybridized with a β-actin probe. For IKKε amplification by real time PCR, Quantitative Real Time PCR (Q-RT-PCR) Applied Biosystems assays-on-demand 20× mix of primers and TaqMan MGB probes (FAM-dye labeled) for target genes and 18S rRNA (VIC-dye labeled probe) TaqMan assay reagent (P/N 4319413E) for controls were used. Separate tubes (singleplex) one-step RT-PCR was performed with 80 ng RNA for both target genes and endogenous control. The cycling parameters for one-step RT-PCR was: reverse transcription 48^{o}C for 30 min, AmpliTaq activation 95^{o}C for 10 min, denaturation 95^{o}C for 15s and annealing/extension 60^{o}C for 1 min (repeat 30 times) on ABI7000. Duplicate CT values were analyzed in Microsoft Excel using the comparative CT (ΔΔCT) method as described by the manufacturer (Applied Biosystems). The amount of target (2−ΔΔCT) was obtained by normalizing to endogenous reference (18S) sample.

Plasmid construction and cell transfection

The PGL2-220 plasmid, containing the first 220 nucleotides of the RANTES promoter, the IL-8 LUC, containing the first −162 nucleotides of the IL-8 promoter, as

well as the plasmid containing multiple copies of the RANTES ISRE site linked to the luciferase reporter gene, have been previously described (11-12,45). The IKKε wild type and catalytically-inactive (K38A) plasmids were created by cloning the PCR product corresponding to bases 324 to 2477 of the human IKKε gene into the pcDNA3 expression vector, using the BamHI and XbaI cloning sites, as previously described (89). Mutation of the lysine 38 residue to alanine was introduced by overlapping PCR (89). The plasmid expressing a kinase inactive (DN) IKKβ was a generous gift of Dr. Mercurio, Signal Pharmaceutics, and has been previously described (90).

Logarithmically growing A549 or 293 cells were transfected in triplicate in 60mm dishes using Fugene 6 (Roche). One μg of the reporter gene plasmid, 0.5μg of β-galactosidase and 0.5μg of either IKKε wild type or K38A or IKKβ DN expression plasmid were premixed with FuGene6 in a 1:3 ratio (μg/μl), and added to the cells in 3ml of regular medium. The next morning, cells were infected with RSV and at 12 or 24h post-infection cells were lysed to measure independently luciferase and β-galactosidase reporter activity, as previously described (11). Luciferase was normalized to the internal control β-galactosidase activity. All experiments were performed at least three times.

IKKε stable cell lines

Tetracycline-inducible 293-IKKε wild type and kinase inactive cell lines were generated using a modified version of the Tet-on system (91). 293T cells were transfected with plasmids encoding a reverse tetracycline-inducible transactivator, a tetracycline-regulated repressor, the puromycin resistance gene and IKKε (wild type or K38A mutant) and GFP under the control of a bi-directional promoter (plasmids were kindly provided by Dr. Jay Morgenstern, Millennium Pharmaceuticals). Transfection was performed using Fugene 6, according to the manufacturer's instructions. Stably transfected cell lines were selected in the presence of puromycin. Flow cytometry sorting was used to select

cells that were GFP-negative in the absence of doxycycline and GFP-positive in its presence. Cells were sorted as single cells into 96-well plates and resulting clones were tested for inducible IKKε protein expression by Western blot analysis.

Kinase assays

A549 cells were resuspended in lysis buffer [25mM Tris, pH 7.5, 150mM NaCl, 1.0% Triton X-100, 10.0% Glycerol. 1mM DTT, 20mM β-glycerolphosphate, 0.2mM sodium orthovanadate, 20mM p-Nitrophenyl enhanceosome phosphate (PNPP), 1mM PMSF, 1mM Benzamidine, and supplemented with 1 mini protease inhibitor tablet per 10ml]. Lysates were cleared by centrifugation at 14,000rpm for 10min at 4°C. 0.5mg protein lysate was incubated for 3h at 4 with 7.5mg of IgG-purified anti-IKKε antibody, followed by 1h incubation at 4°C with 20ml of protein G slurry (Amersham). Samples were rotated end-over-end during all incubations. Protein G beads were pre-blocked and equilibrated with lysis buffer containing 0.2 mg/ml BSA. After the immunoprecipitation, the beads were collected by centrifugation for 3 min at 6,000 rpm and washed twice with lysis buffer. Kinase assays with biotinylated IRF-3 peptide aa 380–406 (GGASSLENTVDLHISNSHPLSLTSDQ) as substrate were performed out in a total volume of 10 ml in kinase buffer containing 100 mM ATP, 1.0 mg of substrate and 0.33 μCi of 32P-γATP. The reaction was carried out for 30 min at 37°C and was terminated by addition of 20ml of 7.5 M guanidine hydrochloride. The phosphorylated substrate was spotted on SAM2, a biotin capture membrane (Promega). Filters were washed several times with 2M NaCl solution and phosphorylated substrate was visualized and analyzed by PhosphoImager after overnight exposure.

RESULTS

RSV infection of airway epithelial cells induces IKKε activation

IKKε is an IKK-like kinase identified as part of a novel kinase complex which can activate NF-κB following certain inducers like LPS and PMA (89,92). Recent studies have reported a fundamental role of IKKε in IRF-3 activation and induction of IRF-3-dependent genes, like IFN-α, IFN-β and RANTES (85-86). Expression of IKKε can be either constitutive or inducible, depending on the cell type (85). To investigate whether RSV infection of A549 cells induced IKKε expression, we performed Western blot analysis of total cell lysates prepared from A549 cells uninfected or infected for various lengths of time. As shown in Figure 3.1A, RSV infection caused a marked increase in IKKε protein synthesis, starting around 6 h post-infection (p.i.) and peaking at 12 h. To determine whether IKKε protein synthesis was paralleled by changes in steady-state level of its mRNA, total RNA was extracted from cells uninfected and infected for various length of time, and used to amplify IKKε gene by RT-PCR (93). As shown in Figure 3.1B, RSV-induced IKKε gene expression followed a kinetic similar to the one seen for protein induction, with up-regulation occurring between 6 and 12h p.i.

We then asked whether RSV-induced IKKε was catalytically active and could phosphorylate IRF-3. For this purpose, we performed kinase assays using IKKε immunoprecipitated from A549 cell uninfected or infected with RSV for various lengths of time and an IRF-3 peptide corresponding to amino acids 380–406, which contains the major viral-inducible phosphorylation sites (84), as substrate. As shown in Figure 3.1C, IKKε catalytic activity was significantly increased, following viral infection, starting at 6h p.i., with maximal activity at 12h. This pattern is similar to the kinetics of RSV-induced IRF-3 nuclear translocation and DNA binding, as well as to the kinetics of RSV-induced RANTES gene expression (29). Viral-induced IRF-3 activation occurs through

phosphorylation of specific C-terminal serine residues, located between amino acids 386 and 405 (84), of which Ser396 has been shown to be necessary for viral-induced IRF-3 activation (87).

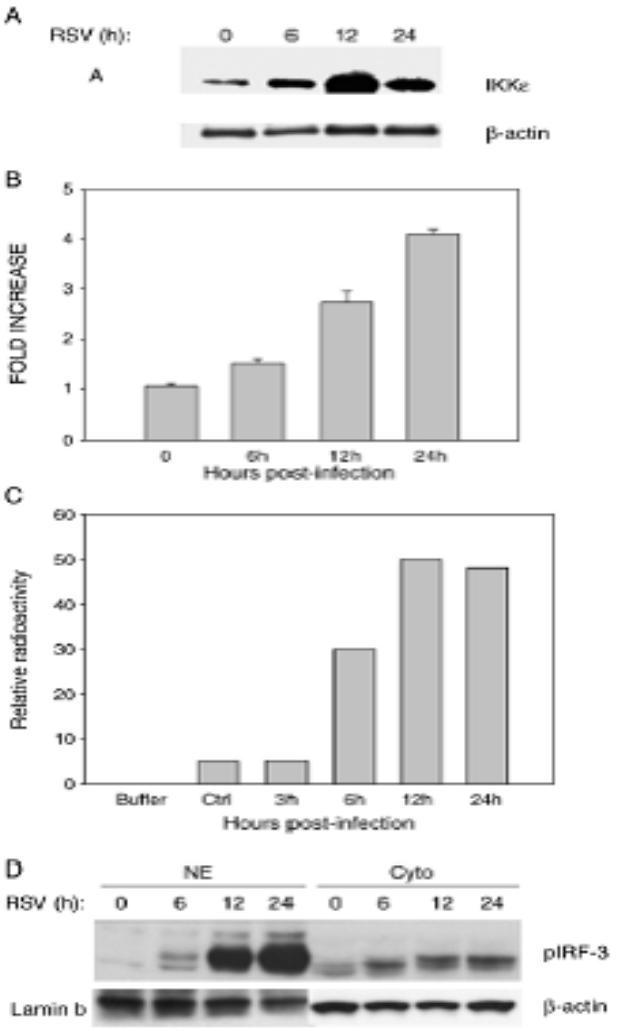

FIGURE 3.1 RSV INFECTION INDUCES IKKε ACTIVATION IN A549 CELLS A) IKKε protein levels. Total cell lysates, prepared from A549 cells uninfected or infected with RSV for 6, 12 and 24 h, were resolved on 10% SDS-PAGE and Western blot was performed using an anti-IKKε antibody. Membrane was stripped and reprobed for β-actin. B) IKKε mRNA. A549 cells were infected with RSV for various lengths of time (hours). Total RNA was extracted from control and infected cells and used to amplify IKKε by Q-RT-PCR. C) IKKε kinase activity. Total cell lysates were prepared from uninfected (Ctrl) or RSV-infected cells for 3, 6, 12 and 24 h. IKKε was immunoprecipitated with a specific antibody for in vitro kinase assay. Amount of 32P-phosphate incorporated into the IRF-3 substrate was quantified by exposure to PhosphoImager cassette and analyzed with Molecular Dynamics Storm imaging system software. Relative radioactivity is expressed in arbitrary units after subtraction of the background radioactivity present in the buffer alone sample. Data are representative of one of two independent experiments. D) Kinetics of IRF-3 phosphorylation. A549 cells were infected with RSV for various lengths of time and harvested to prepare cytoplasmic (Cyto) and nuclear extracts (NE). Equal amounts of protein from uninfected and infected cells were analyzed by Western immunoblot probed with anti Ser396 phospho-IRF-3 antibody. Membrane was stripped and reprobed for β-actin (cytoplasmic extracts) and lamin b (nuclear extracts).

To determine whether IRF-3 was phosphorylated following RSV infection, cytoplasmic and nuclear extracts were prepared from A549 cells uninfected or infected for various length of time and used for Western blot analysis of Ser396 phosphorylated IRF-3. As shown in Figure 3.1D, RSV infection induced IRF-3 phosphorylation both in the cytoplasmic and nuclear compartment, starting at 6h p.i. and peaking at 24h p.i. The kinetics of phospho-Ser396 IRF-3 formation is similar to RSV-induced IKKε activation, suggesting that indeed IKKε could play an important role in IRF-3 activation following RSV infection.

IKKε regulates RSV-induced RANTES promoter activation through the ISRE site.

Since IRF-3 activation plays a fundamental role in RSV-induced chemokine gene expression (45), we investigated the effect of overexpressing catalytically inactive IKKε (mutated on the lysine residue 38 of the catalytic domain by substitution with alanine and defined as K38A) (89) on RSV-induced RANTES gene transcription. 293 cells were cotransfected with a construct containing the minimal RSV-inducible RANTES promoter-luciferase reporter gene, PGL2-220, and a pcDNA3-based expression plasmid containing FLAG-tagged IKKε K38A (45). Expression of the dominant negative mutant IKKε significantly reduced, in a dose-dependent manner, RSV-induced luciferase activity of the RANTES promoter construct, indicating a role of this kinase in viral-induced RANTES gene transcription (Figure 3.2A).

RANTES promoter activation, following RSV infection, is controlled by multiple regulatory elements (45). Both an intact NF-κB site and ISRE, the IRF binding site, are important for RSV-stimulated RANTES gene transcription, with the ISRE site being absolutely necessary (45). To determine whether IKKε activation was sufficient to induce RANTES transcription and whether this occurred through the ISRE site, 293 cells were transiently transfected with a plasmid expressing wild type IKKε and RANTES promoter

plasmids either wild type or containing site-mutations of the ISRE or the NF-κB binding sites. As shown in Figure 3.2B, overexpression of IKKε caused a significant (~6-fold) activation of the RANTES promoter, which was abolished by mutation of the ISRE site. On the contrary, the RANTES NF-κB site mutation significantly reduced basal promoter activity, yet showed a 20-fold induction by IKKε expression (45). Together these data indicate that IKKε is a potent activator of the ISRE.

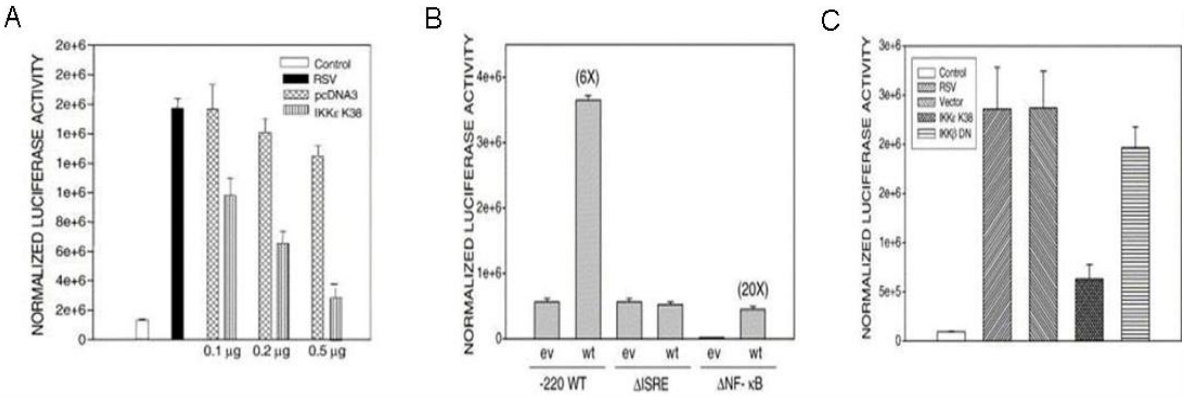

FIGURE 3.2 EFFECT OF OVEREXPRESSING CATALYTICALLY-INACTIVE OR WILD TYPE IKKε ON RANTES TRANSCRIPTION A) 293 cells were transfected with the PGL2-220 RANTES promoter and the pcDNA3-IKKε K38A plasmid or the empty vector at different indicated concentrations, and infected with RSV. Cells were harvested 24 h post-infection to measure luciferase activity. Uninfected plates served as controls. For each plate luciferase was normalized to the β-galactosidase reporter activity. Data are expressed as mean ± standard deviation of normalized luciferase activity. B) 293 cells were transfected with the PGL2-220 RANTES promoter wild type (WT) or mutated in the ISRE (ΔISRE) or NF-κB (ΔNF-κB) site and the pcDNA3-IKKε wild type (WT) or the empty vector (EV). Cells were harvested 48 h later to measure luciferase activity. C) 293 cells were transiently transfected with multimers of the RANTES ISRE site and either the pcDNA3-IKKε K38A plasmid or a kinase-inactive (DN) IKKβ expression plasmid and infected with RSV. Cells were harvested 12 h post-infection to measure luciferase activity. Uninfected plates served as controls. For each plate luciferase was normalized to the β-galactosidase reporter activity. Data are expressed as mean ± standard deviation of normalized luciferase activity.

To further confirm that expression of the catalytically inactive IKKε affected RSV-induced RANTES promoter activation through the ISRE site, 293 cells were transiently transfected with a construct containing multiple copies of the isolated RANTES ISRE site linked to the luciferase reporter gene (12), and the IKKε K38A plasmid. Expression of IKKε K38A caused a significant inhibition, between 70 and 80%, of IRF-driven transcription (Figure 3.2C). This effect was specific to IKKε since expression of catalytically inactive (DN) IKKβ only modestly reduced RSV-induced ISRE activation (Figure 3.2C).

IKKε regulates RSV-induced RANTES gene expression and IRF-3 phosphorylation

To further investigate the role of IKKε in transcription factor activation and gene expression following RSV infection, we established 293 stable cell lines expressing K38A FLAG-tagged IKKε, under the control of a tetracycline-regulated promoter. As a control cell line, we used a clone containing the empty vector (EV) only. To induce IKKε expression, doxycycline (Dox) was added to the culture medium and IKKε protein level was monitored at different time points thereafter by Western blot using an anti-FLAG antibody. As shown in Figure 3.3, there was a time-dependent expression of IKKε, which was maximal at 48h following Dox treatment. To confirm the role of IKKε in RSV-induced RANTES gene expression we measured RANTES protein and mRNA induction following RSV infection of the K38A-expressing 293 cell line. Cells were treated with Dox for 48h, infected with RSV for 24h and harvested to measure RANTES protein by ELISA and RANTES mRNA by Northern blot (29). Expression of kinase-inactive IKKε significantly blocked viral-induced RANTES secretion (Figure 3.4A), as well as mRNA induction (Figure 3.4B), indicating a fundamental role of IKKε in the expression of this viral-induced chemokine.

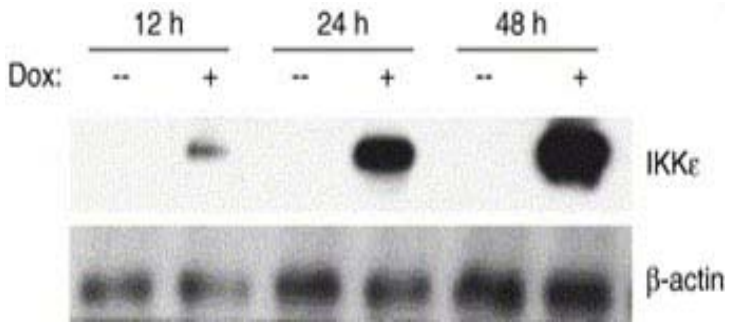

FIGURE 3.3 KINETICS OF CATALYTICALLY INACTIVE IKKε EXPRESSION IN 293 STABLE CELL LINE 293 stable cell lines IKKε K38A were treated with Dox for 12, 24 and 48h and harvested to prepare total cell lysates. Equal amounts of protein from uninfected and infected cells were assayed by Western blot for FLAG-IKKε expression. Membrane was stripped and reprobed for β-actin to control the equal loading of the samples.

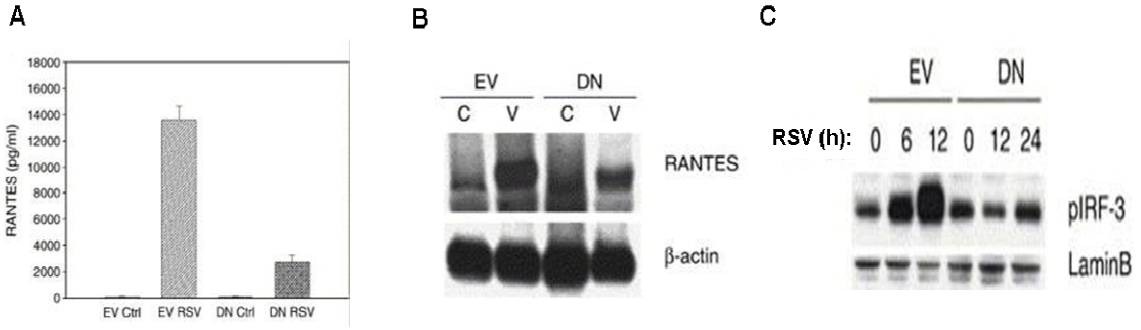

FIGURE 3.4 EXPRESSION OF CATALYTICALLY INACTIVE IKKε BLOCKS VIRAL-INDUCED RANTES EXPRESSION AND IRF-3 PHOSPHORYLATION. A) RANTES protein secretion. 293 control cell line (EV) and IKKε K38A cell line (DN) were treated with tetracycline for 48 h and then infected with RSV. Culture supernatants, from uninfected (Ctrl) and infected (RSV) cells, were assayed 24 h later for RANTES production by ELISA. Data are expressed as mean ± standard deviation of triplicate samples. B) RANTES mRNA induction. Total RNA was extracted from control (C) and 24h infected (V) cells. Twenty micrograms of RNA were fractionated on a 1.2% agarose-formaldehyde gel, transferred to nylon membrane and hybridized to a radiolabeled RANTES cDNA probe. Membrane was stripped and hybridized with a radiolabeled β-actin probe, to show equal loading of the samples. C) IRF-3 phosphorylation. Control and IKKε K38A 293 cell lines were infected with RSV for 6, 12 and 24h and harvested to prepare nuclear extracts. Equal amounts of protein from uninfected and infected cells were fractionated on a 10% SDS-PAGE, transferred to PVDF membrane and probed with anti Ser396 phospho-IRF-3 antibody. Membrane was stripped and reprobed for lamin b to control the equal loading of the samples.

Furthermore, to determine whether inhibition of IKKε activation would block RSV-induced IRF-3 activation, we measured phospho Ser396 IRF-3 formation in 293 cells expressing IKKε K38A. Nuclear extracts were prepared from control (EV) or IKKε K38A (DN) expressing 293 cells infected with RSV for various lengths of time and used for Western blot analysis of phospho Ser396 IRF-3. As shown in Figure 3.4C, expression of catalytic-inactive IKKε significantly blocked viral-induced IRF-3 phosphorylation, indicating that IKKε plays a fundamental role in RSV-induced IRF activation.

ROS regulate viral-induced IRF-3 activation

We have previously shown that RSV infected airway epithelial cells generate ROS and that antioxidant treatment with butylated hydroxyanisole (BHA), as well as a panel of chemically unrelated antioxidants, blocks RSV-induced signal transduction cascade leading to chemokine expression in vitro, through inhibition of transcription factors belonging to IRF and Signal Transducers and Activators of Transcription (STAT) families (29) and (83). BHA treatment blocks RSV-induced IRF-1 and -7 gene expression and inhibits IRF-3 nuclear translocation and DNA binding to the RANTES Interferon Stimulated Responsive Element (ISRE), an event that is absolutely required for RSV-stimulated RANTES gene transcription. To determine whether antioxidant treatment inhibits RSV-induced IRF-3 activation, we examined RSV-induced IRF-3 serine phosphorylation in A549 cells treated with 400μM BHA. A549 cells were infected with RSV in the presence or absence of BHA and harvested at 12 and 24h p.i. to extract nuclear proteins for Western blot analysis of phosphor Ser396 IRF-3. As shown in Figure 3.5A, antioxidant treatment completely blocked RSV-induced IRF-3 phosphorylation, indicating that it is redox-dependent.

Since IKKε plays a major role in RSV-induced IRF-3 activation, we examined IKKε gene expression and protein synthesis in A549 cells infected with RSV in the presence or absence of the antioxidant. As shown in Figure3.5B, RSV-induced IKKε gene expression was significantly inhibited by antioxidant treatment. Similar results were obtained when we examined IKKε protein synthesis, which was strongly induced by RSV infection and abolished by antioxidant treatment (Figure3.5C).

An important source of inducible intracellular ROS, generated in response to a variety of stimuli, is the membrane-bound NAD(P)H oxidase system (62). We have previously shown that treatment of A549 cells with DPI, a known NAD(P)H oxidase inhibitor, significantly blocked RSV-induced STAT activation (83). To test if RSV-induced IRF-3 activation was mediated through ROS production by this enzyme complex, A549 cells were treated with various NAD(P)H oxidase inhibitors, including DPI, apocyanin and AEBSF (94), and infected with RSV for 24h. We then assessed RSV-induced RANTES production and IRF-3 phosphorylation. As shown in Figure 3.6A, all three inhibitors significantly reduced RANTES secretion, as well as IRF-3 phosphorylation (Figure 3.6B). DPI almost completely abolished RSV-induced IKKε gene expression (Figure 3.6C), with a limited effect on viral replication (Figure 3.6D), indicating that the NAD(P)H oxidase system is important for the generation of ROS and subsequent activation of IRF-3 following RSV infection.

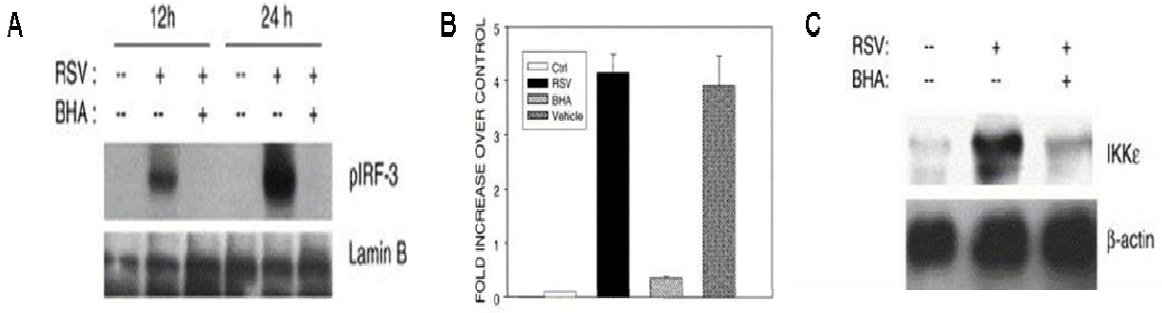

FIGURE 3.5 EFFECT OF ANTIOXIDANT TREATMENT ON RSV-INDUCED IRF-3 AND IKKε ACTIVATION. A) IRF-3 phosphorylation. Nuclear extracts were prepared from A549 cells control and infected with RSV for 12 and 24h, in the absence or presence of 400μM BHA, and assayed for Ser396 phosphorylation by Western blot. Membrane was stripped and reprobed for lamin b to control the equal loading of the samples. B) IKKε mRNA. A549 cells were infected with RSV for 24h, in the absence or presence of 400μM BHA. Total RNA was extracted from control and infected cells and used to amplify IKKε by Q-RT-PCR. C) IKKε protein levels. Total cell lysates, prepared from A549 cells control and infected with RSV for 24h, in the absence or presence of 400μM BHA, were resolved on 10% SDS-PAGE and Western blot was performed using an anti-IKKε antibody. Membrane was stripped and reprobed for β-actin.

DISCUSSION

The innate immune response represents a critical component of the host defense against viruses and is coordinated at the cellular level by activation of transcription factors that regulate the expression of inducible gene products with antiviral and/or inflammatory activity. RSV is the most common cause of epidemic respiratory infections in infants and young children and represents the prototype of mucosal-restricted viral pathogens with epithelial cell tropism and profound proinflammatory activity. RSV replication in airway epithelial cells results in the activation of multiple cellular signaling pathways involved in the expression of early response genes, which is coordinated by a small subset of transcription factors including NF-κB and IRF proteins (11,23,45,95).

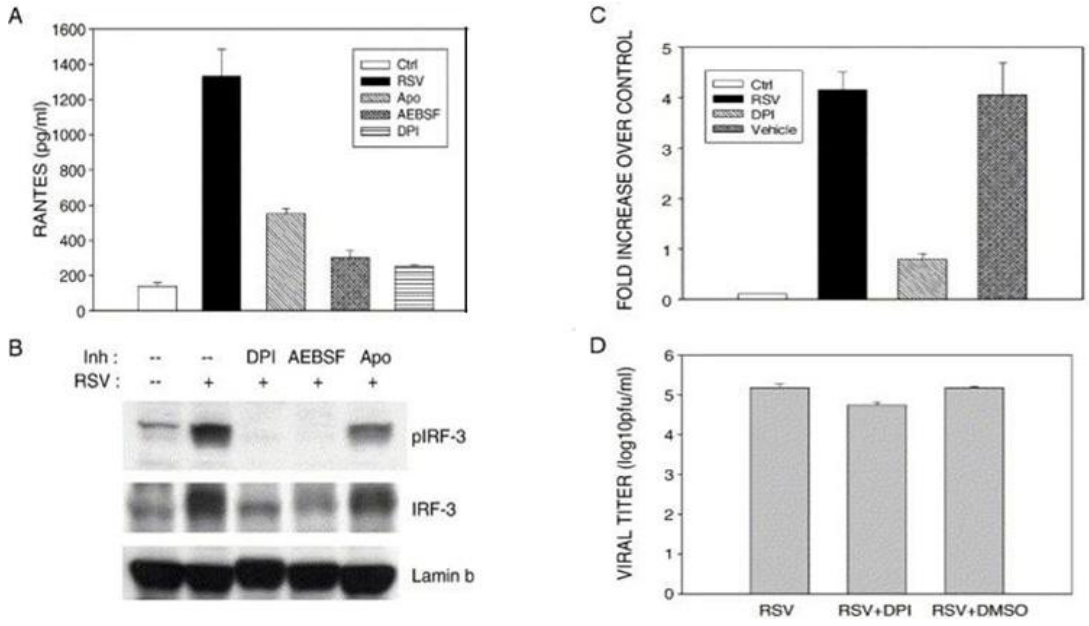

FIGURE 3.6 EFFECT OF NAD(P)H INHIBITION ON RSV-INDUCED IRF-3 AND IKKε ACTIVATION A) RANTES secretion. A549 cells were infected with RSV for 24h, in the absence or presence of either 10μM DPI, 500μM AEBSF or 500μM apocyanin (Apo). Culture supernatants were assayed 24h later for RANTES production by ELISA. Data are expressed as mean ± standard deviation of triplicate samples. B) IRF-3 phosphorylation. Nuclear extracts were prepared from A549 cells control and infected with RSV for 24h, in the absence or presence of either 10μM DPI, 500μM AEBSF or 500μM apocyanin (Apo) and assayed for Ser396 phosphorylation by Western blot. Membrane was stripped and reprobed for total IRF-3 and for lamin b to control the equal loading of the samples. Inh: inhibitor. C) IKKε mRNA. A549 cells were infected with RSV for 24h, in the absence or presence of 10μM DPI. Total RNA was extracted from control and infected cells and used to amplify IKKε by Q-RT-PCR. D) Viral replication. A549 cells were infected with RSV, in the absence or presence of 10μM DPI. Cell culture supernatants were harvested at 24h post-infection and viral load was determined by plaque assay.

Most of the signaling pathways leading to RSV-induced gene expression are still unknown. Free radicals and ROS have recently been shown to function as second messengers influencing a variety of molecular and biochemical processes, including expression of a number of genes (31). In earlier studies, we have shown that ROS play a major role in RSV-induced de novo IRF-1 and -7 genes expression and protein synthesis, by regulating STAT-1 and -3 activation (29,31). We have also shown that inhibition of

ROS production, by antioxidant treatment, blocks IRF-3 nuclear translocation and DNA binding to the RANTES ISRE site (29). However, the intracellular signaling events leading to RSV-induced IRF-3 activation and the mechanism of inhibition of IRF-3 induction by antioxidant treatment were not investigated. In this study, we show that RSV infection of airway epithelial cells induces activation of IKKε, a noncanonical IKK-like molecule, recently identified as an essential component of the virus activated kinase (VAK) complex responsible for IRF-3 activation. Expression of catalytically inactive IKKε significantly inhibits RSV-induced RANTES expression, by blocking RANTES promoter activation and ISRE-driven transcription, through the inhibition of IRF-3 phosphorylation, indicating a fundamental role of this kinase in the pathway leading to RSV-induced IRF-3 activation. We also show that RSV-induced ROS formation, occurring likely through the NAD(P)H oxidase system, is involved in RSV-induced IKKε activation, as indicated by the inhibition of IKKε expression and IRF-3 phosphorylation by antioxidant treatment, as suggested in the schematic model of Figure 3.7.

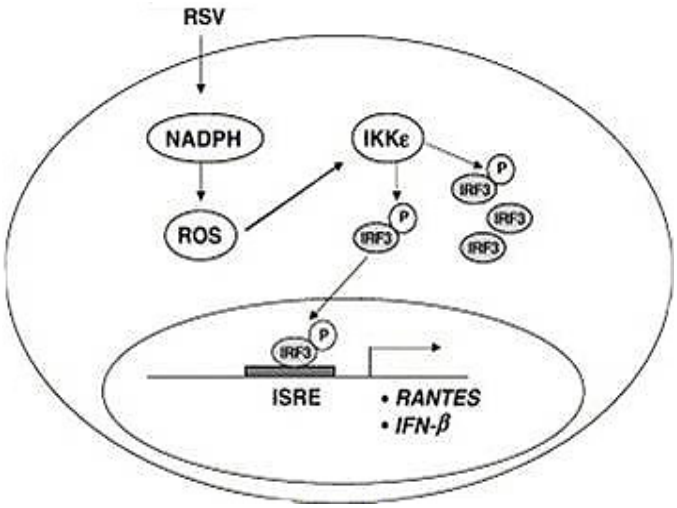

FIGURE 3.7 SCHEMATIC REPRESENTATION OF THE PROPOSED ROLE OF ROS IN VIRAL-INDUCED IKKε AND IRF-3 ACTIVATION Recent findings have revealed a fundamental role of IKKε, in the signaling pathway leading to IRF-3 activation (85,86,96,97) which has been shown to be important for double-stranded RNA and viral-induced IRF-3 phosphorylation and expression of IRF-3 dependent genes.

While TBK1 is constitutively and ubiquitously expressed, expression of IKKε can be induced, in a cell type-dependent manner (92). Splenocytes and thymocytes show constitutive expression of IKKε, while IKKε mRNA can be upregulated in macrophages and cells isolated from the synovia following cytokines, LPS or PMA stimulation (92) and (98). Here, we show that IKKε expression is inducible in airway epithelial cells infected with RSV. The only another report of IKKε induction following a viral infection, is in mouse embryonic fibroblasts infected with Vesicular Stomatitis Virus (VSV) (99). The mechanism(s) regulating IKKε gene expression is not known, however cytokines, LPS, PMA and viruses are all potent activators of NF-κB, therefore it is likely that this master transcriptional regulator plays an important role in IKKε induction. In support of this hypothesis is the lack of IKKε gene expression in LPS-stimulated MEFs which are deficient in the expression of IKKβ, the kinase that controls NF-κB activation following a variety of different stimuli, including viral infections (100-102).

In our study, the kinetics of IKKε kinase activity correlates with its expression. It has been previously shown that recombinant IKKε is phosphorylated during its expression and that this phosphorylation is necessary for kinase activity (92,103). Once the kinase is present, its enzymatic activity cannot be further stimulated by agonist treatment, suggesting that IKKε activity is likely regulated at the level of mRNA induction and not at the level of phosphorylation by stimuli-activated kinases (92,103).

Phosphorylation is a fundamental mechanism of IRF protein activation, necessary for nuclear translocation, dimerization, binding to DNA and activation of transcription (104). Upon viral infection, both IRF-3 and IRF-7 are phosphorylated within the C terminus of the protein (105). Although recent studies indicated that IRF-3 may also be a phosphorylation target following stimulation of cellular stress pathways or the engagement of TLR receptors like TRL3 and 4 (106), only Sendai Virus, Measles Virus,

Newcastle Disease Virus, VSV and RSV have been clearly shown to induce C-terminal phosphorylation of IRF-3 (29,104,107). Among the major viral-inducible phosphoacceptor sites present in the C-terminal portion of IRF-3, Ser396 has been shown to be the minimal phosphoacceptor site involved in IRF-3 activation following infection with Sendai virus and double-stranded RNA treatment (87). Using a novel phosphospecific antibody (87), we show that RSV infection induces Ser396 phosphorylation, which is completely abolished by the expression of catalytically inactive IKKε, indicating a fundamental role of this kinase in RSV-induced IRF-3 activation. The evidence that IKKε, following RSV infection, is able to phosphorylate a C-terminal IRF-3 peptide, containing the major viral-inducible phosphoacceptor sites, with a kinetics very similar to the kinetics of RSV-induced IRF-3 activation (29) strongly suggests that IKKε is a component of the virus-activated kinase complex required for IRF-3 phosphorylation following RSV infection. Since TBK1 has also been shown to play an important role in viral-induced IRF-3 activation, we are currently investigating the contribution of this kinase in IRF-3 activation following RSV infection.

In this study, we show that ROS formation plays a major role in the signaling pathway leading to viral-induced IRF-3 activation. Antioxidant treatment blocks IKKε expression and subsequent IRF-3 phosphorylation, following RSV infection, identifying this pathway as redox-sensitive. This is a novel observation, since it is the first time that viral-induced ROS production are shown to be involved in IKKε activation and subsequent IRF-3 phosphorylation. NF-κB could be the redox-sensitive target involved in IKKε gene transcription, since ROS have been shown to play an important role in NF-κB activation following various stimuli (108-109). Intracellular ROS can be generated by different systems, including the NAD(P)H oxidase system, the mitochondrial electron transport chain and enzymes like xanthine oxidase and cyclooxygenase. ROS play an

important role in the regulation of intracellular signaling cascades in various cell types including fibroblasts, endothelial cells, myocytes, smooth muscle cells, etc. (76). In our study, treatment of RSV-infected alveolar epithelial cells with a panel of inhibitors of the NAD(P)H complex significantly reduced RANTES production and IRF-3 activation. DPI also almost completely abolishes viral-induced IKKε gene expression. These data suggest that NAD(P)H oxidase is an important system for the generation of ROS and subsequent activation of IRF-3, following RSV infection. Since inhibitors may not be completely specific for NAD(P)H oxidase, current studies are in progress to better define the role of this complex in RSV-induced ROS formation and IRF-3 activation. However, the recent finding that Rac1, a small GTPase part of the NAD(P)H complex , is necessary for influenza virus-induced activation of IRF-3 and IRF-3-dependent genes (110), supports the role of NAD(P)H-generated ROS as fundamental mediators of the viral-induced signaling pathway leading to IRF-3 activation.

In summary, RSV-induced chemokine gene expression is controlled by numerous ROS-sensitive signaling molecules. This study indicates that viral-induced ROS formation, occurring likely through the NAD(P)H oxidase-generated system, is necessary for IRF-3 phosphorylation, through modulation of IKKε activation, and identifies a novel molecular target for the development of strategies aimed to modulate the inflammatory response associated with RSV infection of the lung.

CHAPTER 4: ANTIOXIDANT TREATMENT AMELIORATES RESPIRATORY SYNCYTIAL VIRUS–INDUCED DISEASE AND LUNG INFLAMMATION*

ABSTRACT

Respiratory syncytial virus (RSV) is a major cause of lower respiratory tract infection in children. No treatment has been shown to significantly improve the clinical outcome of patients with this infection. Recent evidence suggests that oxidative stress could play an important role in the pathogenesis of acute and chronic lung inflammatory diseases. It is not known whether RSV induces pulmonary oxidative stress and whether antioxidant treatment can modulate RSV-induced lung disease. Therefore, we tested the hypothesis that antioxidant administration could attenuate RSV-induced lung inflammation, clinical disease, and airway hyperreactivity (AHR). The BALB/c mouse model was infected with 10^7 plaque-forming units of RSV, in the presence or absence of orally administered butylated hydroxyanisole (BHA), an antioxidant. Malondialdehyde and 4-hydroxynonenal were measured in bronchoalveolar lavage (BAL) by colorimetric assay. Cytokines and chemokines were measured in BAL by Bio-Plex and leukotrienes were measured by enzyme-linked immunosorbent assay. AHR to methacholine challenge was measured by whole-body plethysmography. Our findings indicate that BHA treatment significantly attenuated RSV-induced lung oxidative stress, as indicated by the decrease of malondialdehyde and 4-hydroxynonenal content in BAL of RSV-infected mice. RSV-induced clinical illness and body weight loss were also reduced by BHA treatment, which inhibited neutrophil recruitment to the lung and significantly reduced

* "Reprinted from American Journal of Respiratory and Critical Care Medicine, Vol. 174, Pages No. 1361-1369 Guerrero-Plata A., Suarez-Real G., Adegboyega P. A., Colasurdo G. N., Khan A. M., Garofalo R. P., and Casola A., Antioxidant Treatment Ameliorates Respiratory Syncytial Virus–induced Disease and Lung Inflammation , Copyright (2006), with permission from the American Thoracic Society"

pulmonary cytokine and chemokine production after RSV infection. Similarly, antioxidant treatment attenuated RSV-induced AHR. Therefore, modulation of oxidative stress represents a potential novel pharmacologic approach to ameliorate RSV-induced acute lung inflammation and potentially prevent long-term consequences associated with RSV infection, such as bronchial asthma.

INTRODUCTION

Respiratory syncytial virus (RSV) is a major cause of respiratory tract infection in children worldwide and is the leading cause of virally induced bronchiolitis (80). Each year, approximately 100,000 children are hospitalized with RSV disease, with an estimated annual cost close to $300 million in the United States alone (2,111). There is no safe and efficacious vaccine for RSV, and immunity is incomplete, resulting in repeat attacks of acute illness throughout adulthood. The long-term consequences of RSV infection, which include increased airway resistance and recurrent wheezing (80), are associated risk factors for the development of asthma (7). Although the mechanisms of RSV-induced airway disease and the associated long-term consequences have yet to be clearly defined, the local inflammatory response is believed to play a fundamental role. Airway epithelial cells are the target of RSV infection, and they respond to the infection by producing a variety of mediators involved in lung immune/inflammatory responses, like cytokines, chemokines, and interferons, and by up-regulating adhesion molecules and major histocompatibility complex antigens on the cell surface (44).

Reactive oxygen species (ROS) are highly reactive molecules implicated in cellular damage. In the past few years, there has been increased recognition of their role as redox regulators of cellular signaling (31) and (46). We have previously shown that RSV-infected airway epithelial cells generate ROS and that antioxidant treatment with butylated hydroxyanisole (BHA), as well as a panel of chemically unrelated antioxidants,

blocks RSV-induced signal transduction cascades, leading to chemokine expression in vitro through inhibition of transcription factors belonging to interferon regulatory factor (IRF) and signal transducers and activators of transcription (STAT) families (29,83). Recent studies have indicated, directly or indirectly, an important role of ROS produced by epithelial and inflammatory cells in the pathogenesis of acute and chronic lung inflammatory diseases, such as acute respiratory distress, asthma, and chronic obstructive pulmonary disease (33,112-113). Surprisingly, little is known regarding the oxidative stress response in patients with virally induced lung inflammation. In an animal model of influenza infection, inhibition of oxygen radicals through administration of antioxidants or increased lung superoxide dismutase levels significantly reduced lung injury and improved the survival rate of infected animals, suggesting that oxidative stress can play a significant role in the pathogenesis of virally induced pneumonia (114-118). We have previously shown that RSV induces reactive nitrogen species and nitric oxide synthase (NOS) in the lungs of infected mice, and that inhibition of NOS expression significantly reduces RSV-induced lung inflammation (119). However, it is not known whether RSV infection induces significant lung oxidative stress damage and whether inhibiting ROS production by antioxidants modifies RSV-induced lung disease. Therefore, the aim of this study was to investigate the effect of antioxidant administration on RSV-induced lung inflammation, clinical disease, and airway hyperreactivity (AHR).

MATERIALS AND METHODS

RSV Preparation

The RSV A2 strain was grown in Hep-2 cells and purified by centrifugation on discontinuous sucrose gradients as described elsewhere (47). The virus titer of the purified RSV pools was 8 to 9 $\log_{10}$ plaque-forming units (PFU) per milliliter using a methylcellulose plaque assay. No contaminating cytokines were found in these sucrose-

purified viral preparations (48). LPS, assayed using the limulus hemocyanin agglutination assay, was not detected. Virus pools were aliquoted, quick-frozen on dry ice/alcohol, and stored at −70°C until used. Sucrose-purified extracts from uninfected Hep-2 cells were also generated under the same conditions.

Inoculation Procedure and Mice

Female BALB/c mice were purchased from Harlan and were housed in pathogen-free conditions, in accordance with the National Institutes of Health and UTMB institutional guidelines for animal care. Under light anesthesia, mice were inoculated intranasally with either sucrose-purified Hep-2 extracts (sham-infected) or sucrose-purified RSV at 1 x 10^7 PFU, diluted in sterile phosphate-buffered saline (PBS) for a total inoculation volume of 50µl, as previously described (28). BHA was prepared by dissolving the right amount of compound in a 100µl volume of corn oil, which was administered by gavage, once a day, without anesthesia. A total of four experimental groups consisting of two treatment groups, vehicle (corn oil) and BHA, for each infection group, sham and RSV, were used for all experiments. There was no effect of the vehicle alone; therefore, the groups sham + vehicle and RSV + vehicle are usually identified in the figures as sham and RSV. In AHR experiments, mice were infected with RSV at 1 x 10^5 PFU.

Clinical Illness

We used a well-established clinical illness grading scale for mice to establish the severity of infection (0 = healthy; 1 = barely ruffled fur; 2 = ruffled fur but active; 3 = ruffled fur and inactive; 4 = ruffled fur, inactive, and hunched; 5 = dead) (28). In addition, daily determination of body weight was used to monitor the progression of disease over the experimental period. These parameters have been shown to closely

correlate with lung pathology in experimental paramyxovirus infection of BALB/c mice (120). Visual differences were observed and captured by digital photography.

AHR

The effect of BHA on RSV-induced AHR was measured in mice using a whole-body plethysmograph (Buxco) as previously described (119;121). Measurement of airway responses was performed on individual, unrestrained, and nonanesthetized mice within a two-chamber plethysmograph. AHR was expressed as an enhanced pause (Penh). Penh, a dimensionless parameter used to measure pulmonary resistance, is calculated by changes in chamber pressure induced by methacholine challenge during inspiration and expiration. After a brief acclimatization to the chamber, the mice received an initial baseline challenge of saline followed by increasing doses of nebulized methacholine (3, 6, 12, 24, and 50 mg/ml). Recordings were taken for 3 min after each nebulization. The respiratory rate in breaths per minute was extrapolated from readings of every 10 breaths. The box pressure waveforms generated from the respiratory cycle were used to calculate peak expiratory pressure (PEP), peak inspiratory pressure (PIP), and the time of expiration. Penh was then calculated using the following formula: Penh = Pause x PEP/PIP. Penh values were averaged and reported as a percentage of baseline saline values.

Pulmonary Inflammation

Bronchoalveolar lavage (BAL) was obtained from the lungs of mice at various time points postinfection. In brief, anesthetized and tracheotomized mice were cannulated with a 1 ml syringe, and the lungs flushed three times with 1 ml of sterile, cold PBS. Total cellular influx and differential cell counts were measured in the BAL of all experimental groups. Total cell counts were determined by staining 50 µl of BAL with trypan blue and counting viable cells using a hemocytometer. For differentials, 100 µl of

BAL was used to generate cytospin preparations. Slides were dried, fixed, and stained with Protocol Hema3 (Fisher Diagnostics). A total of 300 cells were counted per sample using light microscopy.

Lung Pathology

Selected mice in each group were killed at various time points, and the entire lung was perfused, removed, and fixed in 10% buffered formalin and embedded in paraffin. Multiple 4 μm longitudinal cross-sections were stained with hematoxylin and eosin. The slides were analyzed and scored for cellular inflammation under light microscopy by a board-certified pathologist, as previously described (28). The pathology score reported includes the number of abnormal perivascular and peribronchial regions divided by the total number of perivascular and peribronchial regions and are reported as the percentage of inflamed tissue.

Effect of Antioxidants on Viral Replication

Lungs were excised on Days 3, 5, and 7 postinfection, snap-frozen in liquid nitrogen, and stored at –70°C. Viral titers were determined by plaque assay using confluent Hep-2 cells grown in 24 well plates, as previously described (122).

Lipid Peroxidation in BAL

BAL was centrifuged at 15,000 rpm for 1 min at 4°C. BHT was added to the supernatant to prevent further oxidation, and the samples were immediately frozen in liquid nitrogen. Measurement of lipid peroxidation markers malondialdehyde (MDA) and 4-hydroxynonenal (4-HNE) was carried out using a lipid peroxidation kit from Calbiochem. To detect MDA and 4-HNE, 200 μl of BAL was added to 650 μl of a 3:1 solution of N-methyl-2-phenylindole in acetonitrile:ferric ions in methanol and quickly vortexed. A total of 150 μl of methanesulfonic acid were added and incubated at 45°C for 1 h. The samples were cooled and measured at 586 nm using a spectrophometer.

Measurements of 8-isoprostane were performed using a competitive enzyme immunoassay from Cayman Chemical, according to the manufacturer's instructions.

Chemokine and Cytokine Protein Profile

To assess the production of chemokines and cytokines, BAL was obtained at 12, 24, 48, and 72 h postinfection. Samples were tested for multiple cytokines using the Bio-Plex Cytokine Mouse 18-Plex panel (Bio-Rad Laboratories), according to the manufacturer's instructions, as previously described (123). The panel includes the following cytokines: interleukin (IL)-1α, IL-1β, IL-2, IL-3, IL-4, IL-5, IL-6, IL-10, IL-12 (p40), IL-12 (p70), IL-17, granulocyte colony–stimulating factor, granulocyte-macrophage colony–stimulating factor, IFN-γ, KC, MIP-1α, MCP-1, RANTES, and tumor necrosis factor (TNF)-α. The broad assay range was from 0.2 to 5,000 pg/ml.

Cysteinyl Leukotriene Determination

BAL was used to measure leukotriene C4 (LTC_4) by a competitive ACE enzyme immunoassay (Cayman Chemical). The sensitivity of the assay was 7.8 pg/ml. The specificity of the assay for traditionally classified cysteinyl leukotrienes (cys-LTs) LTC_4 and LTC_5 was 100%. The cross-reactivities of the assay with LTC_4 metabolites are 48% with LTD_5, 46% with LTD_4, 28% with LTE_4, 7% with LTE_5, and 2% with LTE_4.

Statistical Analysis

Statistical analysis was performed with the biostatistics software program GraphPad Prism (GraphPad Software, Inc.). Comparisons between all experimental groups were done using a one way-analysis of variance (ANOVA) with Dunnett's multiple comparison test, to analyze body weight loss. Comparisons between two groups were done using an unpaired, two-tailed, student's t-test. Data are presented as mean ± SD unless otherwise stated. A p value <0.05 was considered significant and indicated by the symbol * in comparing RSV versus RSV + BHA.

RESULTS

RSV infection induces oxidative stress in the lung. Lipid peroxidation products, such as MDA, 4-HNE, and isoprostanes, are useful markers of pulmonary oxidative stress and by themselves have been shown to mimic all the pathophysiological features of asthma (bronchoconstriction, AHR, mucus hypersecretion, enhanced arachidonic acid cascade, increased synthesis of chemoattractants, epithelial damage, and microvascular leakage (124). To determine whether RSV infection induced oxidative damage of the lung, MDA and 4-HNE were measured in the BAL of RSV-infected mice at different times postinfection. As shown in Figure 4.1, RSV infection was associated with a significant increase of MDA and 4-HNE levels in BAL samples at all time points tested, when compared with sham mice, indicating that lung oxidative stress damage indeed occurs in RSV infection. MDA and 4-HNE values from the sham group did not change over time (data not shown).

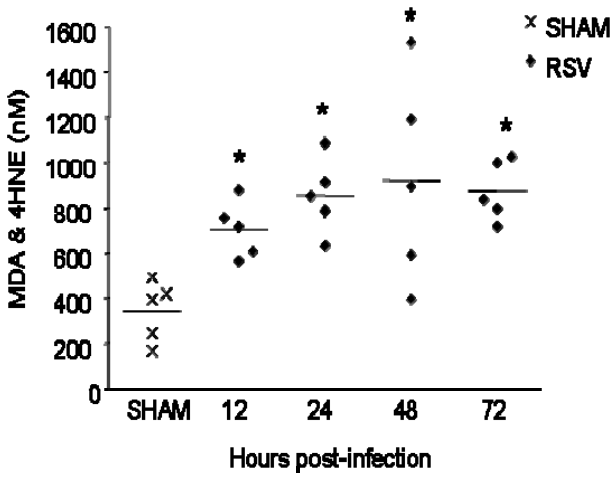

FIGURE 4.1 LIPID PEROXIDATION PRODUCTS IN THE BRONCHOALVEOLAR LAVAGE (BAL) Malondialdehyde (MDA) and 4-hydroxynonenal (4-HNE) were detected by a colorimetric assay in BAL of RSV (♦) and sham-infected (x) mice at various times postinfection. The *bar* in the scatter plot represents the mean of five different animals. The figure is representative of two different experiments. *$p<0.01$ relative to sham-infected mice.

BHA Attenuates RSV-induced Clinical Illness

To determine whether antioxidant administration was capable of altering RSV-induced disease, we initially assessed the effect of three different BHA treatment protocols on body weight loss. In protocol 1, animals were pretreated with various doses of BHA, ranging from 50 to 250 mg/kg, 3 d before and during the first 5 d of infection. As shown in Figure 4.2, mice inoculated with RSV alone progressively lost weight during the first 3 d of infection, with a peak of 15 to 20% loss at Day 3 postinfection. The 250 mg/kg dose of BHA consistently attenuated RSV-induced body weight loss, as the mice experienced a weight loss of 6% and regained their original body weight earlier. A statistically significant difference in body weight loss was also observed with the 150 mg/kg dose, whereas the 100 mg/kg had some effect only at Day 3 postinfection, which represents the peak of body weight loss. We then determined whether the 250 mg/kg dose was still effective if treatment was started the same day of RSV infection (protocol 2) or at 1 d postinfection (protocol 3). Protocol 3, or post-treatment with BHA, failed to attenuate RSV-induced body weight loss and was not further investigated (data not shown). There was no statistically significant difference in body weight loss between protocols 1 and 2 (data not shown); therefore, all subsequent experiments were performed using the dose of BHA 250 mg/kg given during the first 5 d of RSV infection.

A positive effect of antioxidant treatment was also observed on other clinical parameters of RSV infection that constitute the viral-induced illness score (see METHODS for details). Typically, the peak of illness severity coincides with the peak of RSV-induced body weight loss and occurs between Day 3 and 4 of infection (35). We observed a significant difference in appearance of BHA-treated versus untreated RSV-infected mice (Figure 4.3A), as well as in the total illness score, starting at Day 3

postinfection (Figure 4.3B), indicating that antioxidant treatment is effective in modulating RSV-induced clinical disease.

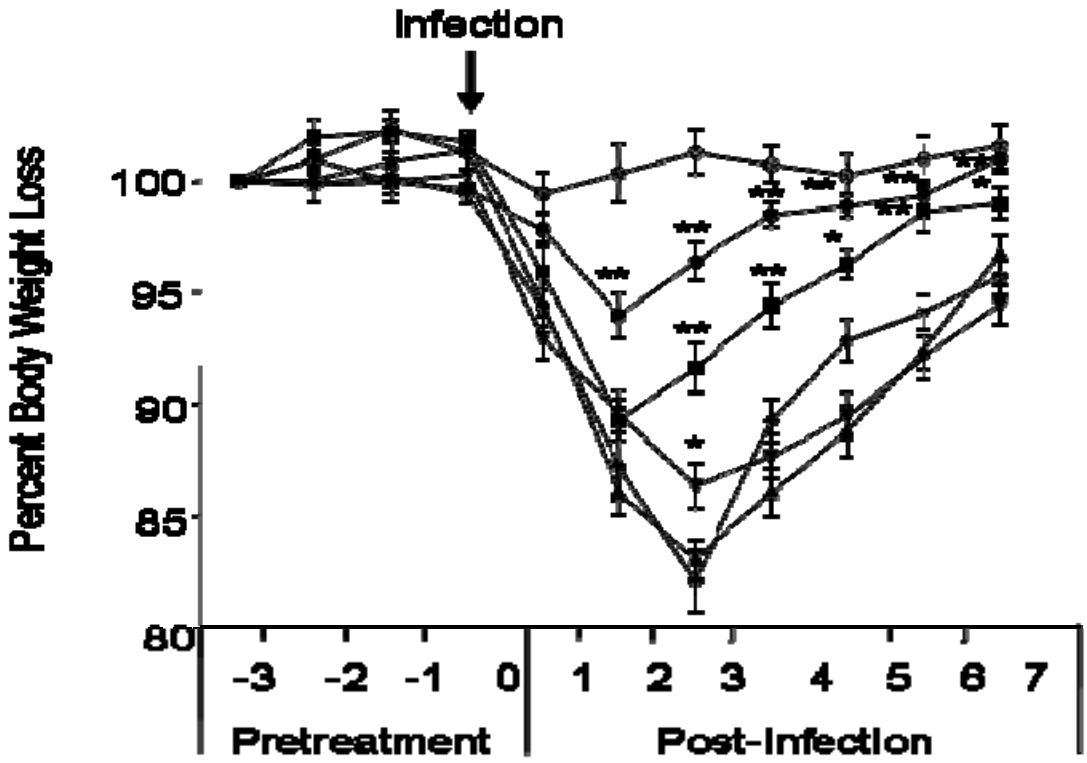

FIGURE 4.2 EFFECT OF BUTYLATED HYDROXYANISOLE (BHA) ADMINISTRATION ON RSV-INDUCED WEIGHT LOSS. Mice were treated with increasing concentrations of BHA for 3 d before RSV infection and during the first 7 d of infection. The following is a representative diagram of three different experiments. All data points represent the mean of at least four animals. *Open circles*, sham; *cross marks*, RSV; *triangles*, RSV + BHA 50 mg/kg; *inverted triangles*, RSV + BHA 100 mg/kg; *solid squares*, RSV + BHA 150 mg/kg; *solid circles*, RSV + BHA 250 mg/kg. *$p<0.05$ relative to sham-infected mice; **$p<0.01$ relative to sham-infected mice.

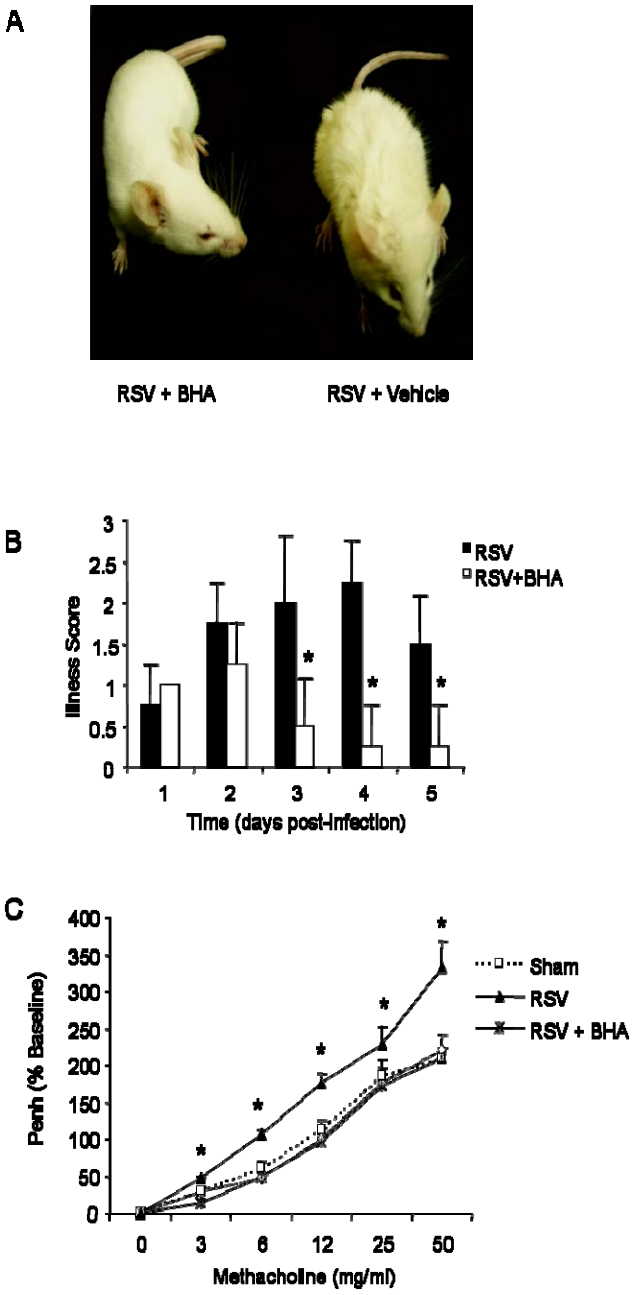

FIGURE 4.3 EFFECT OF BHA ON CLINICAL ILLNESS AND AIRWAY HYPERREACTIVITY (AHR). Mice were infected with RSV and treated with BHA 250 mg/kg for the following 7 d. A) Differences in the appearance of fur in RSV + BHA–versus RSV + vehicle–treated mice at Day 3 postinfection. B) Clinical illness scores of RSV + BHA (open squares) and RSV + vehicle (solid squares) were measured from Day 1 to Day 5 postinfection. Sham-infected mice treated with either vehicle or BHA received a healthy illness score = 0 throughout the course of the experiment (data not shown). Data are expressed as mean ± SD of five different animals and are representative of three different experiments. *$p<0.01$ relative to RSV-infected mice. C) The effect of BHA treatment on RSV-induced AHR during methacholine challenge was measured at Day 4 postinfection by whole-body plethysmography. All treatment groups were given an initial dose of saline and subsequently challenged with increasing concentrations of methacholine (mg/ml). Penh is reported as a percentage increase from baseline saline challenge. Data are expressed as mean ± SD of eight different animals. *Open squares*, sham; RSV, *solid triangles*; *cross marks*, RSV + BHA. *$p<0.01$ relative to RSV-infected mice.

We and others have previously shown that RSV infection induces AHR in response to methacholine challenge (119,121,125). As shown in Figure 4.3C, we observed a significant difference between RSV and RSV + BHA treated animals, because administration of BHA strongly attenuated RSV-induced AHR at all methacholine doses. BHA treatment did not alter baseline Penh values or airway response to methacholine in sham-infected animals.

Effect of BHA on RSV-induced Pulmonary Inflammation

To determine whether BHA altered RSV-induced lung inflammation, total and differential cell counts in the BAL were measured. We observed a significant attenuation of cellular influx by BHA treatment in RSV-infected mice, starting at Day 1 postinfection and continuing throughout the infection, with the most significant difference observed at Day 3 postinfection (Figure 4.4A), which, in our mouse model, corresponds to the peak of inflammatory cell recruitment in the BAL after RSV infection. Macrophages are the normal resident cell type found within the airways in uninfected mice. RSV infection induces a significant lung recruitment of neutrophils, which become the predominant inflammatory cell observed in the BAL in the first few days of infection (126). As shown in Figure 4.4B, BHA administration significantly blocked neutrophil recruitment into the airways, with little difference observed among the different experimental groups in lymphocyte and eosinophil populations.

To further examine the effect of BHA treatment on RSV-induced inflammation, lungs of infected mice were analyzed for histopathology. The perivascular and peribronchial mononuclear cell recruitment in the lung was examined at Days 3, 5, 7, and 9 postinfection. A dramatic decrease in lung inflammation between untreated and BHA-treated infected mice was observed as early as Day 3 postinfection, bringing the histopathology score of the treated RSV infected mice to levels similar to that of

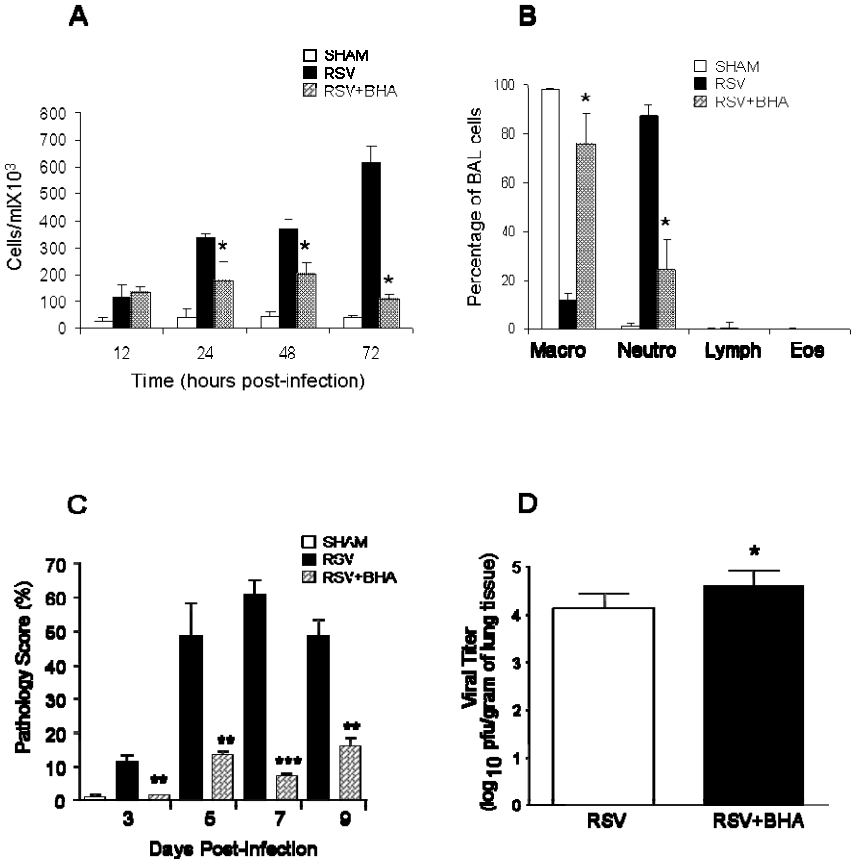

FIGURE 4.4 EFFECT OF BHA ON AIRWAY INFLAMMATION AND VIRAL REPLICATION A) Total number of cells was measured in BAL of sham and RSV-infected mice, either untreated or treated with BHA, at various times postinfection. Data are expressed as mean ± SD of five different animals and representative of three different experiments. *$p<0.01$ relative to RSV-infected mice. B) Differential cell count was measured in BAL of sham and RSV-infected mice, either untreated or treated with BHA, at Day 3 postinfection. *$p<0.01$ relative to RSV-infected mice. C) Mice were infected with RSV or sham-infected and treated with either vehicle or BHA. At various days postinfection, mice were killed and lungs were excised, fixed in 10% buffered formalin, and embedded in paraffin. Lung sections were stained with hemotoxylin and eosin, and peribronchial, perivascular inflammation was scored. Data are expressed as mean ± SD of four animals/group. Data shown are representative of three independent experiments. **$p<0.01$ relative to RSV-infected mice; ***$p<0.001$ relative to sham-infected mice. D) Mice were infected with RSV and either treated with vehicle or BHA. At Day 5 postinfection, lungs were excised and viral load was determined by plaque assay. Data shown are representative of three independent experiments (n = 10, mean ± SD). *$p<0.05$ relative to RSV-infected mice.

uninfected control animals, with a similar, although less striking, effect at Days 5, 7, and 9 postinfection, as shown in Figure 4.4C.

Because inflammatory cells, especially neutrophils, can play an important role against viral replication, at the early stage of infection (127), we examined whether BHA altered RSV replication. In our mouse model of RSV infection, increased viral titer can be detected as early as Day 3 postinfection, with peak viral titer occurring at Day 5 postinfection, and viral clearance by Day 7 postinfection (35). We found a consistent increase of approximately a half log in viral titer in BHA-treated animals at Days 4 and 5 postinfection, as shown in Figure 4.4D, where antioxidant administration increased peak viral load from 4.12 ± 0.31 to 4.59 ± 0.32 log10. RSV replication was usually no longer detectable at Day 7 postinfection in both untreated and BHA-treated infected mice, although occasionally we could recover virus at a very low titer (101) in the treated animals.

BHA Attenuates RSV-induced Oxidative Stress in the Lung

To determine whether antioxidant treatment affected RSV-induced oxidative damage of the lung, MDA and 4-HNE, as well as 8-isoprostanes, were measured in the BAL of RSV-infected mice, with or without BHA treatment. As shown in Figure 5, the average levels of MDA and 4-HNE were between 2 and 2.5 fold higher in RSV infected BAL samples in comparison to control mice at all time points of RSV infection. BHA administration clearly lowered RSV-induced lipid peroxidation to values equivalent to control at all time points. Similarly, RSV-induced 8-isoprostane production was significantly reduced at all time points tested.

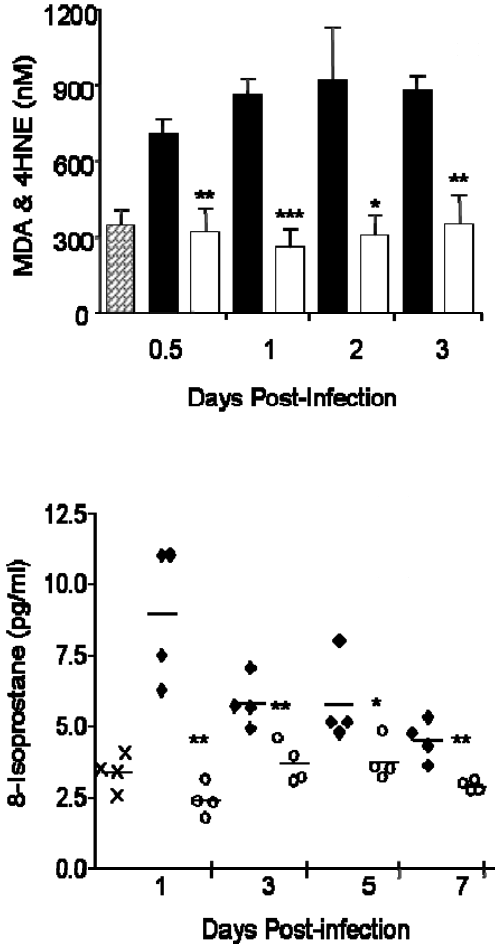

FIGURE 4.5 EFFECT OF BHA ON LIPID PEROXIDATION A) MDA and 4-HNE or B) 8-isoprostane were detected by either colorimetric assay or ELISA in BAL of mice infected with RSV and treated with either vehicle (solid bars) or BHA (open bars) at various times postinfection. Hatched bars, sham-treated mice. The bar in the scatter plot represents the mean of five different animals. x, sham; solid diamonds, RSV; open circles, RSV + BHA. Data shown are representative of two independent experiments. *$p<0.05$; **$p<0.01$; ***$p<0.001$ relative to RSV-infected mice.

Effect of BHA on Chemokine and Cytokine Induction

RSV infection is a potent inducer of chemokine production, and increased chemokine release has been shown to play an important role in RSV-induced lung inflammation and to correlate with disease severity (44). In our model, the peak of chemokine production occurs during the first 3 d of infection (123), after which chemokines are no longer measurable. To determine whether BHA treatment was able to modulate RSV-induced chemokine secretion, we analyzed chemokine levels in BAL samples collected during the first 3 d of infection. As shown in Figure 4.6, RANTES, KC, and MIP-1α were strongly up-regulated in the lungs of infected animals starting as early as 12 h postinfection. BHA treatment consistently reduced all three chemokine protein levels, especially at 48 and 72 h postinfection.

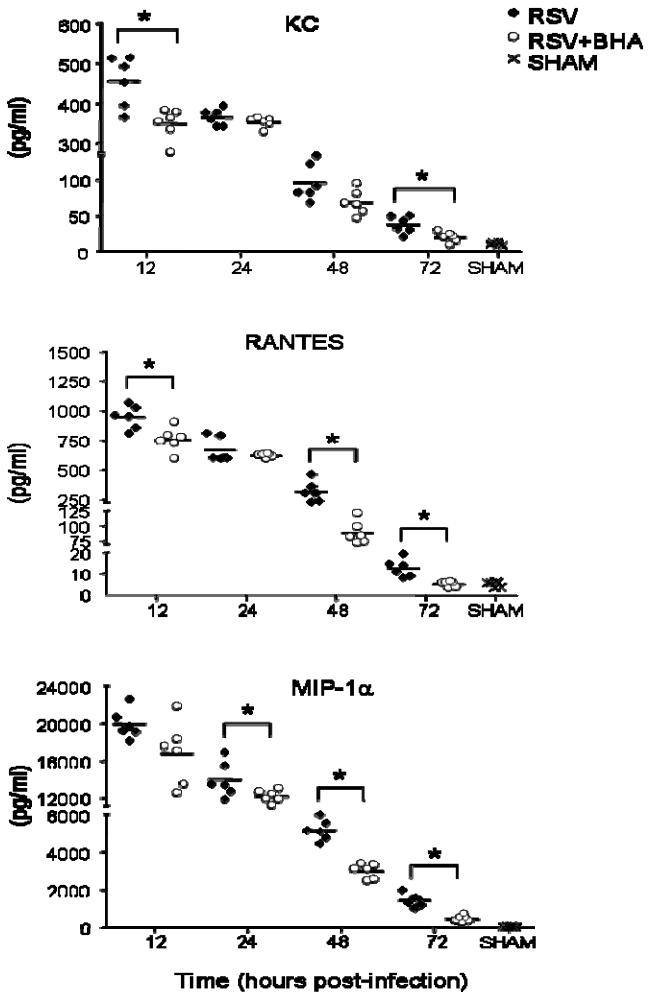

FIGURE 4.6 EFFECT OF BHA ON CHEMOKINE RELEASE IN THE BAL. Chemokine production was measured by Bio-Plex bead suspension array in the BAL of mice infected with RSV and treated with either vehicle or BHA at various times postinfection. The *bars* in the scatter plot represent the mean of six different animals. Data shown are representative of three independent experiments. *$p<0.01$ relative to RSV-infected mice.

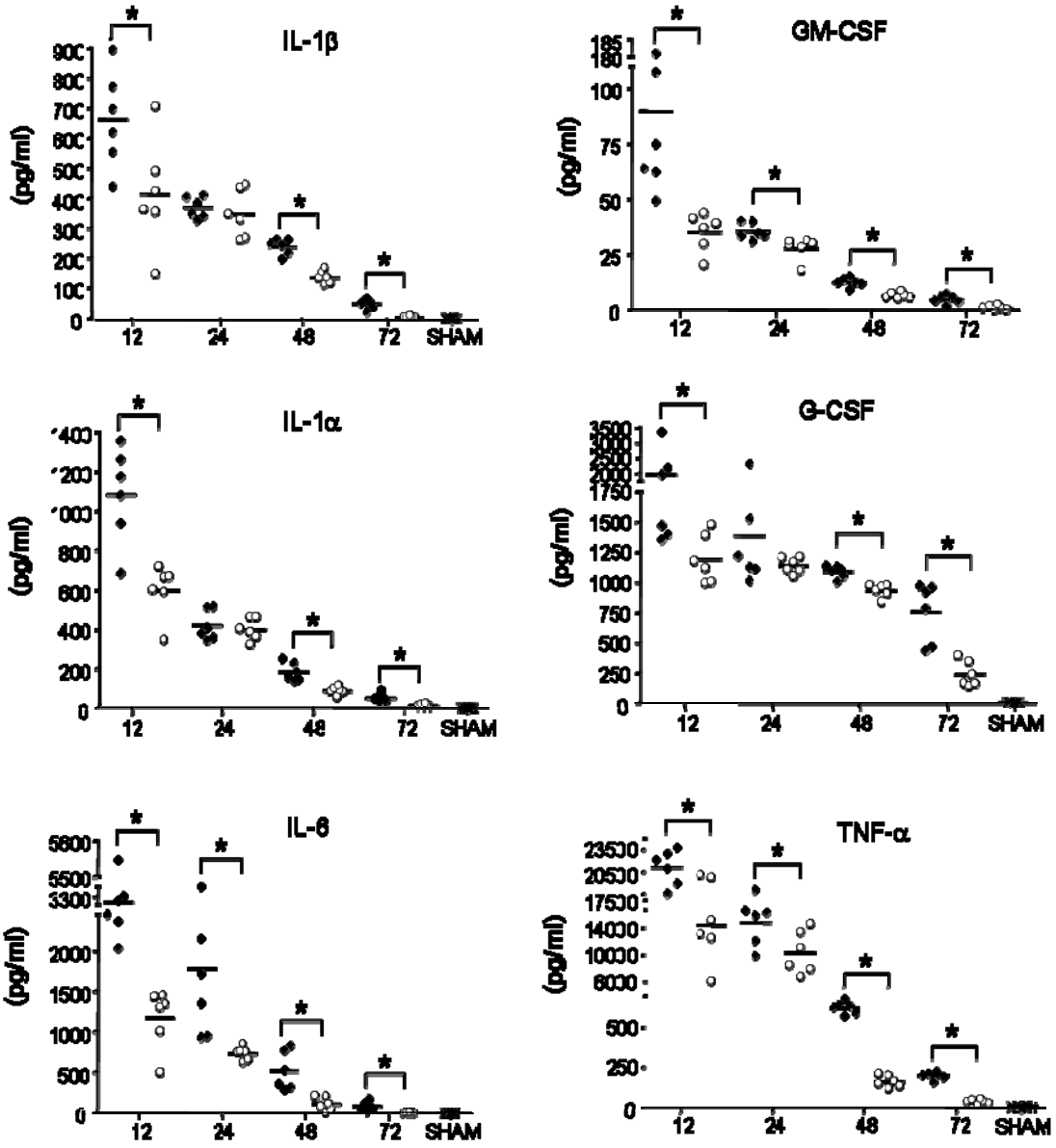

FIGURE 4.7 EFFECT OF BHA ON PROINFLAMMATORY CYTOKINES RELEASE IN BAL
Cytokine production was measured by Bio-Plex bead suspension array in the BAL of mice infected with RSV and treated with either vehicle or BHA at various times postinfection. The bars in the scatter plot represent the mean of six different animals. Data shown are representative of three independent experiments. x, sham; solid diamonds, RSV; open circles, RSV + BHA.*$p < 0.01$ relative to RSV-infected mice.

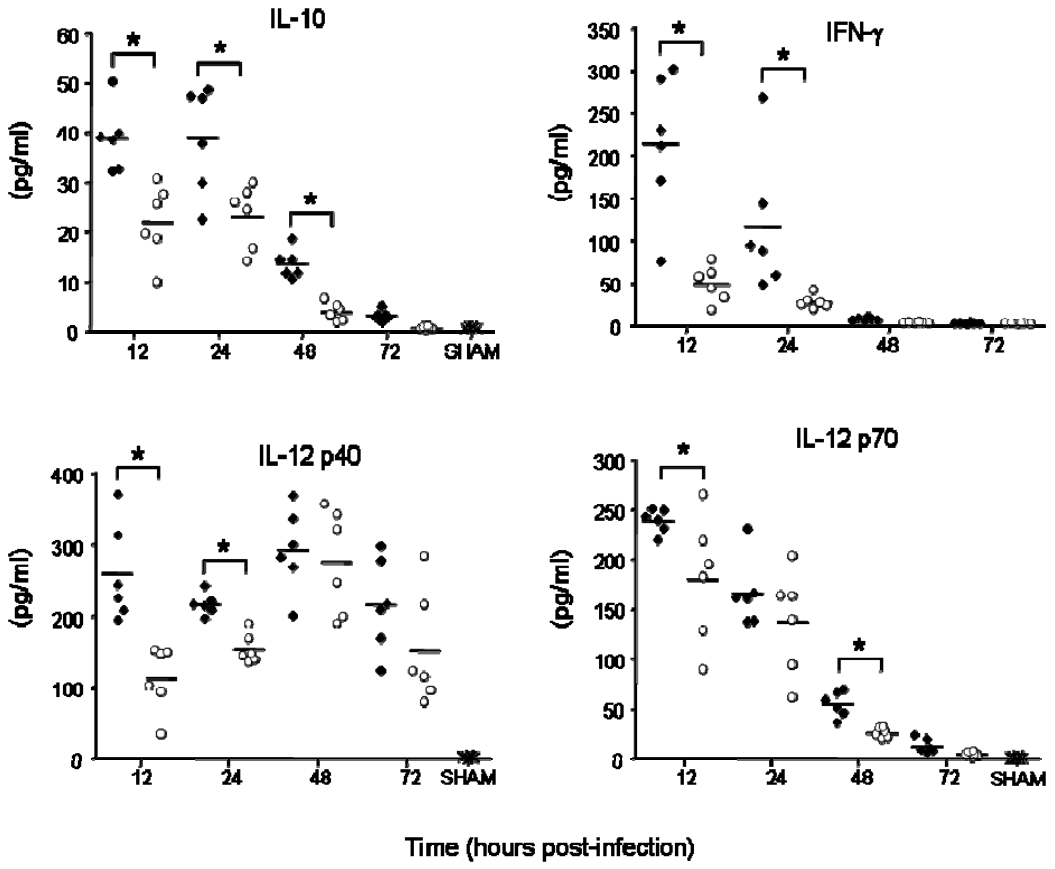

FIGURE 4.8 EFFECT OF BHA ON IMMUNOMODULATORY CYTOKINES IN BAL Cytokine production was measured by Bio-Plex bead suspension array in the BAL of mice infected with RSV and treated with either vehicle or control at various times postinfection. The bars in the scatter plot represent the mean of six different animals. Data shown are representative of three independent experiments. x, sham; solid diamonds, RSV; open circles, RSV + BHA. *$p < 0.01$ relative to RSV-infected mice.

Proinflammatory cytokines, such as IL-1, IL-6, and TNF, as well as immuno-modulatory cytokines, such as IL-10, IL-12, and IFN-γ, have been implicated in the pathogenesis of RSV-induced lung disease (44,128). As with chemokine secretion, significant cytokine production after RSV infection can be measured mainly during the first 3 d of infection, with the exception of IL-12 and IFN-γ (123). Similar to what we observed for chemokine production, BHA treatment effectively reduced the secretion of

all tested RSV-induced cytokines at Days 1, 2, and 3 postinfection (Figures 4.7 and 4.8). IFN-γ secretion was also significantly reduced at later time points (Day 5: RSV, 128.7 ± 63.3, vs. RSV + BHA, 22.1 ± 5.3 pg/ml; Day 7: RSV, 294.8 ± 69, vs. RSV + BHA, 5.8 ± 1.7), indicating that antioxidant treatment exerts a general anti-inflammatory activity in the context of RSV infection of the lung.

Effect of BHA on RSV-induced LT Production

Cys-LTs, which include LTC_4, LTD_4, and LTE_4, are important mediators of airway inflammation and bronchoconstriction (129). They have been shown to increase in the respiratory secretion of children infected with RSV (130) and are associated with RSV-induced wheezing (131). We and others have shown that inhibition of LT synthesis (132) or treatment with LT receptor antagonist (133) inhibits lung inflammation and AHR in a mouse model of RSV infection. To determine whether the antioxidant BHA had an effect on RSV-induced cys-LT release, LTC_4 was measured in BAL at various times postinfection. As shown in Figure 4.9, BHA-treated mice had significantly lower levels of LTC_4, which was particularly evident at Days 3 and 5 postinfection.

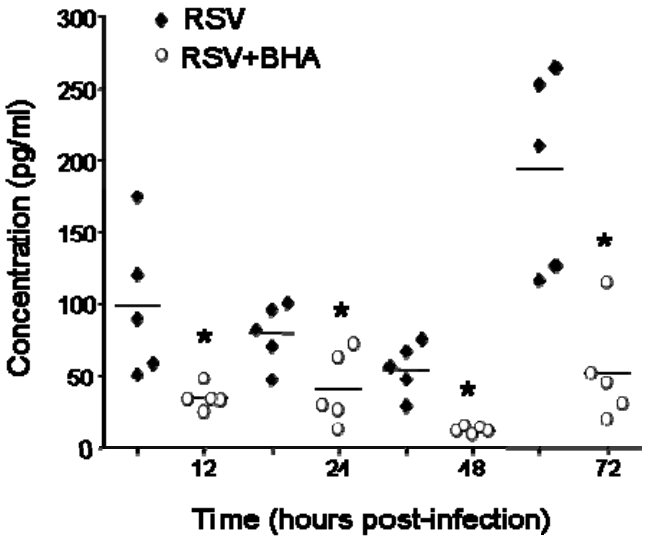

FIGURE 4.9 EFFECT OF BHA ON RSV-INDUCED LEUKOTRIENE RELEASE Leukotriene C_4 production was measured by ELISA in BAL of RSV-infected mice treated with either vehicle or BHA at various time points after infection. The *bars* in the scatter plot represent the mean of five different animals. Data shown are representative of three independent experiments. *$p<0.05$; **$p<0.01$; ***$p<0.001$ relative to RSV-infected mice.

DISCUSSION

Oxidative stress has been implicated in the pathogenesis of several acute and chronic airway diseases, such as asthma and chronic obstructive pulmonary disease (134). ROS generation, due to the respiratory burst of activated phagocytic cells recruited to the airways during viral infections, is an important antiviral defense, necessary for viral clearance. However, a robust production of ROS can lead to depletion of antioxidants and cause oxidative stress. Surprisingly, little is known regarding the role of ROS in respiratory virus–induced lung diseases, with the exception of influenza. It was not known whether modulation of ROS production with antioxidants would be of clinical benefit in the contest of RSV infection, for which no effective therapeutic treatment is currently available. In this study, we took advantage of an in vivo model of RSV infection to test the effect of antioxidant treatment on RSV-induced lung disease. We show for the first time that RSV infection induces lung oxidative stress, as evidenced by increase in the lipid peroxidation products. This is an important finding, because this information was available only for a mouse model of influenza infection (116). Remarkably, there are no studies investigating lipid peroxidation products in children or adults infected with respiratory viruses. These biomarkers of oxidative stress have been shown to be elevated in plasma and breath condensate of patients, both children and adults, with various acute and chronic inflammatory lung diseases, and to correlate with severity of illness in certain disease conditions (135). In our study, antioxidant treatment with BHA significantly decreased the content of MDA and 4-HNE in BAL of RSV-infected mice and ameliorated both body weight loss and clinical illness, indicating that modulation of oxidative stress in the context of RSV infection can lead to improvement in lung disease. It is important to note that these findings were reproduced by the use of another antioxidant agent, dimethyl sulfoxide (DMSO). Oral administration of DMSO at

the time of infection significantly reduced RSV-induced body weight loss and clinical disease (data not shown). However, given the systemic toxicity of DMSO, we did not use it for further experiments.

Although it is difficult to determine the precise mechanisms by which antioxidants provided protection in the context of RSV infection, attenuation of inflammation is likely a key one. We and others have shown that RSV-induced chemokine and cytokine release and subsequent pulmonary inflammation play a fundamental role in the pathogenesis of RSV-induced disease (44,136,137). Lack of production of specific chemokines, such as MIP-1α (28), or modulation of chemokine secretion, for example by perflubron treatment (122), has been shown to significantly reduce RSV-induced pulmonary inflammation. BHA treatment significantly reduced pulmonary cytokine and chemokine production after RSV infection, resulting in inhibition of lung recruitment of inflammatory cells, especially neutrophils, which are the major cell type responsible for oxidative burst in response to infectious stimuli. BHA treatment was effective if given before or at the moment of RSV infection, but did not result in significant improvement of clinical disease administered 1 d after infection, when clinical disease and lung inflammation are already present. This finding suggests that early therapeutic intervention may be necessary to improve clinical outcome in RSV infection. In fact, treatment of children with RSV-induced lower respiratory tract infection with anti-inflammatory drugs, such as steroids, has been shown to be mostly ineffective in improving clinical disease, as these drugs are usually administered when children are hospitalized, days after manifestation of initial symptoms (138).

Although BHA administration slightly increased RSV replication in the lung, there is no documented correlation between RSV viral titer and severity of illness. Antiviral treatment with ribavirin alone or immunotherapy with specific immunoglobulin

does not provide significant clinical improvement, indicating that RSV-induced lung disease is most likely the result of the inflammatory response more than a direct viral cytopathic (139). On the other hand, inhibition of NO production, which is antiviral against RSV in vitro and in vivo (119,140), significantly reduces pulmonary inflammation and airway hyper-responsiveness, although it increases viral replication (119), suggesting again that modulation of inflammation is fundamental to controlling RSV disease.

RSV infection early in life has been associated with AHR and recurrent wheezing, and possibly long-term pulmonary abnormalities (7,141-142). In the mouse model of RSV infection, whole-body plethysmography has been used to measure airway resistance, and we have found that AHR to inhaled methacholine correlates with pulmonary resistance when measured with more invasive techniques (119,133,143). In our study, we found that antioxidant treatment attenuated RSV-induced AHR, possibly due to a reduction in cys-LT production. Cys-LTs are potent bronchoconstrictors, as well as proinflammatory mediators, and their role in the pathogenesis of airway inflammation and obstruction has been recently recognized as a new target for therapeutic intervention (129). They have been shown to increase in the respiratory secretion of children infected with RSV (130,144) and are associated with RSV-induced wheezing (131). In a mouse model of RSV infection, increased levels of cys-LTs correlate with increased airway responsiveness (132), and either inhibition of LT production (132) or treatment with LT receptor antagonist (133) inhibits AHR. In children, treatment with a cys-LT receptor antagonist decreased exacerbations of reactive airway disease after RSV bronchiolitis (145). In our study, BHA administration significantly decreased LTC_4 secretion, with parallel reduction of AHR after methacholine challenge, suggesting a causal relationship

of the two phenomena, although we cannot exclude that inhibition of other important mediators could be responsible for AHR reduction after BHA treatment.

Although little information is available regarding respiratory infections, there is a body of literature showing that antioxidants can afford protection against virally induced morbidity and mortality and are important in host immune responses (146-147). For example, butylated hydroxytoluene, an analog of BHA, provided increased survival of chickens infected with Newcastle disease virus (148). In conclusion, the ability of antioxidants to attenuate symptoms and pathology in RSV infection warrants further investigation of these agents as a novel therapeutic approach to virally induced pulmonary disease.

CHAPTER 5: ANTIOXIDANT AND ANTIVIRAL COMBINATION THERAPY AMELIORATES RESPIRATORY SYNCYTIAL VIRUS-INDUCED LUNG DISEASE

ABSTRACT

Respiratory syncytial virus (RSV) is a potent inducer of pulmonary inflammation and oxidative stress in the lung. In a mouse model of acute RSV infection, treatment with the antioxidant butylated hydroxyanisol (BHA) significantly ameliorates clinical illness, proinflammatory mediator induction and pulmonary inflammation. However, this amelioration of lung disease is accompanied by an increased viral yield. In this study, we treated RSV-infected mice with a combination therapy of BHA and interferon alpha (IFN-α). The combined therapy of antioxidant and antiviral agents protected against RSV-induced pathology and reduced lung viral replication, thus representing a more efficient treatment for acute RSV infection.

INTRODUCTION

RSV is the most common cause of viral lower respiratory tract infections leading to severe bronchiolitis and pneumonia in infants and children worldwide (149). An effective vaccine for RSV is not yet available, therefore various alternative treatment options are being currently investigated (150). We have recently reported that antioxidant administration was able to attenuate RSV-induced lung inflammation, pathology, and severity of clinical disease in mice. However, the antioxidant treatment concurrently increased RSV viral replication in the lung (151). In contrast, we have also reported that direct nasal administration of IFN-α before or after infection decreased viral replication in RSV-infected mice (35). Therefore, our goal for this study was to test the therapeutic advantage of combination therapy with an antioxidant and antiviral agent in ameliorating

RSV-induced clinical disease and inflammation, using a well established experimental mouse model of RSV infection. However, there are no reports about the efficacy of antioxidant and antiviral combination therapy for acute RSV infection.

MATERIALS AND METHODS

Virus

RSV A2 was grown in HEp-2 cells (American Type Culture Collection, Manassas, VA) and purified by polyethylene glycol precipitation and sucrose gradient centrifugation as previously described (47,93).

RSV inoculation and treatment protocol

Female BALB/c mice were purchased from Harlan (Houston, TX) and were housed in pathogen-free conditions in the animal research facility at the University of Texas Medical Branch (UTMB), Galveston, Texas. All animal care and treatment was in accordance with the National Institutes of Health and UTMB institutional guidelines for animal care. Mice were treated with the antioxidant BHA (250 mg/kg) or control solvent corn oil in a total volume of 100μl by gavage daily throughout the duration of the experiment. After a two day pretreatment with BHA mice were lightly anesthetized and intranasally (i.n.) inoculated with 10^7 PFU of RSV diluted in PBS to a total volume of 50 μl or sham infected with PBS (28). On day 2 RSV post-infection (p.i), mice were i.n. treated with 10^4 IU of murine recombinant interferon alpha (IFN-α) (PBL Biomedical Laboratories) or 50 μl of vehicle control (Minimum essential medium plus 2% of fetal bovine serum). For all endpoints tested there were no measured effects with the vehicle and sham infected experimental group (data not shown).

Viral titration

Lungs were excised on day 5 p.i., snap frozen in liquid nitrogen, and stored at -70^{o}C. Serial dilutions of lung homogenates were subjected to the methylcellulose plaque assay to determine viral titer as previously described (152).

Pulmonary histophathology

On day 7 p.i, lungs were flushed with phosphate buffered saline, perfused and fixed with 10% buffered formalin, removed, and embedded in paraffin. Multiple 4 μm-thick sections were stained with hematoxylin and eosin. Slides were analyzed and scored for cellular inflammation under light microscopy by a board certified pathologist as previously described (28,153). Briefly, inflammatory infiltrates were scored by enumerating the layers of inflammatory cells surrounding the vessels and bronchioles. Finding zero to three layers of inflammatory cells was considered normal. Moderate to abundant infiltrate consisting of 50% or more of the circumference of the vessel or bronchioles was considered abnormal. The pathology score reported includes the number of abnormal perivascular and peribronchial regions divided by the total number of perivascular and peribronchial regions and are reported as the percentage of inflamed tissue.

Disease Severity

Illness score and body weight were measured to monitor the progression of disease. We used a well-established clinical illness grading scale to establish the severity of infection. Mice were scored daily by two investigators (0 = healthy; 1 = barely ruffled fur; 2 = ruffled fur but active; 3 = ruffled fur and inactive; 4 = ruffled fur, inactive, and hunched; 5 = dead) (28). Daily determination of body weight was used to monitor the progression of disease over the experimental period. These parameters have been shown

to closely correlate with lung pathology in experimental paramyxovirus infection of BALB/c mice (120).

Statistical Analysis

Statistical analysis was performed with the biostatistics software program GraphPad Prism (GraphPad Software, Inc.). Comparisons between all experimental groups were done using a one way-analysis of variance (ANOVA) with Dunnett's multiple comparison test. Comparisons between two groups were done using an unpaired student's t-test. Data are presented as mean ± standard error of the mean (SEM). A p value <0.05 was considered significant. The symbol * is used in comparing RSV versus RSV + Treatment Group. The symbol # is used to denote significance between RSV-infected Treatment Groups.

RESULTS

Antioxidant and antiviral treatments in RSV-infected mice were previously developed in our laboratory as separate protocols (35,151). Figure 5.1A illustrates the experimental design used to investigate the combined effects of BHA and IFN-α on clinical illness, lung disease, and viral load. Body weight loss and clinical illness score were evaluated daily, as shown in Figure 5.1B and 5.1C. Combination therapy protected against RSV-induced body weight loss, although to a lesser degree than BHA treatment, while p.i. treatment with IFN-α failed to attenuate RSV-induced weight loss (data not shown). Combination therapy also reduced the severity of RSV-induced illness as early as day 2 p.i. as opposed to isolated treatment with BHA, which did not reduce RSV-illness until day 3 p.i. or IFN-α which displayed little or no benefit at all timepoints measured (data not shown). To further examine the effect of the combination treatment on RSV-induced pulmonary inflammation, the lungs of infected mice were collected at day 7 p.i. to evaluate the pathology score, an index of pulmonary inflammation assessed

by perivascular and peribronchial mononuclear cell recruitment to the lung. In mice given the combination therapy, we observed a decrease in RSV-lung inflammation slightly lower than the administration of BHA alone (Figure 5.1D). There was no marked difference among the different treatment groups in comparison to RSV+BHA.

We evaluated effect of combined therapy on viral replication in RSV infected mice at 5 days p.i. since this time corresponds to the peak of RSV viral titer in the mouse model of RSV infection used for this study.

RSV viral load in the lung is shown in logarithmic scale (Figure 5.2A) and percentage of RSV viral yield (Figure 5.2B), which conveys a more visual depiction of the effects of BHA and combination therapy. Consistent with our previous study (151), administration of BHA to RSV-infected mice resulted in a greater than 3 fold increase lung viral replication. As previously reported by (35), treatment with IFN-α significantly reduced RSV viral load, with no significant differences measured in viral load between IFN-α versus BHA+IFN-α treatment groups (data not shown). However, combination treatment produced a 2 fold reduction of viral replication compared to untreated mice, and led to striking 6 fold reduction in comparison to BHA treated mice.

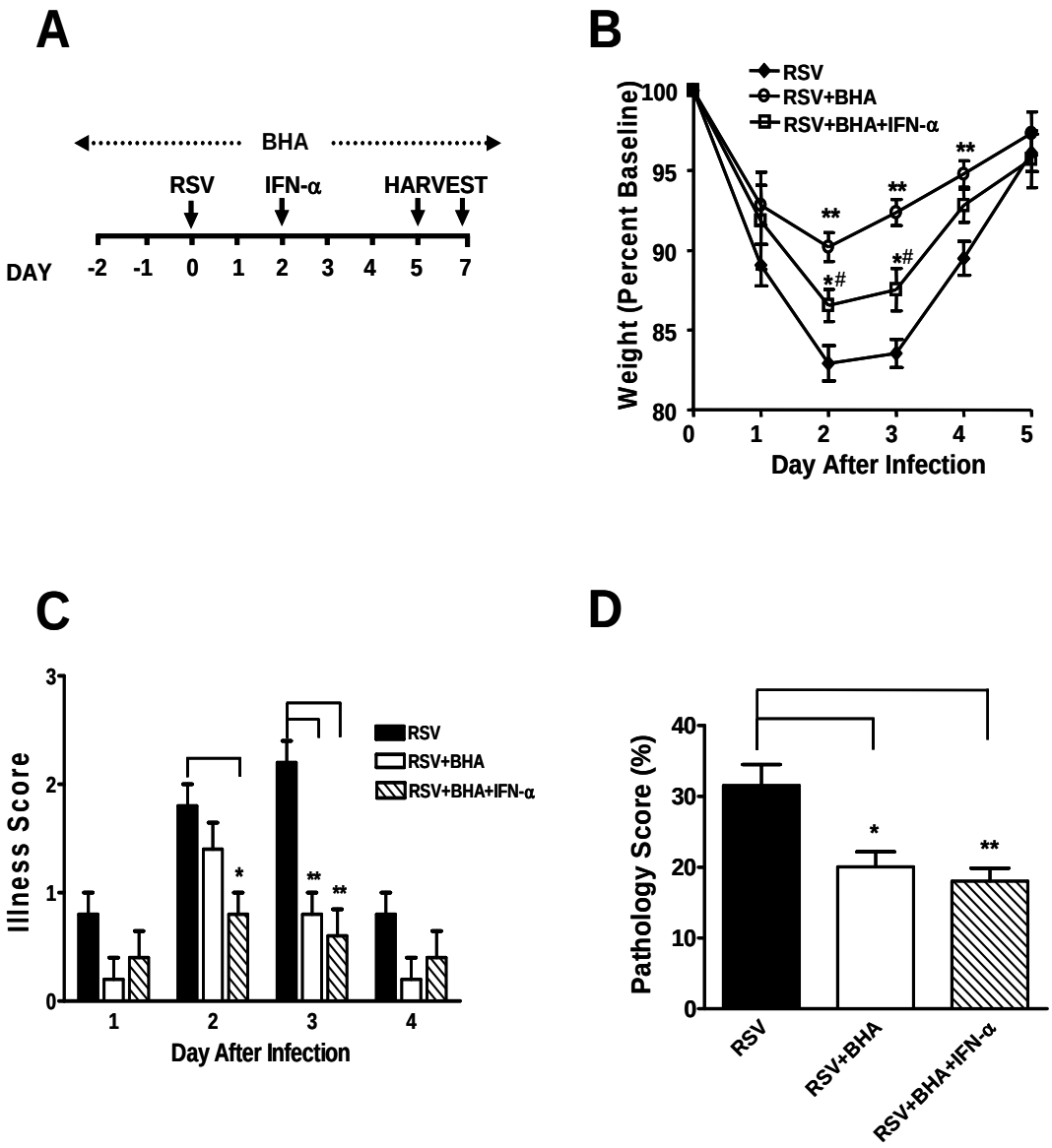

FIGURE 5.1 EFFECT OF COMBINATION THERAPY ON RSV INDUCED ILLNESS AND INFLAMMATION A. Experimental design for antioxidant administration and IFN-α treatment in the context of RSV infection. Effects of combination treatment on RSV-induced B. body weight and C. illness score and D. airway inflammation. N=5, mean±SEM *p<0.05, **p<0.01.

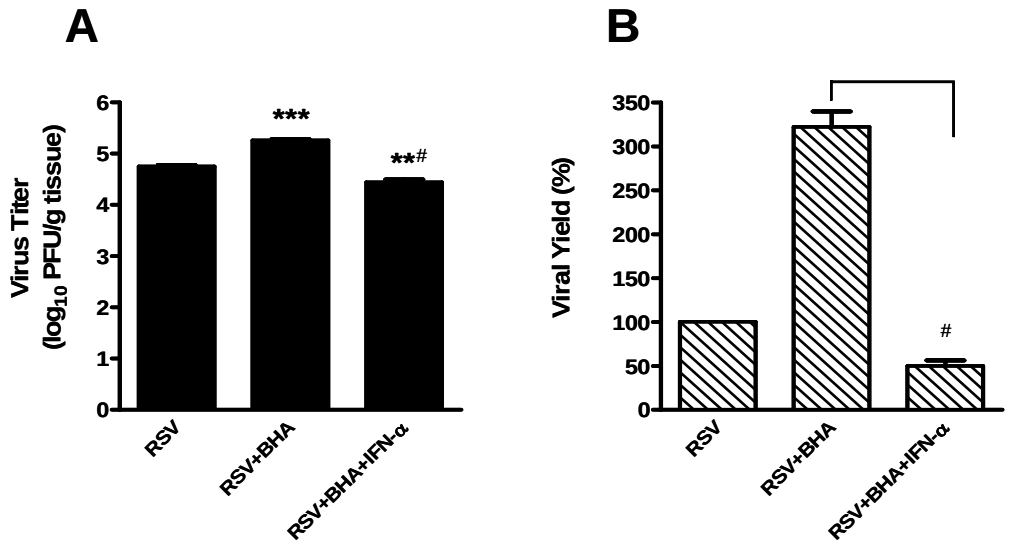

FIGURE 5.2 EFFECT OF COMBINATION TREATMENT ON VIRAL REPLICATION A. Lung viral titer following antiviral and antioxidant treatment at day 5 p.i. B. Virus yield is expressed as percentage of RSV and calculated as [(RSV + Treatment viral titer)/ (RSV viral titer)] X 100. * represents comparisons with RSV as reference group, # represents comparison between RSV+BHA vs. RSV+BHA+IFN-α **p<0.01, ***p<0.001, #p<0.001, N=5, mean ± SEM.

DISCUSSION

There are currently no reports about the efficacy of antioxidant and antiviral combination therapy for acute RSV infection. Therefore, our observations in this study provide the first documentation of ameliorating the symptoms associated with the onset of RSV infection by combination therapy with the antioxidant BHA and an antiviral IFN-α, specifically reducing of RSV-induced body weight loss, illness score, and pulmonary inflammation as well as diminished viral load.

The use of combination therapy with BHA and IFN-α mirrored findings reported during combination treatment with triamcinolone acetonide (TA), a potent anti-inflammatory glucocorticoids and the antiviral Synagis (154). Similar to treatment with BHA alone TA resulted in a profound decrease in RSV-induced inflammatory infiltrates in the lung (151) and delay in viral clearance (154). While combination therapy with TA

and Synagis decreased both RSV-induced lung pathology and viral replication (154). In comparing the antivirals Synagis and IFN-α both diminished RSV viral replication, however only IFN-α improved RSV-induced lung pathology (35,154).

Antioxidant therapy with BHA alone strongly attenuated several RSV induced disease parameters. However, the half log increase in viral titer was a notable and undesirable side effect. Since, we had previously shown the potent beneficial effects of IFN-α on viral replication and lung pathology (35) we investigated the potential for combination therapy with BHA and IFN-α to attenuate RSV-induced pulmonary inflammation and viral replication.

Antioxidants display various protective effects against viral-induced. For example, a related study by Ghezzi and Ungheri, found that combination therapy with the antioxidant N-Acetylcysteine (NAC) and antiviral drug ribavirin produced a synergistic increase in survival rate in mice infected with a lethal dose of influenza virus in comparison to treatment with just ribavirin alone (117). The protective benefits from adding antioxidant therapy suggest that a bolstered antioxidant capacity either enhances host defenses against viral infection or protects against the pathogenesis of viral-induced lung inflammation. For infants at high risk for developing severe RSV infections such as those born premature with underdeveloped immune systems or infants exposed to oxidant producing environmental stimuli such as environmental tobacco smoke, fortifying the antioxidant status of the lung through nutritional supplementation could protect against oxidative damage and oxidative injury warrants further investigation.

The anti-inflammatory agent, dosage, and time of administration have also been identified as critical factors in determining a successful treatment regimen in combating RSV infection and inflammation (155). For example, we have found that the antioxidant BHA also had a narrow effective dosing range of (150-250mg/kg) with 250mg/kg being

the most effective dose for decreasing RSV-induced pulmonary inflammation and improving acute clinical symptoms. Another advantage of adjuvant antioxidant therapy could be widening the therapeutic index of anti-viral agents by lowering their effective dose which should alleviate associated adverse side effects and enhance efficacy of antiviral therapy.

Similar to other reported antiviral agents that lowered RSV-induced viral replication and lung inflammation (156), IFN-α also reduced RSV-induced lung inflammation. When given prior to RSV infection, IFN-α also prevented RSV-induced body weight loss (35). However, post-infection treatment of mice with IFN-α produced marginal benefit in alleviating RSV-induced clinical illness and body weight loss (data not shown). The beneficial effect of IFN-α when given during the clinically relevant post-infection time frame supports previous reports (157) that prophylactic anti-viral administration yields the most therapeutic benefit. For example, reports on Synagis prophylaxis in premature infants results in fewer hospitalizations, suggesting a reduction in the severity of RSV-induced clinical symptoms of disease (158). Prophylaxis with Synagis is currently limited to high risk groups. Therfore attenuation of the inflammatory response with readily available antioxidants such as BHA in children already infected with RSV, in addition to targeting the infectious agent, is an important avenue for future investigations since RSV-induced pulmonary inflammation is believed to be a key process in the pathogenesis of RSV induced lung disease.

One possible explanation for the higher viral load from BHA is this agents known ability to reduce the expression of antiinflammatory chemokines or cytokines (151) which stimulate the recruitment of inflammatory cells. Activated phagocytic cells recruited to the airways during viral infections undergo a respiratory burst and release ROS, an important antiviral defense necessary for viral clearance. Therefore, the

antioxidant BHA could reduce the migration of the immune cells involved in viral clearance, mitigate the stimulation oxidative stress, and thereby enhance RSV viral replication in the lung. The likely role of IFN-α in the combination therapy is to diminish viral replication in cells already infected with RSV. The strategic combination of drugs that work through different but complementary mechanistic pathways demonstrates the clinical efficacy of successfully targeting both the infectious agent and viral-induced oxidative lung injury and pulmonary inflammation.

In summary, our new observations extend and further validate the potential efficacy of combination therapy with an antiviral and anti-inflammatory agent in alleviating RSV induced lung injury and eliminating viral persistence. Due to the pervasive nature of RSV, the lack of an effective vaccine and the high cost and limited use of preventative therapy, there is an urgent need to discover new treatments that diminish the clinical symptoms during RSV infection and aid in viral clearance.

CHAPTER 6: A ROLE FOR POLY (ADP) RIBOSE-POLYMERASE (PARP) IN MEDIATING RESPIRATORY SYNCYTIAL VIRUS INDUCED PULMONARY INFLAMMATION

ABSTRACT

Respiratory Syncytial Virus (RSV), a major cause of lower respiratory infections in children world wide, is a potent inducer of pulmonary inflammation. Here, we demonstrate that RSV is also a potent inducer of Poly (ADP)-Ribose Polymerase (PARP) nuclear enzymatic activity in vivo and that pharmacological inhibition of PARP attenuated RSV-induction of PARP activity, the release of pro-inflammatory mediators, airway cellular influx, and lung inflammation. Therefore, PARP inhibition could represent a novel target for ameliorating RSV induced lung disease.

INTRODUCTION

RSV, the major cause of viral-induced lower respiratory tract infection, is a potent inducer of pulmonary inflammation. We and others have recently reported that RSV infection produces a condition of acute oxidative stress of the airways which coincides with a rapid stimulation of pulmonary inflammation (119,151). Investigations into the pathogenesis of various lung inflammatory disorders, also characterized by the condition of oxidative stress, have identified an associative activation with the nuclear enzyme PARP (159). Oxidative stress triggers the rapid formation of single stranded DNA breaks, a necessary event for PARP activation. Interestingly, inhibition of PARP, either through genetic manipulation or pharmacological inhibition, provides protection against oxidative stress-induced cellular injury and pro-inflammatory responses in model systems of acute lung diseases in vivo (37-38).

Recent studies suggest that PARP mediates lung inflammation by regulating cytokine and chemokine gene expression (160). However, no published reports describing effects of PARP inhibition on viral-induced pulmonary inflammation. Therefore, the primary goal of this study was to determine whether PARP plays a role in RSV-induced pulmonary inflammation by modulating the expression of inflammatory chemokine and cytokine production. We selected INO-1001, a potent isoindolinone-based inhibitor of PARP catalytic activity to diminish PARP activity.

MATERIALS AND METHODS

Treatment Protocol and Innoculation

Female BALB/c mice (Harlan, Houston, TX), 8-10 weeks of age, were pretreated one hour prior to RSV infection with an intraperitoneal injection of 200 mg/kg INO-1001 (Inotek Pharmaceuticals Corporation, Beverly, Massachusetts) in 5% dextrose or control diluent in a total volume of 0.5ml. The dosage, route, and timing of INO-1001 were based on suggestions from Inoteck Pharmaceuticals Corporation. Mice were anesthetized and intranasally inoculated with either sucrose purified HEp-2 extracts (Sham) or sucrose purified RSV at $1x10^7$ PFU as previously described elsewhere (47,123). Subsequently, mice received additional treatments with the same dosage of INO-1001 at 6 and 12 hours post-infection (p.i.) and then once daily from day 1 p.i. until p.i. day 5 for viral titration and histopathology. Experimental groups labeled as control and INO were treated with vehicle and INO-1001 respectively and sham infected. RSV and RSV+INO were treated with vehicle and INO-1001 respectively and RSV infected.

PARP Enzymatic Activity

At 24 hours p.i., lungs were removed and immediately snap frozen. Nuclear extracts isolated from the lung tissue of RSV-infected and INO-1001 treated mice were isolated using the hypotonic/nonionic detergent lysis method as previously described

(161). PARP activity was measured using 25 μg of nuclear extract incubated at 30°C for 30 min in a 40 μl reaction mixture containing 3% glycerol, 50 mM HEPES (pH 7.8), 5 mM MgCl2, 50 mM 0.5 mM DTT, 0.4 mM EDTA, 20 μg/ml bovine serum albumin, 2 mM ATP, and 0.5μCi (3000 mCi/mol) [^{32}P] NAD+ (Amersham) (162). The reaction was stopped by the addition of 50μl acetone and ribosylated nuclear acceptor proteins were analyzed by 8% SDS PAGE and visualized by ImageQuant (Molecular Dynamics).

Pulmonary Inflammation and Histopathology

Total leukocyte cell counts in bronchoalveolar lavage (BAL) obtained at day 1 p.i. were determined by counting the viable cells which excluded trypan blue stain. To measure cell differentials in BAL, cytospin slide preparations were stained and viewed by light microscopy. For histopathology, slides of conventionally formaldehyde-fixed lung sections were prepared and scored for cellular inflammation by a board certified pathologist as previously described (28,151).

Chemokine and Cytokine Protein Profiles

To assess the production of chemokines and cytokines released into the airspace, BAL was obtained at 24 hours p.i. and multiple inflammatory mediators were measured using the Bio-Plex Cytokine Mouse Multi-Plex panel (Bio-Rad Laboratories) according to the manufacture instructions, as previously described (123).

Viral Titration

Lungs from RSV-infected mice treated with INO-1001 or vehicle were excised at day 5 p.i., snap frozen in liquid nitrogen, and stored at -70^{o}C. Serial dilutions of lung homogenates were subjected to the methylcellulose plaque assay to determine viral titer as previously described (122).

Statistical Analysis

Statistical analysis was performed with the biostatistics software program GraphPad Prism (GraphPad Software, Inc.). Comparisons between two groups were done using an unpaired student's t-test. Data are presented as mean ± standard error of the mean (SEM). A p value <0.05 was considered significant.

RESULTS

As shown in Figure 6.1, RSV was a potent inducer of PARP enzymatic activity, as indicated by the formation of ribosylated ADP units to nuclear acceptor proteins. Treatment with INO-1001 completely blocked RSV-induced PARP activity, as well as basal levels of sham-infected mice (data not shown). PARP activity was detectable in INO-1001 treated and sham+vehicle groups only upon prolonged exposures (data not shown).

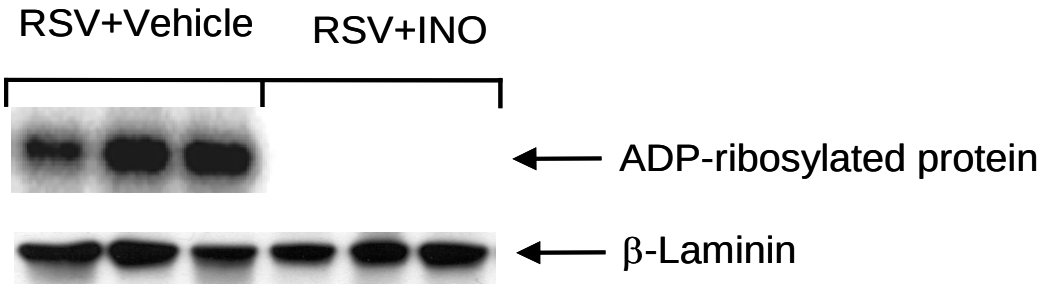

FIGURE 6.1 PARP INHIBITION WITH INO-1001 SUPPRESSES RSV-INDUCED PARP. Enzymatic PARP activity was assayed in lung nuclear extracts obtained at day 1 p.i. from RSV infected mice treated with either vehicle or INO-1001. Figure is representative of two independent experiments.

We have published numerous reports using the Balb/c mouse model of RSV infection and routinely measure inflammatory parameters associated with the progression of RSV-induced acute lung injury (28,123). To investigate the effect of PARP inhibition

on RSV-induced acute lung inflammation, bronchoalveolar lavage (BAL) samples obtained from the lungs of treated mice on day 1 p.i. were used to measure total cellular influx, perform differential cell counts, and measure inflammatory cytokine and chemokine proteins. As previously observed, the number of cells in BAL from RSV infected mice was an order of magnitude higher than in sham infected mice. Treatment with INO-1001 led to a significant 3 fold decrease in total cellular influx (Figure 6.2A) and reduced neutrophil migration into the airspace of lungs by ~ 4 fold both sham and RSV–infected mice in comparison to their respective controls (Figure 6.2B). Similarly,

lung pathology analysis showed that PARP inhibition significantly reduced RSV-induced cellular infiltrate within the perivascular and peribronchiol regions of the lung. These observations clearly indicate that INO-1001 treatment dramatically attenuates RSV-induced lung inflammation (Figure 6.2C). To examine whether the decrease in RSV-induced lung inflammation was due to a decrease on RSV replication, mice were administered INO-1001 and lungs were obtained at day 5 p.i to measure viral load. In contrast to the dramatic effects of INO-1001 on RSV-induced lung inflammation, there was no change in RSV viral titer (Figure 6.2D).

To determine whether treatment with INO-1001 altered the secretion of RSV-induced inflammatory mediators, BAL obtained on day 1 p.i. was analyzed by Bio-Plex. As shown in Figure 6.3 and 6.4, PARP inhibition significantly attenuated the secretion of nine different RSV-induced inflammatory cytokines (Figure 6.3) and three chemokines (Figure 6.4). Some measurements for control groups were below the limit of detection and therefore are not shown.

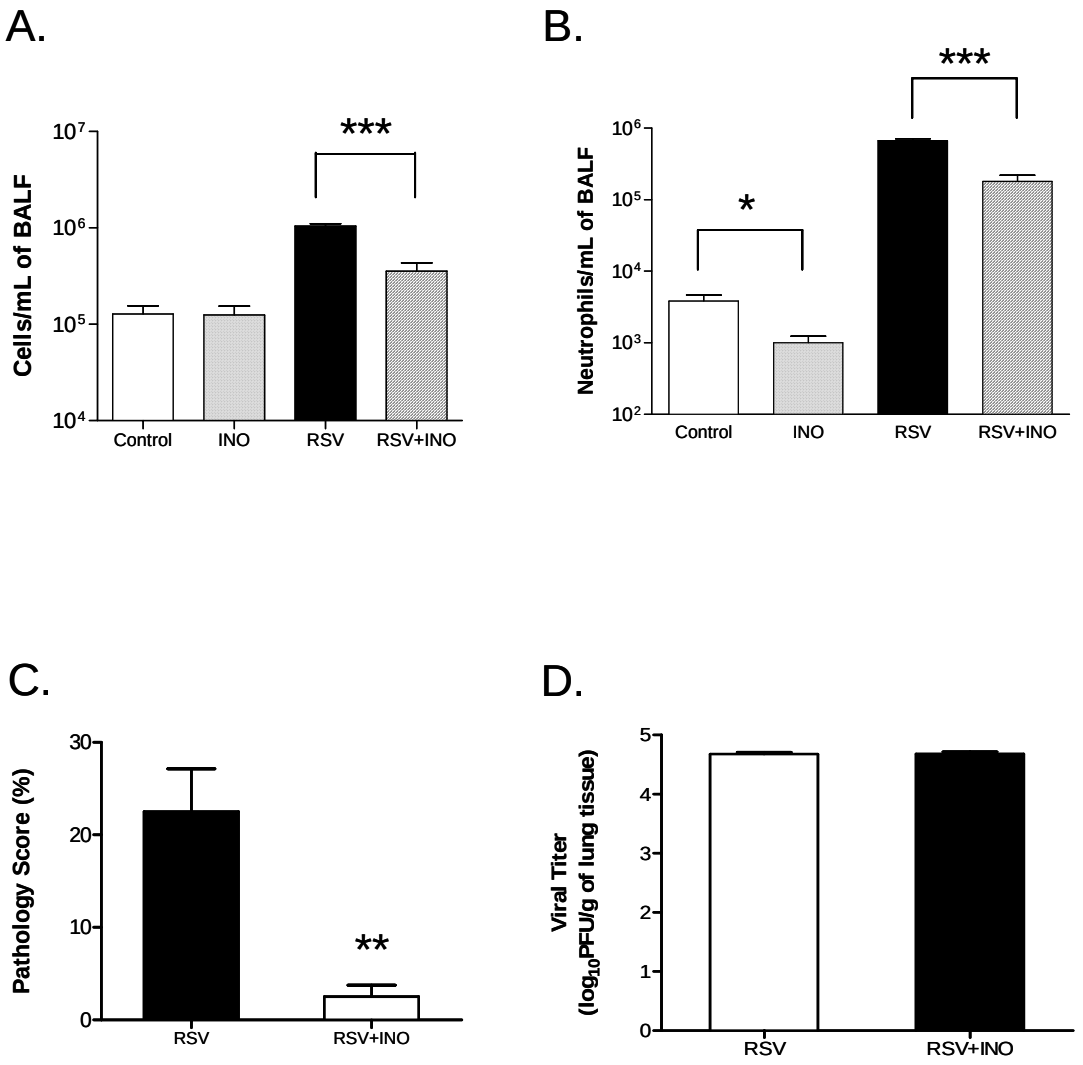

FIGURE 6.2 THE EFFECT OF INO-1001 ON RSV INDUCED PULMONARY INFLAMMATION AND VIRAL TITER. BAL was collected at day 1 p.i. to measure: A) Total leukocyte cell counts in BAL, B) Percentage of neutrophils in BAL, C) Lung pathology, D) Viral load. N=4, mean±SEM, *p<0.05, **p<0.01, ***p<0.001.

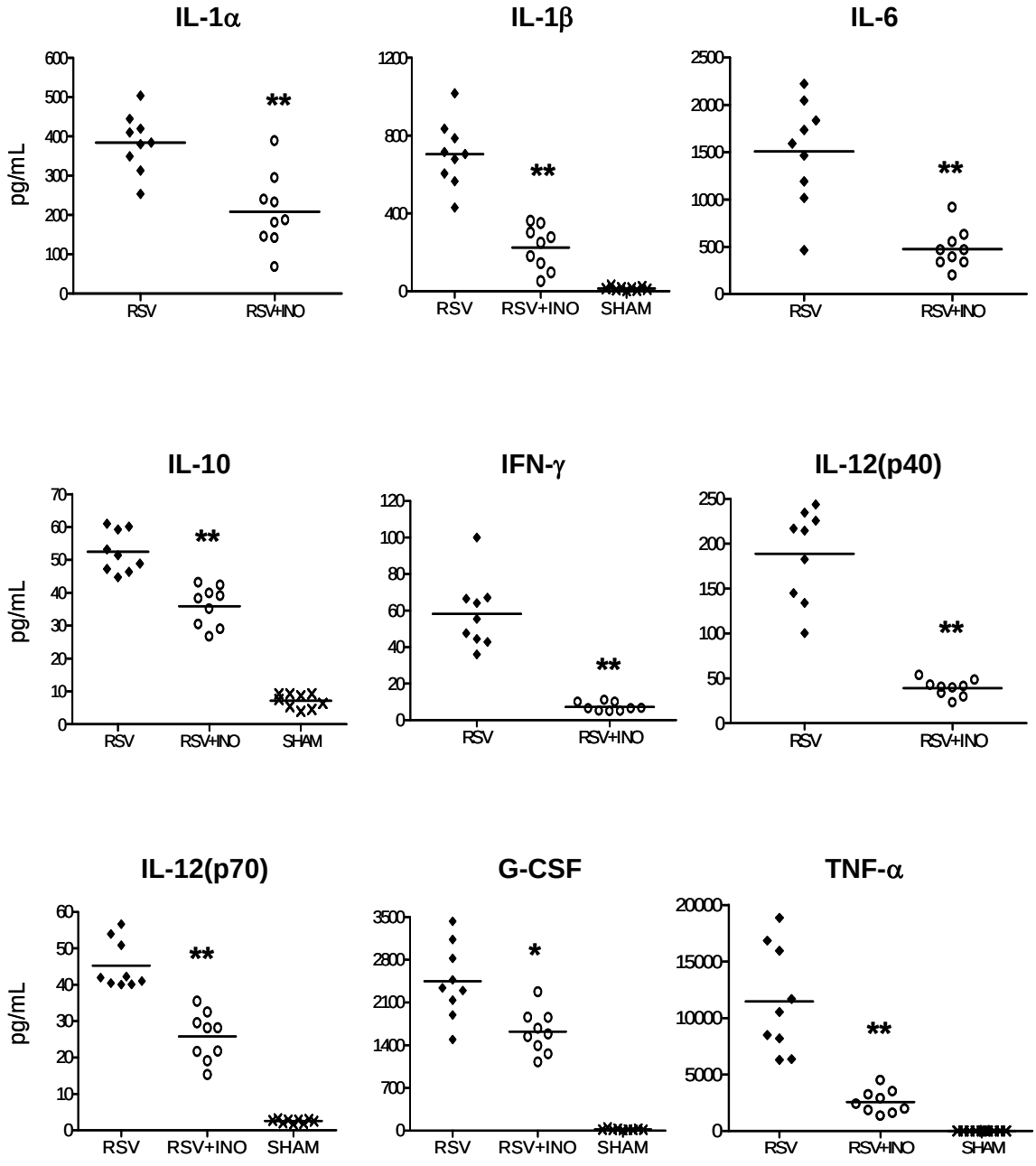

FIGURE 6.3 EFFECT OF PARP INHIBITION ON RSV-INDUCED INFLAMMATORY CYTOKINE SECRETION. The release of inflammatory mediators was measured by Bio-Plex in the BAL at day 1 p.i. to quantitate. Results values from individual mice in one experiment which was representative of three independent experiments, N=9, — symbol represents mean, * $p<0.01$, **$p<0.001$.

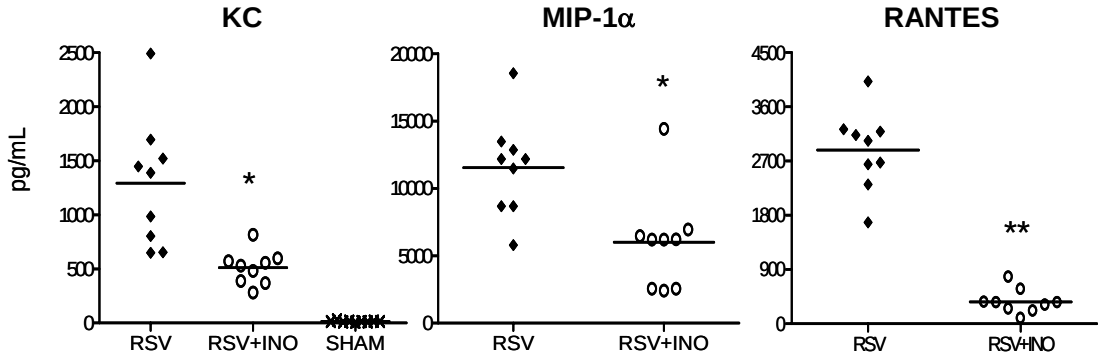

FIGURE 6.4 EFFECT OF PARP INHIBITION ON RSV-INDUCED INFLAMMATORY CHEMOKINES PRODUCTION. The release of inflammatory mediators was measured by Bio-Plex in the BAL at day 1 p.i. to quantitate. Results are representative of three independent experiments, N=9, — symbol represents mean, * $p<0.01$, **$p<0.001$.

DISCUSSION

Although numerous studies utilizing various models of pulmonary inflammation have reported that PARP knockout or INO-1001 pharmacological inhibition modulate the innate inflammatory response (159,163), no published reports have investigated the role of PARP in RSV-induced pulmonary inflammation. Our observations include the novel finding the RSV is a potent inducer of PARP activation. Of concern, is the rapid over-activation of PARP could rapidly deplete cellular NAD+ and ultimately lead to cell death through the necrotic pathway. Prevention of PARP mediated cell necrosis during acute tissue injury is currently being explored since the leakage of cellular contents from necrotic cells releases powerful inflammatory stimuli, which does not occur during the more controlled process of cell death by apoptosis. Efforts to block overactive PARP mediated inflammatory responses in favor of the more benign apoptotic cascade could thus reduce acute lung injury during RSV infection. PARP activation is also mediated by free radicals and oxidative stress. We have previously reported that RSV induces

oxidative stress in the lung of infected mice (151). Therfore, treatment with INO-1001 may have blocked the positive feedback cyle leading to RSV induced PARP activation by preventing cell necrosis, inflammation and subsequent downstream oxidative stress (164).

This study also demonstrated that pharmacological inhibition of PARP with inhibition INO-1001 also decreased immune cell migration into the airspace of the lung. Several studies using other models of lung inflammation (165,166) have observed similar findings indicating that PARP is involved in regulating leukocyte trafficking into the lung and that PARP inhibition selectively decreases neutrophil chemotaxis. The observed effect of PARP inhibition on RSV induced lung pathology was both striking and profound. Another function of PARP is regulating endothelial permeability as supported by the finding that treatment with PARP inhibitor 3-aminobenzamide significantly reduced the lipopolysaccharide-induced lung hyperpermeability (167). Since reduced levels of cellular infiltrates were observed both in the surrounding airways and vasculature, PARP inhibition could have decreased RSV-induced vascular permeability in the lung. As reported for other models of pulmonary inflammation (159) pharmacological inhibition of PARP resulted in a widespread reduction in RSV-induced chemokines and cytokines. Treatment with PARP inhibitior PJ34 similarly reduced inflammatory chemokine MIP-1α cytokines TNF-α and IL-12 in a mouse model of asthma (160). In conclusion, our observations of the dramatic protective effects of PARP inhibition warrant further inquiries about the role of PARP in ameliorating RSV-induced acute lung inflammation and possibly preventing the long term consequences of lung injury, critical concerns in the rapidly developing infant.

CHAPTER 7: CIGARETTE SMOKE CONDENSATE ENHANCES RESPIRATORY SYNCYTIAL VIRUS-INDUCED CHEMOKINE RELEASE BY MODULATING NF-KAPPA B AND INTERFERON REGULATORY FACTOR ACTIVATION

ABSTRACT

Exposure to cigarette smoke is a risk factor contributing to the severity of respiratory tract infections associated with respiratory syncytial virus (RSV). Exposure of airway epithelial cells to either RSV or cigarette smoke condensate (CSC) has been shown to induce secretion of the pro-inflammatory chemokines. We tested the hypothesis that co-exposure of airway epithelial cells to CSC would enhance RSV-induced chemokine production. Co-exposure of A549 human type II cells to CSC and RSV synergistically increased RSV-induced chemokine gene and protein expression of IL-8 and MCP-1. Promoter deletion studies identified the interferon stimulatory response element (ISRE) of the IL-8 promoter as a critical region responsible for the synergistic increase of IL-8 gene transcription by the co-exposure. CSC enhanced RSV-induced activation of the interferon regulatory factors (IRF)-1 and IRF-7, which bind to the ISRE site. Co-exposure also furthered RSV-induced activation of the transcription factor NF-κB, as shown by increased NF-κB DNA- binding to its specific site of the IL-8 promoter and increased NF-κB-driven gene transcription. Therefore, our observations that a combined exposure to CSC and RSV synergistically increases chemokine expression in airway epithelial cells, suggesting that CSC enhances the already exuberant immune response to RSV by stimulating overlapping signal transduction pathways.

INTRODUCTION

Respiratory syncytial virus (RSV) is a major cause of lower respiratory infection in infants, elderly, and immuno-compromised patients (168-169) By the age of 2, nearly all children have been infected with RSV (170). An effective vaccine for RSV has yet to be developed and immunity to infection is incomplete. Therefore, repeated attacks of RSV infection occur, causing symptoms ranging from mild nasal discharge greater morbidity, such as bronchiolitis and pneumonia requiring hospitalization. In addition to the acute morbidity of RSV infection, long-term consequences include the development of hyperractive airway disease (171) and recurrent wheezing, both risk factors for the development of asthma (7).

Although the mechanisms of acute RSV-induced lung disease have not been clearly elucidated, strong experimental evidence indicates that early inflammatory and immune events play critical roles. Therefore, exposure to external stimuli that either contribute to or enhance the inflammatory response to RSV infection could consequently increase the severity of RSV-induced lung disease and/or the long-term consequences associated with RSV infection. One such external stimulus is exposure to environmental tobacco smoke (ETS). In the United States, exposure to ETS may occur in up to 60% of the infants with RSV bronchiolitis and multiple epidemiological studies have suggested that ETS exposure contributes to the severity of RSV LRTI, (172). ETS has also been linked to an increased frequency of lower respiratory tract infection (LRTI), persistent wheezing, increased incidence and severity of asthma episodes (40) and overall decreased pulmonary function (40,173). Known responses to ETS exposure that could worsen RSV-induced acute lung inflammation and delay viral clearance include oxidative stress (174), mucosal edema, decreased mucocilliary clearance, and bronchial inflammation (40).

The airway epithelial cell, a primary target of RSV infection, plays a key role in regulating pulmonary inflammation by producing potent immuno-modulatory and inflammatory mediators, such as chemokines. Chemokines are small cytokines that recruit and activate leukocytes into the airway mucosal. Therefore, chemokines play a pivotal role in regulating acute inflammatory and infectious processes (175). Monocyte chemoattractant protein-1 (MCP)-1 and interleukin-8 (IL-8) are two chemokines found in samples derived obtained from the airways of hospitalized infants with naturally-acquired RSV infection (25,27) and in the bronchoalveolar lavage of mice following exposure to ETS (176). MCP-1 is a major recruiter of monocytes and macrophages, whereas IL-8 promotes primarily the migration and activation of neutrophils.

Pathological mechanisms underlying the epidemiologic association between cigarette exposure and the severity of RSV infection are unclear. In various experimental model systems, independent stimulation with either RSV or cigarette smoke condensate (CSC), a tar phase extract of cigarette smoke, has been linked to the activation of NF-κB (23,177,178). NF-κB is a ubiquitous multifunctional transcription factor involved in the expression of RSV-induced chemokines IL-8 and MCP-1 (23,179). However, the impact of a mixed exposure of CSC during RSV infection on chemokine secretion, as well as on activation of NF-κB and other transcription factors that regulate chemokine gene expression, has not been investigated.

In this study, we show that the presence of CSC increased the production of IL-8 and MCP-1 in RSV-infected airway epithelial cells. The synergistic induction of IL-8 gene transcription by RSV and CSC co-exposure required the participation of the IL-8 promoter ISRE site, which binds transcription factors belonging to the IRF family. RSV and CSC co-exposure induced increased nuclear translocation and binding of IRF proteins to the ISRE site. Furthermore, we observed enhanced NF-κB activation and NF-

κB-driven gene transcription during RSV and CSC co-stimulation. These studies reveal important new mechanistic information on how cigarette smoke is an associative factor capable of contributing to the severity of RSV-induced inflammatory response.

MATERIALS AND METHODS

RSV and CSC Preparation

The RSV A2 strain was grown in HEp-2 cells and purified by centrifugation on discontinuous sucrose gradients as described elsewhere (47). The virus titer of the purified RSV used ranged form 8-9 $\log_{10}$ plaque forming units (PFU)/ml using a methylcellulose plaque assay. No contaminating cytokines were found in these sucrose-purified viral preparations (48). LPS, assayed using the limulus hemocyanin agglutination assay, was not detected. RSV pools were aliquoted, quick-frozen in liquid nitrogen, and stored at -70^{o}C until used. The CSC was purchased from Murty Pharmaceuticals and prepared by smoking University of Kentucky's Standard Research Cigarettes on an FTC Smoke Machine. The total particulate matter (TPM) collected was extracted with DMSO (CSC diluent vehicle) to generate a 4% solution.

CSC treatment and infection of epithelial cells with RSV

A549, human alveolar type II-like epithelial cells, and 293, a human embryonic kidney epithelial cell line (ATCC, Manassas, VA), were maintained in F12K and MEM medium respectively, containing 10% (v/v) FBS, 10 mM glutamine, 100 IU/ml penicillin and 100 μg/ml streptomycin. Cell monolayers were serum starved for 4 hours prior to CSC exposure. Cells were then pre-treated with equivalent volumes of DMSO (control) or CSC (1 μg/ml) for 2 h prior and subsequently infected with 30% sucrose solution (control) or sucrose purified RSV at a multiplicity of infection (MOI) of 1. Cells were harvested at various times post-infection. No cell toxicity was observed by measurements

of total cell number and viability at 24 hour following treatment with CSC 1 μg/ml by trypan blue exclusion.

Chemokine Protein Determination

Supernatants from treated and infected cells were harvested at 24 h post-infection (p.i.) to measure the release of inflammatory mediators. Both IL-8 (DuoSet) and MCP-1 (Quantikine) proteins were quantified by ELISA following the manufacturer's protocol (R&D Systems). The production of chemokines and cytokines were measured using the Bio-Plex Cytokine Mouse Multi-Plex panel (Bio-Rad Laboratories) according to the manufacture instructions as previously described (123).

Quantitative Real Time Polymerase Chain Reaction (Q-RT-PCR)

Total RNA was extracted from A549 cells harvested at 6, 12, and 24 h p.i. using the RNeasy Mini Kit (Qiagen). RNA integrity was assessed by gel electrophoresis and quantitated with absorbance A_{260}> 1.5. For IL-8 and MCP-1 gene transcript amplification by Q-RT-PCR, Taqman® Gene Expression Assay singleplex containing a 20 X mix of primers and FAM™ TaqMan® MGB probes for target genes and 18S rRNA VIC™ TaqMan® assay reagent were used (Applied Biosystems). Separate tubes (singleplex) one-step RT-PCR was performed with 100ng RNA for both target genes and endogenous control. The cycling parameters using TaqMan® master mix one-step RT-PCR were: reverse transcription 48°C for 30 min, AmpliTaq activation 95°C for 10 min, denaturation 95°C for 15 sec and annealing/extension 60°C for 1 min (repeat 30 times) on ABI7000. Duplicate CT values were analyzed in Microsoft Excel using the comparative CT (ΔΔCT) method as described by the manufacturer (Applied Biosystems). The amount of target ($2^{-\Delta\Delta CT}$) was obtained by normalizing to endogenous reference (18S) sample.

Plasmid Construction and Cell Transfections

We used previously described (11) luciferase reporter gene plasmid constructs containing 5' deletions of the human IL-8 promoter at upstream positions -162, -132, and -99, multimeric ISRE and NF-κB binding sites and mutations within the ISRE (RSVRE) site. Luciferase reporter constructs were transiently transfected into A549 and 293 cells using Fugene 6 (Roche Applied Science). Logarithmically growing cells were transfected with 1ug of the reporter gene plasmid and 0.5 μg of β-galactosidase premixed with Fugene 6 in a 1:3 ratio (μg/μl). After 18 h of transfection, triplicate plates were treated with either control solvent (DMSO), CSC (1μg/ml), RSV (MOI 1), or RSV+CSC. At indicated times cells were harvested to measure luciferase and β-galactosidase activity as previously described (23). Luciferase activity was normalized to the internal control β-galactosidase activity and results reported as fold induction over baseline control values. Results are representative of three independent experiments.

Electrophoretic Mobility Shift Assay (EMSA)

Nuclear extracts were prepared from A549 cells infected or treated with either CSC or RSV or a combination of the two at 6 and 12 p.i. using the hypotonic/nonionic detergent lysis as previously described (11). Protein concentrations of the nuclear extracts were quantitated by protein assay (Bio-Rad) and incubated with oligonucleotides corresponding to the interferon stimulated response element (ISRE) and the NF-κB wild-type (WT) and mutated (MUT) binding sites of the IL-8 promoter. Sequences for the oligonucleotides are shown below with mutated nucleotides that disrupt NF-κB binding shown in bold font and underlined. Oligonucleotides were synthesized by Integrated DNA Technologies, Coralville, IA. The DNA binding reaction for the NF-κB probe contained 10 μg of nuclear protein, 1 μg of polydeoxyadenylicthymidylic acid (polydA-dT), 5% glycerol and 50,000 cpm α^{32}P –labeled double stranded oligonucleotide in a total

volume of 20 μl. Additional reagents for the ISRE binding reactions included 5mM dithiothreitol (DTT). For competition assays, 2 pmol of unlabeled wild-type or mutated competitor was included in the binding reaction. The resulting hybridized DNA-protein complexes were resolved using a 6% non-denaturing polyacrylamide gel and visualized by autoradiography.

ISRE-IL-8: 5'-GATCCACCGTA TTT GATAAGGAACAAATAGGAGTGTTA- 3'

3'-CTAGGTGGCATAAACTATT CC TT GTTT AT CC TCACAAT-5'

NF-KB-IL-8(WT): 5'-GATCCATCAGTTGCAAATCGTGGAATTTCC T CTA-3'

3'-GTAGTCAACG TTTAGCACCTTAAAGGAGATCTAG-5'

NF-KB-IL-8(MUT): 5'-GATCCATCAGTTGCAAATCG T**TT**AATTT**AA** TCTA-3'

3'-GTAGTCAACGTTT AGCA**AA**TTAAA**TT**AGATCTAG-5'

Western Immunoblot

Nuclear extracts from treated A549 cells were seperated by SDS-PAGE, transferred to a PVDF membrane, and probed with commercially available primary rabbit polyclonal IgG antibodies against IRF-1, IRF-3, IRF-7 (Santa Cruz Biotechnology); anti-phospho-IRF-3(Ser396), anti-NF-κBp65 (Upstate); and LaminB (Zymed Laboratories, Inc.). Following probing with HRP-secondary antibody, proteins were detected using an Enhanced Chemiluminescence system (Amersham Life Science) and visualized through autoradiography. Protein bands were quantitated using Alpha Imager (AlphaInnotech).

Viral Titration

Supernatants from treated A549 cells were obtained at 24 h p.i., snap frozen in liquid nitrogen, and stored at -70^{o}C. Serial dilutions of the supernatants were added to

confluent HEp-2 cells grown in 24-well plates and viral titers were determined by the methylcellulose plaque assay, as previously described (177).

Statistical Analysis

Statistical analysis was performed with the biostatistics software program GraphPad Prism (GraphPad Software, Inc.). Comparisons between the two treatment groups RSV versus RSV + CSC were analyzed using an unpaired student's t-test. Data are presented as mean ± standard error of the mean (SEM). A p value <0.05 was considered significant.

RESULTS

The Effect of CSC exposure on RSV-Induced Chemokine Production in Airway Epithelial Cells

To study the effect of CSC on RSV-induced chemokine secretion in airway epithelial cells, we used A549 cells, a human cell line which resembles type II alveolar epithelial cells, because this model system had previously been shown to be both suitable and useful for investigating RSV infection (23,45). Since RSV is a potent inducer of inflammatory mediators in our model system of A549 cells, we tested increasing concentrations of CSC (0.1, 0.5, 1, 10 μg/ml) in combination with low MOIs of RSV infection (0.1, 0.5 and 1) to identify a potential effect of CSC on RSV infection. Cell-free supernatants of treated and infected cells were obtained at 12, 24, and 48 h p.i. for measurements of IL-8 and MCP-1 secretion by ELISA. Co-exposure yielded additive increased trends in chemokine secretion at 12 and 48 h p.i (data not shown). The treatment conditions with CSC (1 μg/ml) and RSV (MOI of 1) at 24 h p.i. was selected used for all future experiments unless otherwise noted based on the consistently observed synergistic increases in IL-8 and MCP-1 protein secretion (Figure 6.1). To identify the potential release of additional inflammatory mediators, supernatants were also analyzed

by Bio-Plex Multiplex Suspension Array (Bio-Rad), as previously described (123). However, no significant additive or synergistic increase of other chemokine or cytokine was observed in the combination treatment versus RSV alone (data not shown).

To evaluate whether CSC potentiates RSV-induced chemokine production at the level of gene expression, IL-8 and MCP-1 mRNA abundance was determined by Q-RT-PCR. A549 cells were treated with control solvent or CSC and either mock or RSV infected as previously described. Cells were harvested at 6, 12, and 24 h p.i. to extract total RNA. CSC treatment alone produced only slightly increased levels of IL-8 and MCP-1 mRNA, while there was a significant increase in expression for both genes in RSV-infected cells compared to uninfected cells. CSC and RSV co-exposure led to a synergistic increase in the level of IL-8 and MCP-1 mRNA compared to CSC exposure or RSV infection alone (Figure 7.1B).

To determine whether the synergistic increase in chemokine secretion following RSV and CSC co-exposure was due to an increase in viral replication, we assessed viral titer in supernatants from treated and infected A549 cells harvested at 24 h p.i. As shown in Figure 7.2, exposure of RSV-infected cells to CSC did not alter RSV viral replication. Therefore stimulation of overlapping signaling pathways, and not enhanced viral replication, could be responsible for the observed increases in chemokine expression.

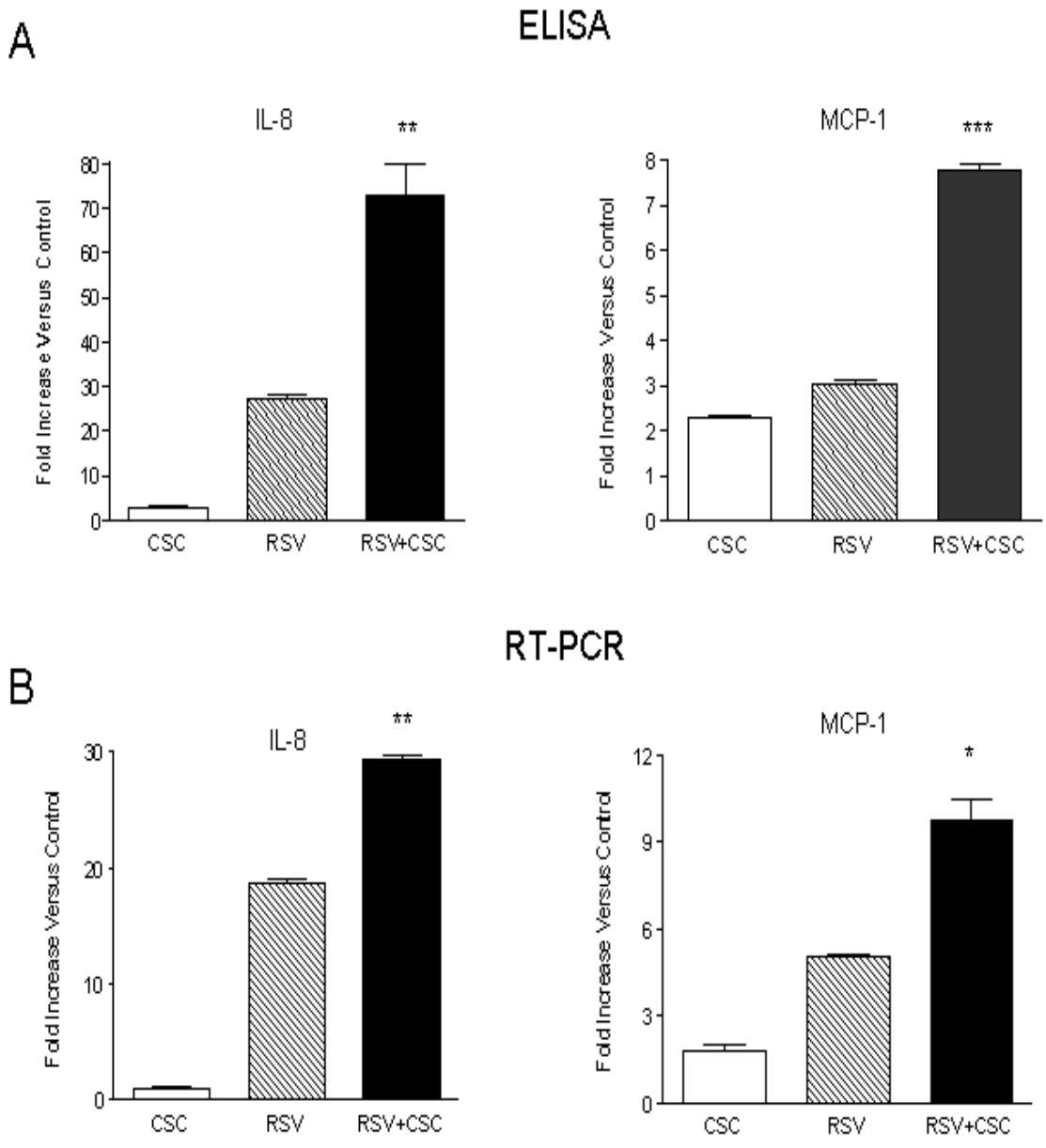

FIGURE 7.1 RSV INFECTION AND CSC TREATMENT OF A549 CELLS SYNERGISTICALLY STIMULATES IL-8 AND MCP-1 PROTEIN RELEASE AND GENE EXPRESSION. A549 cells were treated with vehicle control DMSO and CSC (1 μg/ml) and infected with sham and RSV (MOI of 1). Supernatants were harvested at 24 h p.i. and assayed for IL-8 and MCP-1 protein secretion by ELISA (A). IL-8 and MCP-1 gene expression was quantified by real time PCR at 12 h p.i. (B). Data are presented as fold increases over control and are representative of three independent experiments. *$p<0.05$, **$p<0.01$, ***$p<0.001$ RSV relative to RSV+CSC.

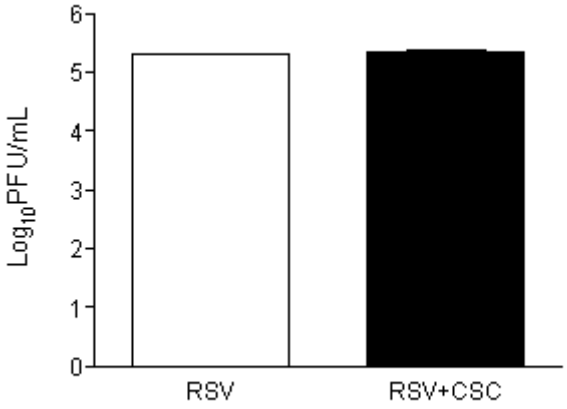

FIGURE 7.2 EFFECT OF CSC ON RSV REPLICATION. Supernatants of A549 cells exposed to DMSO(vehicle control) and CSC 1 μg/ml and infected with RSV at MOI of 1 were harvested at 24 h p.i. to measure RSV viral replication using the methylcellulose plaque assay, n=3.

CSC enhances RSV-Induced IL-8 Transcription Though IRF Activation.

In order to identify the molecular mechanism regulating the increased chemokine production in RSV+CSC treated cells, we investigated the potential roles of specific *cis* regulatory elements to activate the IL-8 promoter and the transcription factors binding to those regulatory elements in response to RSV and CSC co-exposure. A549 cells were transiently transfected with plasmids containing 5' serial deletions, site mutations, or modifications of the human IL-8 promoter linked to the luciferase (LUC) reporter gene. A detailed description of these generated constructs is provided by Casola et al. (11). We have previously shown that nucleotides starting at -162 nt upstream of the transcription start site of the IL-8 promoter are sufficient for RSV-induced promoter activation (23). The diagram in Figure 7.3A depicts the 5' flanking region of the IL-8 promoter starting with the full length wild-type construct designated as the -162/+44 hIL-8 luciferase

(LUC) reporter plasmid. The promoter region contains transcription factor binding sites identified as ISRE (an IRF-1 binding site), AP-1, NF-IL6, NF-κB, and the TATA transcriptional initiation site. All four binding sites play an important role in RSV-induced IL-8 promoter activation in A549 cells (11,23,45).

A549 cells were transfected with the various IL-8 plasmid constructs and 18 hours and treated as previously mentioned. Cells were harvested and assayed for luciferase reporter gene activity at 6, 12, and 24 h p.i. For all constructs, no significant increase of luciferase activity was observed in CSC versus control treated cells, therefore results were reported as fold increases over control (Figure 7.3B). RSV infection led to a 5 fold increase in luciferase activity of the full length promoter (-162/+44 hIL-8 LUC) versus control, as previously observed (23). While, co-exposure with RSV+CSC resulted in a heightened 9 fold synergistic increase in luciferase activity, in comparison to RSV infection alone (Figure 7.3B).

Cells transfected with the 162M/+44 hIL-8 LUC construct, containing a site mutation in the ISRE site, exhibited a slightly lower luciferase induction (4 fold) after RSV infection in comparison to the -162 hIL-8 promoter. With the ISRE mutation, co-exposure with RSV+CSC also failed to enhance IL-8 promoter activation as opposed to the synergistic induction observed with the full length promoter. The -132/+44 hIL-8 LUC construct is a deletion mutant that lacks the ISRE site (11). Similar to the -162M promoter, the -132 deletion mutant showed decreased promoter activation (4 fold) in response to RSV infection and only a slight increase after co-exposure, in comparison to RSV alone (Figure 7.3B).

Consistent with prior observations (45), cells transfected with –99/+44 hIL-8 LUC which contains only the NF-IL6 and the NF-κB sites of the IL-8 promoter, were not inducible in response to RSV or co-exposure with RSV+CSC (data not shown). To

validate the role of the ISRE binding site in RSV+CSC enhanced IL-8 promoter activity, a construct containing two ISRE sites and lacking the AP-1 site, linked to the non-responsive -99/+44 promoter region, designated as 2(ISRE)-99/+44 IL-8 LUC was transfected into A549 cells. Inserting 2 copies of the ISRE site into the –99/+44 hIL-8 LUC restored RSV inducibility of the -99/+44 IL-8 promoter (17 fold) and the re-established the synergistic promoter activation observed following RSV+ CSC co-stimulation (24 fold) (Figure 7.3B). In summary, these results indicate that the IL-8 promoter sequence spanning from -162 to -132, corresponding to the ISRE site, is necessary for enhanced IL-8 gene transcription following RSV and CSC co-exposure.

To further investigate the role of the ISRE site in RSV+CSC-induced enhanced IL-8 gene transcription, we determine whether RSV+CSC co-exposure produced changes in the abundance of ISRE-binding proteins by EMSA, using nuclear extracts prepared from uninfected and RSV-infected cells in the presence or absence of CSC. As shown in Figure 7.4A, three binding complexes, C1, C2 and C3, were detected in control A549 cells. There was a slight induction of C1 complex when treated with CSC alone, and more in response to RSV infection. CSC+RSV co-exposure resulted in a significant increase of C1 complex formation, compared to each stimulus alone (Figure 7.4A). The inducible C1 complex was sequence specific, as demonstrated by its competition by unlabeled wild type. The enhanced induction of C1 complex during co-exposure was sustained until 12 h p.i. (data not shown).

We have previously shown that IRF-1 binds to the ISRE IL-8 promoter in response to RSV infection (11) and that RSV induces the activation of IRF-3 and IRF-7 in airway epithelial cells (29). Therefore, to determine the effect of CSC on IRF activation during RSV infection, we analyzed nuclear translocation of IRF1, -3 and -7 by Western blot following various treatments at 6 h p.i. As shown in Figure 7.4B and 4C,

co-exposure led to an increase in IRF-1 and -7 nuclear translocation compared to RSV alone. A modest increase in IRF-3 phosphorylation, a marker of activation (180), but not in nuclear abundance, was also observed (data not shown).

CSC enhances NF-κB activation in response to RSV infection.

NF-κB is a ubiquitous multifunctional transcription factor that plays an important role in pro-inflammatory gene expression (181). In various experimental systems both RSV and CSC alone, have been shown to induce signaling pathways leading to the NF-κB activation, (23,177-178). We have previously shown that NF-κB is necessary for RSV-induced IL-8 promoter activation (23). To determine whether NF-κB activation was enhanced by RSV+CSC co-exposure, an NF-κB-driven artificial promoter, containing three copies of the IL-8 NF-κB binding site, was used to investigate NF-κB activation following RSV+CSC stimulation. Cells were transfected with the NF-κB-driven luciferase reporter plasmid and either infected with RSV alone or in combination with CSC. Cells were harvested at various time points to measure luciferase activity. As shown in Figure 7.5, CSC alone did not induce luciferase activity, in contrast to RSV which induced a 9 fold increase at 6 h, but not at 12 or 24 h p.i.. While co-stimulation of RSV+CSC produced a synergistic increase in promoter activation, compared to RSV alone at all time points.

Based on the observation that CSC contributed to RSV-induced NF-κB activation, we investigated whether CSC enhanced RSV-induced NF-κB DNA-binding activity by EMSA. Nuclear extracts were incubated with a radio-labeled oligonucleotide corresponding to the IL-8 promoter NF-κB site. RSV infection induced the formation of two DNA-binding complexes, C1 and C2, which were enhanced by RSV and CSC co-exposure, both at 6 and 12 h p.i. C3 was constitutively present in uninfected and infected

cells (Figure 7.6A). C1and C2 binding was specific, as demonstrated by competition assays with wild type (WT) or mutated (MUT) NF-κB binding site.

We have previously shown that the p65 NF-κB subunit is the major protein constituting RSV-induced C1 and C2 complexes (23). To confirm that RSV and CSC co-exposure enhanced NF-κB activation, nuclear extracts were prepared from A549 cells at 6 and 12 h p.i. and NF-κB nuclear translocation by analyzed by Western blot. While there was no significant increase in p65 nuclear translocation after stimulation of A549 cells with CSC alone, nuclear abundance of p65 was higher in co-exposed cells in comparison to RSV alone (Figure 7.6B and C). All together these results indicate that CSC enhances RSV-induced NF-κB activation and subsequent NF-κB-dependent gene transcription.

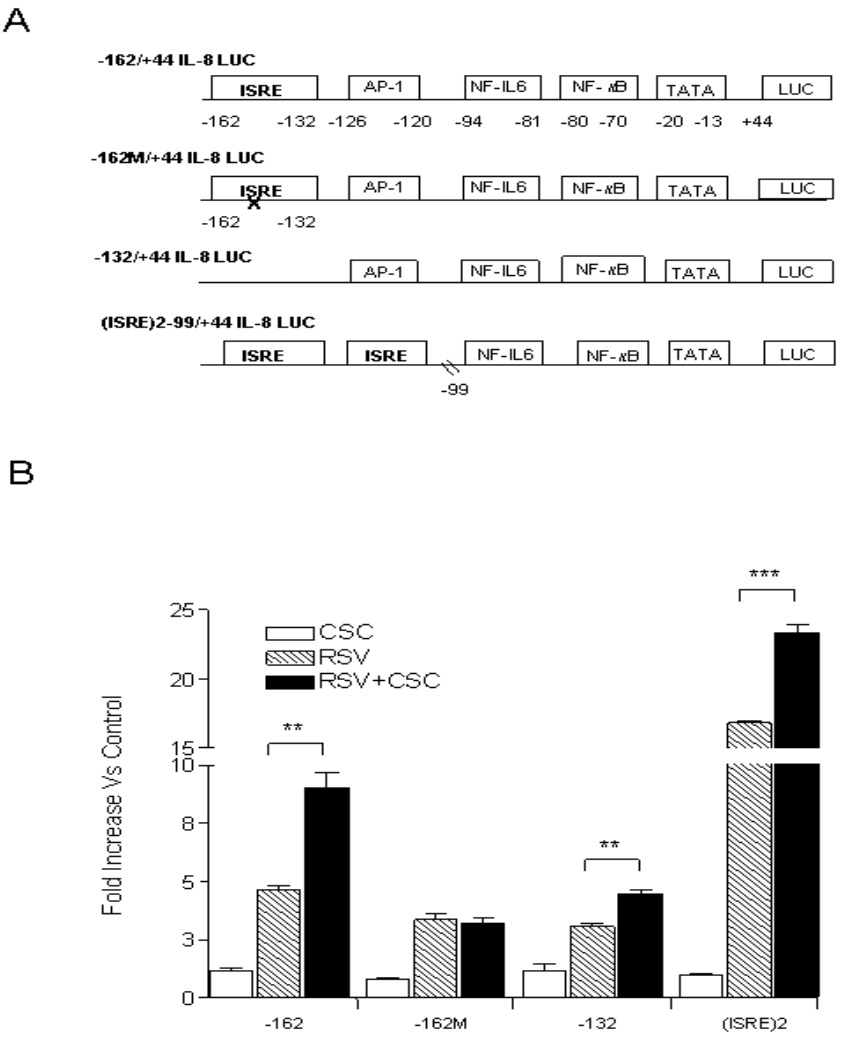

FIGURE 7.3 EFFECT OF CSC TREATMENT ON RSV-INDUCED IL-8 PROMOTER ACTIVATION. (A) Schematic representation of plasmid constructs containing 5' flanking region of the IL-8 promoter region, starting upstream at -162 bp, either wild type or containing modification of the ISRE binding site including ISRE deletion (-132 IL-8), ISRE mutation (-162M), two multiple ISRE binding sites, linked to a luciferase (LUC) reporter gene. Additional regulatory binding sites corresponding to the AP-1, NF-IL6, and NF-κB sites are also shown. The nucleotide numbers indicated their position in relationship to the IL-8 promoter transcriptional initiation site. (B) A549 cells were transfected with various hIL-8 LUC plasmids and treated with vehicle control DMSO or CSC and sham and RSV infected (MOI of 1). Treated and infected cells were harvested at 6 h p.i. to measure luciferase activity measured by luminometer. Data are presented as fold increases over control and are representative of three independent experiments. **p<0.01, ***p<0.001 RSV relative to RSV+CSC.

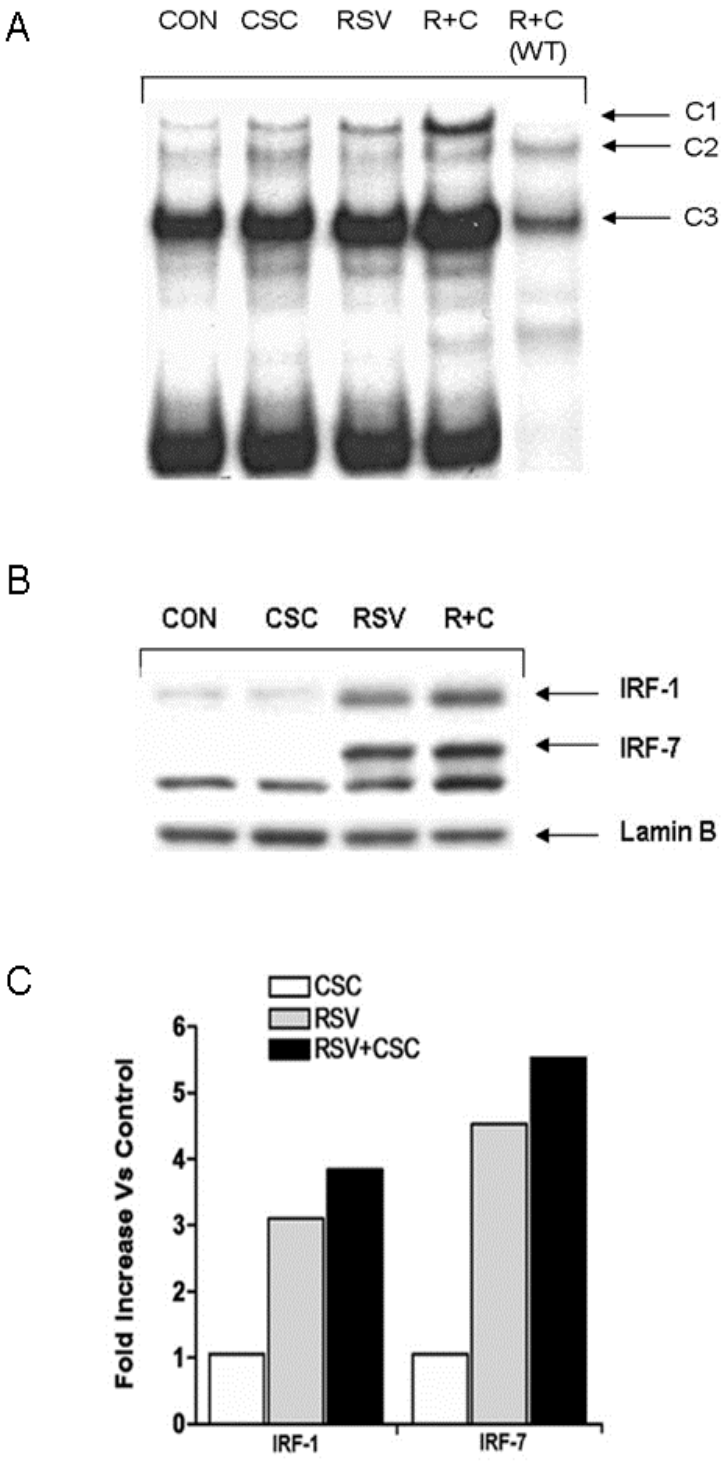

FIGURE 7.4 CSC CO-EXPOSURE ENHANCED RSV-INDUCED IRF PROTEIN ACTIVATION. (A) Nuclear extracts were prepared from the following treatment groups in vehicle+sham (CON), CSC+sham (CSC), vehicle+RSV (RSV), and RSV+CSC (R+C). Cells were harvested at 6 h p.i. and nuclear extracts were used for EMSA using used radiolabeled oligonucleotide corresponding to the IL-8 promoter ISRE site. For the competition assay, an excess of 2 pmol unlabeled wild-type (WT) ISRE probe was included in the binding reactions of RSV and CSC nuclear extracts. (B) Nuclear extracts from treated and infected A549 cells were fractionated by 10% SDS-PAGE, transferred to PVDF membranes and incubated with the appropriate polyclonal primary antibody. Proteins were detected by enhanced chemiluminescence and autoradiography. (C) Densitometric analysis of protein bands from single experiment, representative of two independent experiments.

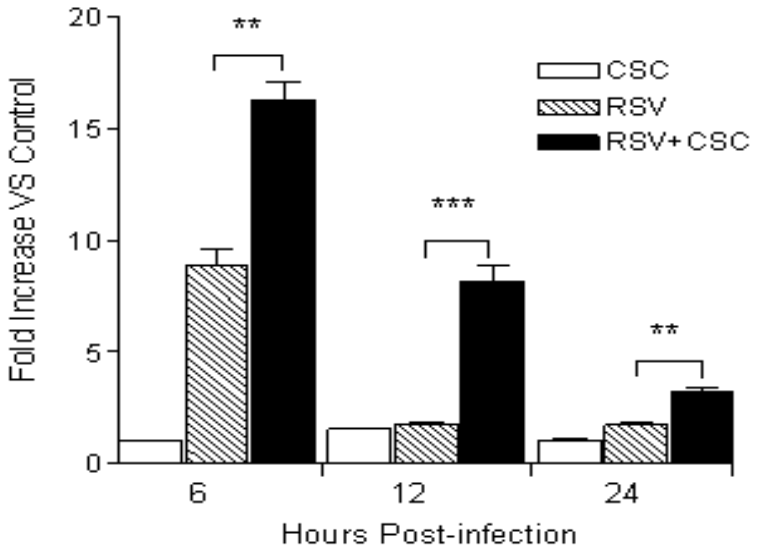

FIGURE 7.5 CSC CO-EXPOSURE ENHANCED RSV-INDUCED NF-κB-DRIVEN GENE TRANSCRIPTION. 293 cells were transiently transfected with a luciferase reporter construct containing multiple IL-8 NF-κB binding sites. Cells were then treated with DMSO (vehicle control) and CSC. Each treatment group was sham and RSV infected. At various times p.i. cells were harvested to measure luciferase activity. Data are presented as fold increases over control and are representative of three independent experiments. **p<0.01, ***p<0.001 RSV relative to RSV+CSC

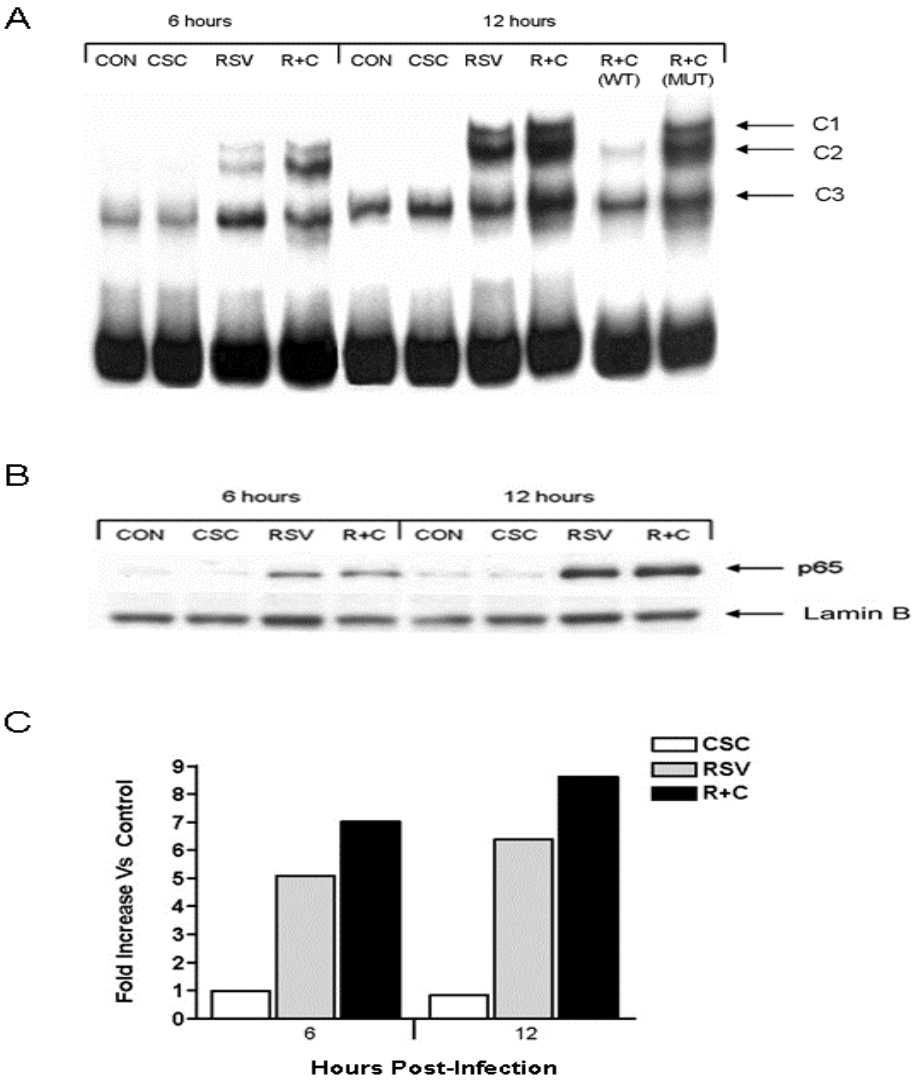

FIGURE 7.6 CSC CO-EXPOSURE ENHANCED RSV-INDUCED NF-κB ACTIVATION. (A) Nuclear extracts were prepared from uninfected (CON), RSV infected, CSC treated and CSC+RSV (R+C) exposed cells at 6 and 12 h p.i. and used for EMSA using a radiolabeled oligonucleotide corresponding to the IL-8 promoter NF-κB site. For the competition assay, an excess of 2 pmol unlabeled wild-type (WT) and mutated (MUT) probe was included in the binding reactions of RSV and CSC nuclear extracts. (B) Nuclear extracts from treated and infected A549 cells were fractionated by 10% SDS-PAGE, transferred to PVDF membranes and incubated with the appropriate polyclonal primary antibody. Proteins were detected by enhanced chemiluminescence and autoradiography. (C) Densitometric analysis of protein bands from single experiment, representative of two independent experiments.

DISCUSSION

In the past few decades, there has been increasing evidence that passive smoking or exposure to ETS increases the incidence and severity of respiratory viral infections. In a recent study, children of smoking parents who were hospitalized with RSV bronchiolitis had a higher level of serum cotinine, a metabolite of nicotine and biomarker of ETS exposure, than children of smoking parents hospitalized with non-respiratory symptoms (5). After one month, children diagnosed with RSV bronchiolitis still had higher cotinine levels than controls suggesting that heavy exposure to ETS may contribute to the development of a more severe respiratory infection (5). An additional investigation, using a neonatal mouse model of RSV infection exposed daily to cigarette smoke, found a priming effect of smoke on RSV replication, diminished Th1, and enhanced Th2 T-cell responses following secondary RSV infection, suggesting that cigarette smoke exposure alters immune responses to RSV infection (182). These investigations on the interactions between RSV and cigarette smoke indicate that cigarette smoke exposure has the potential to modulate and exacerbate the host inflammatory/immune response to RSV infection.

Fundamental events in RSV-induced pulmonary inflammation are thought to involve responses of the airway epithelial cell to RSV infection. Although the pathophysiology of RSV-induced airway disease is not clearly understood, an initial step in RSV-induced pulmonary inflammation is the release of inflammatory chemokines from infected epithelial cells, (13,82). IL-8 is a potent chemokine in recruiting neutrophils and other inflammatory cells. Previous studies have shown that RSV is a potent inducer of IL-8 secretion by airway epithelial cells (183) and that high levels of IL-8 protein have been detected in the nasal lavage washes of children with RSV upper respiratory infections (184). Therefore increased IL-8 chemokine expression by external

environmental stimuli, such as cigarette smoke, could be a critical factor in modulating the severity of RSV-induced lung disease.

In this study, we used CSC, which represents the insoluble tar and particulate component of mainstream cigarette smoke. Cigarette smoke is a highly complex mixture consisting of approximately 4000 chemicals distributed within the gas or particulate phases (185). CSC, a semblance to the mixture of mainstream cigarette smoke, was used as a feasible and readily accessible *in vitro* representative of cigarette smoke. CSC has been shown to activate epithelial and immune cells and stimulate the secretion of inflammatory mediators into the airway mucosa (42,177). Although others have noted a stimulatory and proinflammatory effect of CSC on airway epithelial cells, there are currently no studies that describe the influences of cigarette smoke on the responses of human respiratory epithelial cells to RSV infection.

Our results show that CSC and RSV co-exposure led to an increase in both MCP-1 and IL-8 chemokine gene and protein expression in airway epithelial cells. Increased IL-8 expression was due to enhanced promoter activation following RSV and CSC co-exposure. IL-8 promoter deletion and mutation analysis identified the region between -162 nt and -132 nt as a critical regulatory region contributing to the synergistic transcriptional activation of the IL-8 promoter. We have previously shown that this region contains an ISRE binding site which is as an important regulatory site for IL-8 gene transcription not only in response to RSV infection, but also to other stimuli such as *H. pylori* and hepatitis C virus, (186-187). Co-exposure of a promoter containing a single nucleotide mutation of the ISRE site (-162M IL-8) failed to enhance IL-8 promoter activation, in comparison to RSV stimulation alone. Similarly, co-stimulation of the -132 nt IL-8 promoter, which lacks the ISRE site, resulted in a loss of synergistic induction of promoter activation. On the other hand, the presence of multiple copies of the (ISRE)

upstream an inert IL-8 promoter, restored the enhanced IL-8 promoter activation observed in response to CSC and RSV co-exposure. In agreement with the promoter studies, we found that CSC and RSV co-exposure enhanced nuclear translocation and DNA binding of IRF proteins, which are known to bind to the IL-8 promoter ISRE site.

Although IL-8 transcriptional regulation is modulated by a variety of transcription factors including IRF proteins, NF-κB is essential for IL-8 gene expression in response to all different kind of stimuli. NF-κB has been shown to regulate IL-8 gene expression in response to cigarette smoke alone and to RSV (23,42). Our gene reporter studies, using multimers of the IL-8-NF-κB site showed that, while CSC alone did not strongly induce NF-κB-driven gene transcription, a heightened response was observed with CSC and RSV co-stimulation. Furthermore, CSC and RSV co-stimulation enhanced nuclear translocation and DNA binding of NF-κB proteins, suggesting that CSC likely enhanced RSV-induced IL-8 promoter activation also by contributing to NF-κB activation. The lack of an effect of CSC stimulation alone on NF-κB activation observed in our study is in agreement with a previous study showing that cigarette smoke plays a more important role in inducing NF-κB activation in normal cells compared to cancerous cell lines, (42).

Both RSV and CSC when treated independently of each other have been shown to induce oxidative stress in airway epithelial cells (29,188). We have reported that NF-κB is a redox sensitive transcription factor (189) that RSV –induced IRF-1, and -7 are redox sensitive (29) Therefore, the generation of ROS induced by RSV and CSC co-exposure could serve as a plausible common mediator of transcriptional changes induced by RSV and CSC. Further studies include examining the role of ROS in chemokine expression during co-exposure with the aim of determining whether antioxidant treatment attuenuates chemokine expression and inflammation.

Differential levels of IL-8 gene expression are likely to play an important role in the pathogenesis of RSV-induced lung disease, as recently shown by the association of single gene polymorphisms of the IL-8 promoter with increased disease severity in children with RSV infection, (190)(191). The finding that ETS exposure contributes to the severity of RSV LRTI, (172), could in part be explained by a priming effect of smoke on RSV-induced secretion of proinflammatory mediators by infected airway epithelial cells, which results in enhanced pulmonary inflammation. More studies are needed to fully elucidate the mechanism by which ETS enhances the severity RSV-induced disease, such information could reinforce efforts aimed at reducing ETS exposure in infants particularly, in households were the primary caretakers are smokers. Minimizing the risk of ETS exposure could also potentially decrease the long-term consequences of RSV infection, such as development of asthma.

CHAPTER 8: CONCLUSION

RSV-induced lung inflammation is mediated by the expression of a number of inflammatory mediators particularly chemokines. Therefore, it is important to understand the molecular mechanisms involved in RSV-induced inflammatory gene expression, in order to develope novel therapeutic strategies for the treatment of viral-induced lung inflammation. A unifying question for all of the studies conducted either *in vitro* or *in vivo* was the mechanism by which RSV induced inflammatory mediators. Experiments in chapters 2-4 addressed the first part of the primary hypothesis that a role for **ROS in the pathogenesis of RSV lung injury is the inducing of inflammatory gene expression.**

Major observation included evidence that RSV-induced activation of IRF -1 and -7 gene expression involve the redox sensitive activation of STAT transcription factors, and that treatment with the antioxidant specifically BHA blocked RSV-induced IRF activation by inhibiting STAT activation. BHA blocked RSV-induced STAT phosphorylation, nuclear translocation, and DNA-binding to IRF-1 and -7 promoters which suggests that RSV-induced STAT activation is ROS dependent. The NAD(P)H oxidase inhibitor DPI also blocked RSV-induced STAT activation which further supports a role for ROS likely produced through the NAD(P)H oxidase system, in STAT activation. We also found that RSV inhibited tyrosine phosphatases and that antioxidant treatment restored tyrosine phosphatase activity which indicates that tyrosine phosphatases are redox sensitive regulators of STAT proteins.

Experiments, in chapter 3 revealed that ROS played a major role in the activation of IRF-3. Treatment with a broad range of antioxidants specifically BHA and NAD(P)H

oxidase inhibitors blocked RSV-induced IKKε expression, IRF-3 serine phosphorylation, and RANTES secretion identifying this pathway as redox-sensitive. In this study a novel observation was made that RSV-induced ROS generation was responsible for IKKε activation. This observation identified a new molecular target for strategies aimed to attenuate inflammatory responses associated with RSV infection.

Experiments for chapter 4, tested the second part of the primary hypothesis that **RSV infection induces the condition of oxidative stress in the airway mucosa**. We obtain the first documentation of RSV-induced oxidative stress in the lung, as indicated by elevated levels of the lipid peroxidation products MDA and 4-HNE in the BAL of RSV infected mice. Although BHA treatment had previously been reported to reduce cellular signaling events leading to inflammatory gene expression, it was not known whether attenuation of ROS production by antioxidant treatment would be of clinical benefit. We found that treatment with BHA decreased RSV-induced lipid peroxidation and ameliorated RSV induced body weight loss and clinical illness. BHA treatment also significantly reduced the levels of RSV-induced secretion of chemokines, cytokines, and immuno-modulators in the lung. We also found that antioxidant treatment attenuated RSV-induced airway hyper-responsiveness which could have been mediated by the observed reduction in leukotriene C_4 secretion. Our conclusion is that the ability of antioxidants to attenuate the symptoms and pathology of RSV infection warrants further investigation. Antioxidants could provide a novel therapeutic approach to ameliorating RSV-induced acute lung inflammation and potentially prevent the long term consequences associated with RSV infection, such as bronchial asthma.

However, BHA treatment of acute RSV infection in the mouse model also increased RSV viral yield in the lung. Therefore, to address this negative side effect we investigated the effects of combining BHA with the potent antiviral IFN-α based on prior reports from our lab that postinfection treatment with IFN-α decreased RSV replication in the lung (35). Our experiments demonstrated for the first time that combination therapy, with an antioxidant and antiviral, alleviated symptoms associated with the onset of RSV infection including body weight loss. In addition, combination therapy was more effective than BHA alone in attenuating RSV-induced illness score, inflammation and viral titer. Thus, BHA and post-infection administration of IFN-α delayed an already launched inflammatory cascade, alleviated the severity of RSV-induced acute lung disease and prevented further RSV replication.

Experiments for chapter 6 produced the novel findings that RSV is a potent inducer of PARP enzymatic activity in vivo and that pharmacological inhibition with of PARP with INO-1001 abolished RSV-induced PARP activity and attenuated the release of pro-inflammatory mediators, cellular influx into the airways, and reduced lung inflammation. Further studies on the protective role of PARP inhibition of RSV-induced acute lung inflammation could substantiate PARP as a therapeutic target for ameliorating RSV-induced lung disease.

Experiments for chapter 7 were designed to investigate the potentially synergistic effects of cigarette smoke condensate and RSV on chemokine expression in airway epithelial cells. Results indicated that CSC and RSV co-exposure synergistically induced IL-8 and MCP-1 chemokine gene expression and protein secretion. Investigation into the

mechanism by which CSC increased RSV-induced IL-8 gene expression identified the ISRE and NF-κB site of IL-8 promoter, as a critical regions responsible for the synergistic increase in IL-8 gene transcription through enhanced activation of redox sensitive transcription factors IRF-1, -7, and NF-κB. A recent study showed that low concentrations of CSC (1ug/ml) did not significantly induce ROS or alter cell viability, however higher concentrations of 10ug/ml led to a significant increase in ROS production and decreased GSH/GSSG ratio, a marker of oxidative stress (192). We have found that RSV also induced a number of oxidative stress parameters in A549 cells (193). Therefore future studies involve a dose and time dependent investigation of CSC and RSV to determine whether CSC enhances RSV-induced chemokine expression by further stimulating ROS production or by altering intracellular redox status. Our findings demonstrate that a combined exposure to CSC and RSV synergistically increased chemokine expression in airway epithelial cells, which suggests that CSC enhances the exuberant immune response to RSV by stimulating overlapping signal transduction pathways for the release of pro-inflammatory chemokines. Therefore, prevention efforts aimed at decreasing cigarette smoke exposure in infants could ultimately decrease the severity of RSV-induced lung disease.

Collectively from the studies of this dissertation, we make the following conclusions: 1) RSV-induced ROS serve as signaling molecules for several signal transduction cascades that lead to inflammatory gene expression. 2) Identification of redox-sensitive pathways involved in RSV-stimulated chemokine gene expression revealed numerous therapeutic targets which we demonstrated to be easily abrogated by

antioxidant administration. 3) RSV infection enhanced intracellular ROS production in airway epithelial cells and also induced the condition of oxidative stress in the airway mucosa of the lung. 4) Antioxidant administration diminished RSV-induced oxidative stress responses in the lung, significantly improved the severity of disease and reduced pulmonary inflammation, but enhanced viral load in the lungs. 5) Combining the antioxidant with the antiviral IFN-α had the increased benefit of diminishing viral load which suggests that combination therapy could be a more effective treatment for acute RSV infection. 6) Novel observation about the beneficial effects of inhibiting the oxidative activation of PARP during RSV infection, identified a new target to mediate RSV-induced inflammation. Co-exposure with CSC heightened the release of RSV-induced chemokines, which suggests a mechanism by which this environmental pollutant potentiates RSV lung inflammation; the foremost process in the pathogenesis of RSV induced disease. Together these studies identified new areas of therapeutic intervention that have yet to be clinically explored. This is clinically relevant since RSV infection is pervasive and persistent, lacks of an effective vaccine, and is associated with appreciable morbidity and mortality, particularly in infants and the elderly.

REFERENCES

1. Ruuskanen, O. and Ogra, P. L. (1993). Respiratory syncytial virus. *Curr Prob Pediat* **2,** 50-79.

2. Glezen, W. P., Taber, L. H., and Frank, A. L. (1986). Risk of primary infection and reinfection with respiratory syncytial virus. *Am J Dis Child* **140,** 543-546.

3. Simoes, E. A., Sondheimer, H. M., Top Jr., F. H., Meissner, H. C. W. R. C., Kramer, R. M., and Groothuis, J. R. (1998). Respiratory syncytial virus immune globulin for prophylaxis against respiratory syncytial virus disease in infants and children with congenital heart disease. The Cardiac Study Group. *J Pediatr* **133,** 492-499.

4. Bradley, J. P., Bacharier, L. B., Bonfiglio, J., Schechtman, K. B., Strunk, R., Storch, G., and Castro, M. (2005). Severity of respiratory syncytial virus bronchiolitis is affected by cigarette smoke exposure and atopy *Pediatrics* **115,** e7-14.

5. Gurkan, F., Kiral, A., Dagli, E., and Karakoc, F. (2000). The effect of passive smoking on the development of respiratory syncytial virus bronchiolitis. *Eur J Epidemiol* **16,** 465-468.

6. Al Shehri, M. A., Sadeq, A., and Quli, K. (2005). Bronchiolitis in Abha, Southwest Saudi Arabia: viral etiology and predictors for hospital admission. *West Afr J Med* **24,** 299-304.

7. Sigurs, N., Bjarnason, R., Sigurbergsson, F., Kjellman, B., and Bjorksten, B. (1995). Asthma and immunoglobulin E antibodies after respiratory syncytial virus bronchiolitis: a prospective cohort study with matched controls. *Pediatrics* **95,** 500-505.

8. Sly, P. D. and Hibbert, M. D. (1989). Childhood asthma following hospitalization with acute viral bronchiolitis in infancy. *Pediatr Pulmonol* **7,** 153-158.

9. Hall, C. B. (2001). Respiratory syncytial virus and parainfluenza virus. *N Engl J Med* **344,** 1917-1928.

10. Gardner, P. S., McQuillin, J., and Court, S. D. (1970). Speculation on pathogenesis in death from respiratory syncytial virus infection. *Brit Med J* **1,** 327-330.

11. Casola, A., Garofalo, R. P., Jamaluddin, M., Vlahopoulos, S., and Brasier, A. R. (2000). Requirement of a novel upstream response element in RSV induction of interleukin-8 gene expression: stimulus-specific differences with cytokine activation. *J Immunol* **164,** 5944-5951.

12. Casola, A., Henderson, A., Liu, T., Garofalo, R. P., and Brasier, A. R. (2002). Regulation of RANTES promoter activation in alveolar epithelial cells after cytokine stimulation. *Am J Physiol Lung Cell Mol Physiol* **283,** L1280-L1290.

13. Olszewska-Pazdrak, B., Casola, A., Saito, T., Alam, R., Crowe, S. E., Mei, F., Ogra, P. L., and Garofalo, R. P. (1998). Cell-specific expression of RANTES, MCP-1, and MIP-1alpha by lower airway epithelial cells and eosinophils infected with respiratory syncytial virus. *J Virol* **72,** 4756-4764.

14. Becker, S. and Soukup, J. M. (1999). Airway epithelial cell-induced activation of monocytes and eosinophils in respiratory syncytial viral infection. *Immunobiology* **201,** 88-106.

15. Miller, A. L., Bowlin, T. L., and Lukacs, N. W. (2004). Respiratory syncytial virus-induced chemokine production: linking viral replication to chemokine production in vitro and in vivo. *J Infect Dis* **189,** 1419-1430.

16. Arnold, R., Humbert, B., Werchau, H., Gallati, H., and Konig, W. (1994). Interleukin-8, interleukin-6, and soluble tumour necrosis factor receptor type I release from a human pulmonary epithelial cell line (A549) exposed to respiratory syncytial virus. *Immunology* **82,** 126-133.

17. Mazzarella, G., Ferraraccio, F., Prati, M. V., Annunziata, S., Bianco, A., Mezzogiorno, A., Liguori, G., Angelillo, I. F., and Cazzola, M. (2007). Effects of diesel exhaust particles on human lung epithelial cells: an in vitro study. *Respir Med* **101,** 1155-1162.

18. Sexton, K. G., Jeffries, H. E., Jang, M., Kamens, R. M., Doyle, M., Voicu, I., and Jaspers, I. (2004). Photochemical products in urban mixtures enhance inflammatory responses in lung cells. *Inhal Toxicol* **16 Suppl 1,** 107-114.

19. Puljic, R. and Pahl, A. (2004). Smoke induced changes in epithelial cell gene expression: development of an in vitro model for COPD. *ALTEX* **21,** 3-7.

20. Bacon, K. B. and Schall, T. J. (1996). Chemokines as mediators of allergic inflammation. *Int Arch Allergy Immunol* **109,** 97-109.

21. Gonzalo, J. A., Lloyd, C. M., Wen, D., Albar, J. P., Wells, T. N. C., Proudfoot, A., Martinez-A, C., Dorf, M., Bjerke, T., Coyle, J., and Gutierrez-Ramos, J. C. (1998). The coordinated action of CC chemokines in the lung orchestrates allergic inflammation and airway hyperresponsiveness. *J Exp Med* **188,** 157-167.

22. Alam, R., York, J., Boyers, M., Stafford, S., Grant, J. A., Lee, J., Forsythe, P., Sim, T., and Ida, N. (1996). Increased MCP-1, RANTES, and MIP-1alpha in bronchoalveolar lavage fluid of allergic asthmatic patients. *Am J Respir Crit Care Med* **153,** 1398-1404.

23. Garofalo, R. P., Sabry, M., Jamaluddin, M., Yu, R. K., Casola, A., Ogra, P. L., and Brasier, A. R. (1996). Transcriptional activation of the interleukin-8 gene by respiratory syncytial virus infection in alveolar epithelial cells: Nuclear translocation of the RelA transcription factor as a mechanism producing airway mucosal inflammation. *J Virol* **70,** 8773-8781.

24. Zhang, Y., Luxon, B. A., Casola, A., Garofalo, R. P., Jamaluddin, M., and Brasier, A. R. (2001). Expression of respiratory syncytial virus-induced chemokine gene networks in lower airway epithelial cells revealed by cDNA microarrays.*J Virol* **75,** 9044-9058.

25. Garofalo, R. P., Patti J, Hintz KA, Hill V, Ogra, P. L., and Welliver, R. C. (2001). Macrophage inflammatory protein-1alpha (not T helper type 2 cytokines) is associated with severe forms of respiratory syncytial virus bronchiolitis. *J Infect Dis* **184,** 393-399.

26. Teran, L. M., Seminario, M. C., Shute, J. K., Papi, A., Compton, S. J., Low, J. L., Gleich, G. J., and Johnston, S. L. (1999). RANTES, macrophage-inhibitory protein 1alpha, and the eosinophil product major basic protein are released into upper respiratory secretions during virus-induced asthma exacerbations in children. *J Infect Dis* **179,** 677-681.

27. Sheeran, P., Jafri, H., Carubelli, C., Saavedra, J., Johnson, C., Krisher, K., Sanchez, P. J., and Ramilio, M. O. (1999) Elevated cytokine concentrations in the nasopharyngeal and tracheal secretions of children with respiratory syncytial virus disease. *Pediatrics Infectious Diseases Journal* **18,** 115-122.

28. Haeberle, H. A., Kuziel, W. A., Dieterich, H. J., Casola, A., Gatalica, Z., and Garofalo, R. P. (2001). Multiple *cis* regulatory elements control RANTES promoter activity in alveolar epithelial cells infected with respiratory syncytial virus. *J Virol* **75,** 878-890.

29. Casola, A., Burger, N., Liu, T., Jamaluddin, M., Brasier A.R., and Garofal, R. P. (2001). Oxidant tone regulates RANTES gene expression in airway epithelial cells infected with respiratory syncytial virus. Role in viral-induced interferon regulatory factor activation. *J Biol Chem* **276,** 19715-19722.

30. Schwarz, K. B. (1996). Oxidative stress during viral infection: a review. *Free RadicBiol Med* **21,** 641-649.

31. Allen, R. G. and Tresini, M. (2000). Oxidative stress and gene regulation. *Free Rad Biol Med* **28,** 463-499.

32. Nguyen, H., Hiscott, J., and Pithas, P. M. (1997). The growing family of interferon regulatory factors.*Cytokine Growth Factor Rev* **8,** 293-312.

33. Morcillo, E. J., Estrela, J., and Cortijo, J. (1999). Oxidative stress and pulmonary inflammation: pharmacological intervention with antioxidants. *Pharmacol Res* **40,** 393-404.

34. Soobrattee, M. A., Neergheen, V. S., Luximon-Ramma, A., Aruoma, O. I., and Bahorun, T. (2005). Phenolics as potential antioxidant therapeutic agents: mechanism and actions.*Mutat Res* **579,** 200-213.

35. Guerrero-Plata, A., Baron, S., Poast, J. S., Adegboyega, P. A., Casola, A., and Garofalo, R. P. (2005). Activity and regulation of alpha interferon in respiratory syncytial virus and human metapneumovirus experimental infections. *J Virol* **79,** 10190-10199.

36. Shall, S. and de Murcia, G. (2000). Poly(ADP-ribose) polymerase-1: what have we learned from the deficient mouse model? *Mutat.Res.* **460,** 1-15.

37. Szabo, C., Virag, L., Cuzzocrea, S., Scott, G. S., Hake, P., O'Connor, M. P., Zingarelli, B., Salzman, A., and Kun, E. (1998). Protection against peroxynitrite-induced fibroblast injury and arthritis development by inhibition of poly(ADP-ribose) synthase. *Proc Natl Acad Sci USA* **95,** 3867-3872.

38. Virag, L., Szabo, E., Gergely, P., and Szabo, C. (2003). Peroxynitrite-induced cytotoxicity: mechanism and opportunities for intervention. *Toxicol Lett* **140-141,** 113-124.

39. Bradley, J. P., Bacharier, L. B., Bonfiglio, J., Schechtman, K. B., Strunk, R., Storch, G.., and Castro, M. (2005) *Pediatrics* **115,** e7-14.

40. Cook, D. G. and Strachan, D. P. (1999) *Thorax* **54,** 357-366.

41. Ayer, H. E. and Yeager, D. W. (1982) *Am.J.Public Health* **72,** 1283-1285.

42. Hellermann, G. R., Nagy, S. B., Kong, X., Lockey, R. F., and Mohapatra, S. S. (2002) *Respir.Res.* **3,** 22.

43. Hall, C. B. and McCarthy, C. A. (1995) Respiratory Syncytial Virus. In Mandel, G. L., Bennett, J. E., and Dolin, R., editors. *Principles and practice of infectious diseases*, Churchill Livingston, New York.

44. Garofalo, R. P. and Haeberle, H. (2000) *Am J Respir Cell Mol Biol* **23,** 581-585.

45. Casola, A., Garofalo, R. P., Haeberle, H., Elliott, T. F., Lin, A., Jamaluddin, M., and Brasier A.R. (2001) *J Virol* **75,** 6428-6439.

46. Prasad Gabbita, S., Robinson, K. A., Stewart, C. A., Floyd, R. A., and Hensley, K. (2000) *Arch Biochem Biophysics* **376,** 1-136.

47. Ueba, O. (1978). Respiratory syncytial virus. I. Concentration and purification of the infectious virus. *Acta Med Okayama* **32,** 265-272.

48. Patel, J. A., Kunimoto, M., Sim, T. C., Garofalo, R., Eliott, T., Baron, S., Ruuskanen, O., Chonmaitree, T., Ogra, P. L., and Schmalstieg, F. (1995). Interleukin-1 alpha mediates the enhanced expression of intercellular adhesion molecule-1 in pulmonary epithelial cells infected with respiratory syncytial virus. *Am J Resp Cell Mol* **13,** 602-609.

49. Zhang, Y., Jamaluddin, M., Wang, S., Tian, B., Garofalo, R. P., Casola, A., and Brasier, A. R. (2003). Ribavirin treatment up-regulates antiviral gene expression via the interferon-stimulated response element in respiratory syncytial virus-infected epithelial cells.*J Virol* **77,** 5933-5947.

50. Sims, S. H., Cha, Y., Romine, M. F., Gao, P. Q., Gottlieb, K., and Deisseroth, A. B. (1993). A novel interferon-inducible domain: structural and functional analysis of the human interferon regulatory factor 1 gene promoter. *Mol Cell Biol* **13,** 690-702.

51. Lu, R., Au, W. C., Yeow, W. S., Hageman, N., and Pitha, P. M. (2000). Regulation of the promoter activity of interferon regulatory factor-7 gene. Activation by interferon snd silencing by hypermethylation. *J Biol Chem* **275** 31805-12.

52. Harada, H., Takahashi, E., Itoh, S., Harada, K., Hori, T. A., and Taniguchi, T. (1994). Structure and regulation of the human interferon regulatory factor 1 (IRF-1) and IRF-2 genes: implications for a gene network in the interferon system. *Mol Cell Biol* **14,** 1500-1509.

53. Nelson, P. J., Kim, H. T., Manning, W. c., Goralski, T. J., and Krensky, A. M. (1993). Genomic organization and transcriptional regulation of the RANTES chemokine gene. *J Immunol* **151,** 2601-2612.

54. Boehlk, S., Fessele, S., Mojaat, A., Miyamoto, N. G., Werner, T., Nelson, E. L., Schlondorff, D., and Nelson, P. J. (2000). ATF and Jun transcription factors, acting through an Ets/CRE promoter module, mediate lipopolysaccharide inducibility of the chemokine RANTES in monocytic Mono Mac 6 cells. *Eur J Immunol* **30,** 1102-1112.

55. Stevens, A. M., Wang, Y. F., Sieger, K. A., Lu, H. F., and Yu-Lee, L. Y. (1995). Biphasic transcriptional regulation of the interferon regulatory factor-1 gene by prolactin: involvement of gamma-interferon-activated sequence and Stat-related proteins. *Mol Endocrinol* **9,** 513-525.

56. Imada, K. and Leonard, W. J. (2000). The Jak-STAT pathway. *Mol Immunol* **37,** 1-11.

57. Leonard, W. J. and O'Shea, J. J. (1998). Jaks and STATs: biological implications. *Annu Rev Immunol* **16,** 293-322.

58. Chaturvedi, P., Reddy, M. V., and Reddy, E. P. (1998). Src kinases and not JAKs activate STATs during IL-3 induced myeloid cell proliferation. *Oncogene* **16,** 1749-1758.

59. Moon, S. K., Lee, H. Y., Li, J. D., Nagura, M., Kang, S. H., Chun, Y. M., Linthicum, F. H., Ganz, T., Andalibi, A., and Lim, D. J. (2002). Activation of a Src-dependent Raf-MEK1/2-ERK signaling pathway is required for IL-1alpha-induced upregulation of beta-defensin 2 in human middle ear epithelial cells. *Biochim Biophys Acta* **1590,** 41-51.

60. Hanke, J. H., Gardner, J. P., Dow, R. L., Changelian, P. S., Brissette, W. H., Weringer, E. J., Pollok, B. A., and Connelly, P. A. (1996). Discovery of a novel, potent, and Src family-selective tyrosine kinase inhibitor. Study of Lck- and FynT-dependent T cell activation. *J Biol Chem* **271,** 695-701.

61. Heffetz, D., Bushkin, I., Dror, R., and Zick, Y. (1990). The insulinomimetic agents H2O2 and vanadate stimulate protein tyrosine phosphorylation in intact cells. *J Biol Chem* **265,** 2896-2902.

62. Babior, B. M. (1999). NADPH oxidase: an update. *Blood* **93,** 1464-1476.

63. Flory, E., Kunz, M., Scheller, C., Jassoy, C., Stauber, R., Rapp, U. R., and Ludwig, S. (2000). Influenza virus-induced NF-kappaB-dependent gene expression is mediated by overexpression of viral proteins and involves oxidative radicals and activation of IkappaB kinase. *J Biol Chem* **275,** 8307-8314.

64. Simon, A. R., Rai, U., Fanburg, B. L., and Cochran, B. H. (1998). Activation of the JAK-STAT pathway by reactive oxygen species. *Am J Physiol* **275,** C1640-C1652.

65. Maziere, C., Conte, M. A., and Maziere, J. C. (2001). Activation of JAK2 by the oxidative stress generated with oxidized low-density lipoprotein. *Free Radic Biol Med* **31,** 1334-1340.

66. Maziere, C., Alimardani, G., Dantin, F., Dubois, F., Conte, M. A., and Maziere, J. C. (1999). Oxidized LDL activates STAT1 and STAT3 transcription factors: possible involvement of reactive oxygen species. *FEBS Lett* **448,** 49-52.

67. Gong, G., Waris, G., Tanveer, R., and Siddiqui, A. (2001). Human hepatitis C virus NS5A protein alters intracellular calcium levels, induces oxidative stress, and activates STAT-3 and NF-kappa B. *Proc Natl Acad Sci USA* **98,** 9599-9604.

68. Waris, G., Huh, K. W., and Siddiqui, A. (2001). Mitochondrially associated hepatitis B virus X protein constitutively activates transcription factors STAT-3 and NF-kappa B via oxidative stress. *Mol Cell Biol* **21,** 7721-7730.

69. Lim, C. P. and Cao, X. (2001). Regulation of Stat3 activation by MEK kinase 1. *J.Biol.Chem.* **276,** 21004-21011.

70. Denu, J. M. and Tanner, K. G. (1998). Specific and reversible inactivation of protein tyrosine phosphatases by hydrogen peroxide: evidence for a sulfenic acid intermediate and implications for redox regulation. *Biochemistry* **37,** 5633-5642.

71. Robinson, K. A., Stewart, C. A., Pye, Q., Floyd, R. A., and Hensley, K. (1999). Basal protein phosphorylation is decreased and phosphatase activity increased by an antioxidant and a free radical trap in primary rat glia. *Arch Biochem Biophys* **365,** 211-215.

72. Meng, T. C., Fukada, T., and Tonks, N. K. (2002). Reversible oxidation and inactivation of protein tyrosine phosphatases in vivo. *Mol Cell* **9,** 387-399.

73. Haque, S. J., Flati, V., Deb, A., and Williams, B. R. (1995). Roles of protein-tyrosine phosphatases in Stat1 alpha-mediated cell signaling. *J Biol Chem* **270,** 25709-25714.

74. Tourkine, N., Schindler, C., Larose, M., and Houdebine, L. M. (1995). Activation of STAT factors by prolactin, interferon-gamma, growth hormones, and a tyrosine phosphatase inhibitor in rabbit primary mammary epithelial cells. *J Biol Chem* **270,** 20952-20961.

75. Duff, J. L., Quinlan, K. L., Paxton, L. L., Naik, S. M., and Caughman, S. W. (1997). Pervanadate mimics IFNgamma-mediated induction of ICAM-1 expression via activation of STAT proteins. *J Invest Dermatol* **108,** 295-301.

76. Droge, W. (2002). Free radicals in the physiological control of cell function. *Physiol Rev* **82,** 47-95.

77. Schieffer, B., Luchtefeld, M., Braun, S., Hilfiker, A., Hilfiker-Kleiner, D., and Drexler, H. (2000). Role of NAD(P)H oxidase in angiotensin II-induced JAK/STAT signaling and cytokine induction. *Circ Res* **87,** 1195-1201.

78. Simon, A. R., Vikis, H. G., Stewart, S., Fanburg, B. L., Cochran, B. H., and Guan, K. L. (2000). Regulation of STAT3 by direct binding to the Rac1 GTPase. *Science* **290,** 144-147.

79. Aherne, W. T., Bird, T., Court, S. D. B., Gardner, P. S., and McQuillin, J. (1970). Pathological changes in virus infections of the lower respiratory tract in children.*J Clin Path* **23,** 7-18.

80. Hall, C. B. (1999). Respiratory syncytial virus: A continuing culprit and conundrum. *J Pediatr* **135,** 2-7.

81. Hall, C. B. (2004). Respiratory syncytial virus. Editors. Feigin, D., Cherry, J. D., Demmler G.L., and Kaplan S. L. *Textbook of Pediatric Iinfectious Disease*, W.B.Saunders, Philidelphia, PA.

82. Saito, T., Deskin, R. W., Casola, A., Haeberle, H., Olszewska, B., Ernst, P. B., Alam, R., Ogra, P. L., and Garofalo, R. (1997). Respiratory syncytial virus induces selective production of the chemokine RANTES by upper airway epithelial cells. *J Infect Dis* **175,** 497-504.

83. Liu, T., Castro, S., Brasier, A. R., Jamaluddin, M., Garofalo, R. P., and Casola, A. (2004). Reactive oxygen species mediate virus-induced STAT activation: role of tyrosine phosphatases. *J Biol Chem* **279,** 2461-2469.

84. Lin, R., Heylbroeck, C., Pitha, P. M., and Hiscott, J. (1998). Virus-dependent phosphorylation of the IRF-3 transcription factor regulates nuclear translocation, transactivation potential, and proteasome-mediated degradation. *Mol Cell Biol* **18,** 2986-2996.

85. Fitzgerald, K. A., McWhirter, S. M., Faia, K. L., Rowe, D. C., Latz, E., Golenbock, D. T., Coyle, A. J., Liao, S. M., and Maniatis, T. (2003) *Nat.Immunol* **4,** 491-496.

86. Sharma, S., tenOever, B. R., Grandvaux, N., Zhou, G. P., Lin, R., and Hiscott, J. (2003). Triggering the interferon antiviral response through an IKK-related pathway. *Science* **300,** 1148-1151.

87. Servant, M. J., Grandvaux, N., tenOever, B. R., Duguay, D., Lin, R., and Hiscott, J. (2003). Identification of the minimal phosphoacceptor site required for in vivo activation of interferon regulatory factor 3 in response to virus and double-stranded RNA. *J Biol Chem* **278,** 9441-9447.

88. Chomczynski, P. and Sacchi, N. (1987). Single-step method of RNA isolation by acid guanidinium thiocyanate-phenol-chloroform extraction. *Anal Biochem* **162,** 156-159.

89. Peters, R. T., Liao, S. M., and Maniatis, T. (2000). IKKepsilon is part of a novel PMA-inducible IkappaB kinase complex. *Mol Cell* **5,** 513-522.

90. Mercurio, F., Zhu, H., Murray, B. W., Shevchenko, A., Bennett, B. L., Li, J., Young, D. B., Barbosa, M., Mann, M., Manning, A., and Rao, A. (1997). IKK-1 and IKK-2: cytokine-activated IkappaB kinases essential for NF-kappaB activation. *Science* **278,** 860-866.

91. Yamamoto, A., Hen, R., and Dauer, W. T. (2001). The ons and offs of inducible transgenic technology: a review. *Neurobiol Dis* **8,** 923-932.

92. Shimada, T., Kawai, T., Takeda, K., Matsumoto, M., Inoue, J., Tatsumi, Y., Kanamaru, A., and Akira, S. (1999). IKK-i, a novel lipopolysaccharide-inducible kinase that is related to IkappaB kinases. *Int Immunol* **11,** 1357-1362.

93. Olszewska-Pazdrak, B., Pazdrak, K., Ogra, P. L., and Garofalo, R. P. (1998). Respiratory syncytial virus-infected pulmonary epithelial cells induce eosinophil degranulation by a CD18-mediated mechanism. *J Immunol* **160,** 4889-4895.

94. Schwarzer, C., Machen, T. E., Illek, B., and Fischer, H. (2004). NADPH oxidase-dependent acid production in airway epithelial cells. *J Biol Chem* **279,** 36454-36461.

95. Tian B, Zhang Y, Luxon, B., Garofalo, R. P., Casola, A., Sinha, M., and Brasier A.R. (2002). Identification of NF-kappaB-dependent gene networks in respiratory syncytial virus-infected cells. *J Virol* **76,** 6800-6814.

96. Hemmi, H., Takeuchi, O., Sato, S., Yamamoto, M., Kaisho, T., Sanjo, H., Kawai, T., Hoshino, K., Takeda, K., and Akira, S. (2004). The roles of two IkappaB kinase-related kinases in lipopolysaccharide and double stranded RNA signaling and viral infection. *J Exp Med* **199,** 1641-1650.

97. Perry, A. K., Chow, E. K., Goodnough, J. B., Yeh, W. C., and Cheng, G. (2004). Differential requirement for TANK-binding kinase-1 in type I interferon responses to toll-like receptor activation and viral infection. *J Exp Med* **199,** 1651-1658.

98. Aupperle, K. R., Yamanishi, Y., Bennett, B. L., Mercurio, F., Boyle, D. L., and Firestein, G. S. (2001). Expression and regulation of inducible IkappaB kinase (IKK-i) in human fibroblast-like synoviocytes. *Cell Immunol* **214,** 54-59.

99. TenOever, B. R., Sharma, S., Zou, W., Sun, Q., Grandvaux, N., Julkunen, I., Hemmi, H., Yamamoto, M., Akira, S., Yeh, W. C., Lin, R., and Hiscott, J. (2004). Activation of TBK1 and IKKvarepsilon kinases by vesicular stomatitis virus infection and the role of viral ribonucleoprotein in the development of interferon antiviral immunity. *J Virol* **78,** 10636-10649.

100. Chu, W. M., Ostertag, D., Li, Z. W., Chang, L., Chen, Y., Hu, Y., Williams, B., Perrault, J., and Karin, M. (1999). JNK2 and IKKbeta are required for activating the innate response to viral infection. *Immunity* **11,** 721-731.

101. Delhase, M., Hayakawa, M., Chen, Y., and Karin, M. (1999). Positive and negative regulation of IkappaB kinase activity through IKKbeta subunit phosphorylation. *Science* **284,** 309-325.

102. Israel, A. (2000). The IKK complex: an integrator of all signals that activate NF-kappaB? *Trends Cell Biol* **10,** 129-133.

103. Kishore, N., Huynh, Q. K., Mathialagan, S., Hall, T., Rouw, S., Creely, D., Lange, G., Caroll, J., Reitz, B., Donnelly, A., Boddupalli, H., Combs, R. G., Kretzmer, K., and Tripp, C. S. (2002). IKK-i and TBK-1 are enzymatically distinct from the homologous enzyme IKK-2: comparative analysis of recombinant human IKK-i, TBK-1, and IKK-2. *J Biol Chem* **277,** 13840-13847.

104. Servant, M. J., ten Oever, B., LePage, C., Conti, L., Gessani, S., Julkunen, I., Lin, R., and Hiscott, J. (2001). Identification of distinct signaling pathways leading to the phosphorylation of interferon regulatory factor 3. *J Biol Chem* **276,** 355-363.

105. Mamane, Y., Heylbroeck, C., Genin, P., Algarte, M., Servant, M. J., LePage, C., DeLuca, C., Kwon, H., Lin, R., and Hiscott, J. (1999). Interferon regulatory factors: the next generation. *Gene* **237,** 1-14.

106. Servant, M. J., Grandvaux, N., and Hiscott, J. (2002). Multiple signaling pathways leading to the activation of interferon regulatory factor 3. *Biochem Pharmacol* **64,** 985-992.

107. TenOever, B. R., Servant, M. J., Grandvaux, N., Lin, R., and Hiscott, J. (2002). Transcriptional profiling of interferon regulatory factor 3 target genes: direct involvement in the regulation of interferon-stimulated genes. *J Virol* **76,** 3659-3669.

108. Schieven, G. L., Kirihara, J. M., Myers, D. E., Ledbetter, J. A., and Uckun, F. M. (1993). Reactive oxygen intermediates activate NF-kappa B in a tyrosine kinase-dependent mechanism and in combination with vanadate activate the p56lck and p59fyn tyrosine kinases in human lymphocytes. *Blood* **82,** 1212-1220.

109. Schoonbroodt, S. and Piette, J. (2000). Oxidative stress interference with the nuclear factor-kappa B activation pathways. *Biochem Pharmacol* **60,** 1075-1083.

110. Ehrhardt, C., Kardinal, C., Wurzer, W. J., Wolff, T., Eichel-Streiber, C., Pleschka, S., Planz, O., and Ludwig, S. (2004). Rac1 and PAK1 are upstream of IKK-epsilon and TBK-1 in the viral activation of interferon regulatory factor-3. *FEBS Lett* **567,** 230-238.

111. Groothuis, J. R., Gutierre, K. M., and Lauer, B. A. (1988). Respiratory syncytial virus infection in children with bronchopulmonary dysplasia. *Pediatrics* **82,** 199-203.

112. MacNee, W. (2001). Oxidative stress and lung inflammation in airways disease. *Eur J Pharmacol* **429,** 195-207.

113. Rahman, I., Morrison, D., Donaldson, K., and MacNee, W. (1996). Systemic oxidative stress in asthma, COPD, and smokers. *Am J Respir Crit Care Med* **154,** 1055-1060.

114. Akaike, T., Ando, M., Oda, T., Doi, T., Ljiri, S., Araki, S., and Maeda, H. (1990). Dependence on O2- generation by xanthine oxidase of pathogenesis of influenza virus infection in mice. *J Clin Invest* **85,** 739-45.

115. Akaike, T., Noguchi, Y., Ijiri, S., Setoguchi, K., Suga, M., Zheng, Y. M., Dietzschold, B., and Maeda, H. (1996). Pathogenesis of influenza virus-induced pneumonia: involvement of both nitric oxide and oxygen radicals. *Proc Natl Acad Sci USA* **93,** 2448-2453.

116. Suliman, H. B., Ryan, L. K., Bishop, L., and Folz, R. J. (2001). Prevention of influenza-induced lung injury in mice overexpressing extracellular superoxide dismutase. *Am J Physiol Lung Cell Mol Physiol* **280,** L69-L78.

117. Ghezzi, P. and Ungheri, D. (2004). Synergistic combination of N-acetylcysteine and ribavirin to protect from lethal influenza viral infection in a mouse model. *Int J Immunopathol Pharmacol* **17,** 99-102.

118. Kumar, P., Sharma, S., Khanna, M., and Raj, H. G. (2003). Effect of Quercetin on lipid peroxidation and changes in lung morphology in experimental influenza virus infection. *Int J Exp Pathol* **84,** 127-133.

119. Stark, J. M., Khan, A. M., Chiappetta, C. L., Xue, H., Alcorn, J. L., and Colasurdo, G. N. (2005). Immune and functional role of nitric oxide in a mouse model of respiratory syncytial virus infection. *J Infect Dis* **191,** 387-395.

120. Piedra, P., Camussi, G., and Ogra, P. L. (1989). Immune response to experimentally induced infection with respiratory syncytial virus: possible role in the development of pulmonary disease. *J Gen Virol* **70,** 325-333.

121. Colasurdo, G. N., Hemming, V. G., Prince, G. A., Gelfand, A. S., Loader, J. E., and Larsen, G. L. (1998). Human respiratory syncytial virus produces prolonged alterations of neural control in airways of developing ferrets. *Am J Respir Crit Care Med.* **157,** 1506-1511.

122. Haeberle, H. A., Nesti, F., Dieterich, H. J., Gatalica, Z., and Garofalo, R. P. (2002). Perflubron reduces lung inflammation in respiratory syncytial virus infection by inhibiting chemokine expression and nuclear factor-kappa B activation. *Am J Respir Crit Care Med* **165,** 1433-1438.

123. Guerrero-Plata, A., Casola, A., and Garofalo, R. P. (2005). Human metapneumovirus induces a profile of lung cytokines distinct from that of respiratory syncytial virus. *J Virol* **79,** 14992-14997.

124. Kharitonov, S. A. and Barnes, P. J. (2002). Biomarkers of some pulmonary diseases in exhaled breath. *Biomarkers* **7,** 1-32.

125. Jafri, H. S., Chavez-Bueno, S., Mejias, A., Gomez, A. M., Rios, A. M., Nassi, S. S., Yusuf, M., Kapur, P., Hardy, R. D., Hatfield, J., Rogers, B. B., Krisher, K., and Ramilo, O. (2004). Respiratory syncytial virus induces pneumonia, cytokine response, airway obstruction, and chronic inflammatory infiltrates associated with long-term airway hyperresponsiveness in mice. *J Infect Dis* **189,** 1856-1865.

126. Graham, B. S., Perkins, M. D., Wright, P. F., and Karzon, D. T. (1988). Primary respiratory syncytial virus infection in mice. *J Med Virol* **26,** 153-162.

127. Tsuru, S., Fujisawa, H., Taniguchi, M., Zinnaka, Y., and Nomoto, K. (1987). Protective mechanisms against pulmonary infection with influenza virus. I. Relative contribution of polymorphonuclear leukocytes and of alveolar macrophages to protection during the early phase of intranasal infection. *J Gen Virol* **68(Pt 2),** 419-424.

128. Graham, B. S., Johnson, T. R., and Peebles, R. S. (2000). Immune-mediated disease pathogenesis in respiratory syncytial virus infection. *Immunopharmacology* **48,** 237-247.

129. Kanaoka, Y. and Boyce, J. A. (2004). Cysteinyl leukotrienes and their receptors: cellular distribution and function in immune and inflammatory responses. *J Immunol* **173,** 1503-1510.

130. Dimova-Yaneva, D., Russell, D., Main, M., Brooker, R. J., and Helms, P. J. (2004). Eosinophil activation and cysteinyl leukotriene production in infants with respiratory syncytial virus bronchiolitis. *Clin Exp Allergy* **34,** 555-558.

131. Van Schaik, S. M., Tristram, D. A., Nagpal, I. S., Hintz, K. M., Welliver, R. C. 2., and Welliver, R. C. (1999). Increased production of IFN-gamma and cysteinyl leukotrienes in virus-induced wheezing. *J Allergy Clin Immunol* **103,** 630-636.

132. Welliver, R. C., Hintz, K. H., Glori, M., and Welliver, R. C., Sr. (2003). Zileuton reduces respiratory illness and lung inflammation, during respiratory syncytial virus infection, in mice. *J Infect Dis* **187,** 1773-1779.

133. Fullmer, J. J., Khan, A. M., Elidemir, O., Chiappetta, C., Stark, J. M., and Colasurdo, G. N. (2005). Role of cysteinyl leukotrienes in airway inflammation and responsiveness following RSV infection in BALB/c mice. *Pediatr Allergy Immunol* **16,** 593-601.

134. Folkerts, G., Kloek, J., Muijsers, R. B., and Nijkamp, F. P. (2001). Reactive nitrogen and oxygen species in airway inflammation. *Eur J Pharmacol* **429,** 251-262.

135. Wood, L. G., Gibson, P. G., and Garg, M. L. (2003). Biomarkers of lipid peroxidation, airway inflammation and asthma. *Eur Respir J* **21,** 177-186.

136. Mejias, A., Chavez-Bueno, S., and Ramilo, O. (2005). Respiratory syncytial virus pneumonia: mechanisms of inflammation and prolonged airway hyperresponsiveness. *Curr Opin Infect Dis* **18,** 199-204.

137. Tripp, R. A. (2004). Pathogenesis of respiratory syncytial virus infection. *Viral Immunol* **17,** 165-181.

138. Broughton, S. and Greenough, A. (2004). Drugs for the management of respiratory syncytial virus infection. *Curr Opin Investig Drugs* **5,** 862-865.

139. Blanco, J. C., Boukhvalova, M. S., Hemming, P., Ottolini, M. G., and Prince, G. A. (2005). Prospects of antiviral and anti-inflammatory therapy for respiratory syncytial virus infection. *Expert Rev Anti Infect Ther* **3,** 945-955.

140. Ali-Ahmad, D., Bonville, C. A., Rosenberg, H. F., and Domachowske, J. B. (2003). Replication of respiratory syncytial virus is inhibited in target cells generating nitric oxide in situ. *Front Biosci* **8,** a48-a53.

141. Hamelmann, E., Schwarze, J., Takeda, K., Oshiba, A., Larsen, G. L., Irvin, C. G., and Gelfand, E. W. (1997). Noninvasive measurement of airway responsiveness in allergic mice using barometric plethysmography. *Am J Respir Crit Care Med* **156,** 766-775.

142. Stein, R. T., Sherrill, D., Morgan, W. J., Holberg, C. J., Halonen, M., Taussig, L. M., Wright, A. L., and Martinez, F. D. (1999). Respiratory syncytial virus in early life and risk of wheeze and allergy by age 13 years. *Lancet* **354,** 541-545.

143. Collins, R. A., Gualano, R. C., Zosky, G. R., Atkins, C. L., Turner, D. J., Colasurdo, G. N., and Sly, P. D. (2005). Hyperresponsiveness to inhaled but not intravenous methacholine during acute respiratory syncytial virus infection in mice. *Respir Res* **6,** 142.

144. Garofalo, R. P., Welliver, R. C., and Ogra, P. L. (1991). Concentrations of LTB4, LTC4, LTD4 and LTE4 in bronchiolitis due to respiratory syncytial virus. *Pediatr Allergy Immunol* **2,** 30-37.

145. Bisgaard, H. (2004). Montelukast in RSV-bronchiolitis. *Am J Respir Crit Care Med* **169,** 542-543.

146. Beck, M. A., Handy, J., and Levander, O. A. (2000). The role of oxidative stress in viral infections. *Ann NY Acad Sci* **917,** 906-912.

147. Beck, M. A. (2001). Antioxidants and viral infections: host immune response and viral pathogenicity. *J Am Coll Nutr* **20,** 384S-388S.

148. Brugh, M., Jr. (1977). Butylated hydroxytoluene protects chickens exposed to Newcastle disease virus. *Science* **197,** 1291-1292.

149. Collins, P. L., McIntosh, K., and Chanock, R. M. (1996) Respiratory Syncytial Virus. In Fields, B. N., Knipe, D. M., and Howley, P. M., editors. *Fields Virology*, Lippincott-Raven, Philadelphia.

150. Maggon, K. and Barik, S. (2004). New drugs and treatment for respiratory syncytial virus. *Rev Med Virol* **14,** 149-168.

151. Castro, S. M., Guerrero-Plata, A., Suarez-Real, G., Adegboyega, P. A., Colasurdo, G. N., Khan, A. M., Garofalo, R. P., and Casola, A. (2006). Antioxidant treatment ameliorates respiratory syncytial virus-induced disease and lung inflammation. *Am J Respir Crit Care Med* **174,** 1361-1369.

152. Kisch, A. L. and Johnson, K. M. (1963). A plaque assay for respiratory syncytial virus. *Proc Soc Exp Biol Med* **112,** 583-589.

153. Stack, A. M., Malley, R., Saladino, R. A., Montana, J. B., MacDonald, K. L., and Molrine, D. C. (2000). Primary respiratory syncytial virus infection: pathology, immune response, and evaluation of vaccine challenge strains in a new mouse model. *Vaccine* **18,** 1412-1418.

154. Prince, G. A., Mathews, A., Curtis S.J., and Porter D.D. (2000). Treatment of Respiratory Syncytial Virus Bronchiolitis and Pneumonia in a Cotton Rat Model with Systemically Administered Monoclonal Antibody (Palivizumab) and Glucocorticosteroid. *J Infect Dis* **182,** 1326-1330.

155. Ottolini, M. G., Curtis, S. J., Porter, D. D., Mathews, A., Richardson, J. Y., Hemming, V. G., and Prince, G. A. (2002). Comparison of corticosteroids for treatment of respiratory syncytial virus bronchiolitis and pneumonia in cotton rats. *Antimicrob Agents Chemother* **46,** 2299-2302.

156. Mejias, A., Chavez-Bueno, S., Rios, A. M., Saavedra-Lozano, J., Fonseca, A. M., Hatfield, J., Kapur, P., Gomez, A. M., Jafri, H. S., and Ramilo, O. (2004). Anti-respiratory syncytial virus (RSV) neutralizing antibody decreases lung inflammation, airway obstruction, and airway hyperresponsiveness in a murine RSV model. *Antimicrob Agents Chemother* **48,** 1811-1822.

157. Mejias, A., Chavez-Bueno, S., Rios, A. M., Aten, M. F., Raynor, B., Peromingo, E., Soni, P., Olsen, K. D., Kiener, P. A., Gomez, A. M., Jafri, H. S., and Ramilo, O. (2005). Comparative effects of two neutralizing anti-respiratory syncytial virus (RSV) monoclonal antibodies in the RSV murine model: time versus potency. *Antimicrob Agents Chemother* **49,** 4700-4707.

158. Pedraz, C., Carbonell-Estrany, X., Figueras-Aloy, J., and Quero, J. (2003). Effect of palivizumab prophylaxis in decreasing respiratory syncytial virus hospitalizations in premature infants. *Pediatr Infect Dis J* **22,** 823-827.

159. Liaudet, L., Pacher, P., Mabley, J. G., Virag, L., Soriano, F. G., Hasko, G., and Szabo, C. (2002). Activation of poly(ADP-Ribose) polymerase-1 is a central mechanism of lipopolysaccharide-induced acute lung inflammation.*Am J Respir Crit Care Med* **165,** 372-377.

160. Virag, L., Bai, P., Bak, I., Pacher, P., Mabley, J. G., Liaudet, L., Bakondi, E., Gergely, P., Kollai, M., and Szabo, C. (2004). Effects of poly(ADP-ribose) polymerase inhibition on inflammatory cell migration in a murine model of asthma.*Med Sci Monit* **10,** BR77-BR83.

161. Haeberle, H., Takizawa, R., Casola, A., Brasier A.R., Dieterich, H.-J., van Rooijen, N., Gatalica, Z., and Garofalo, R. P. (2002). Respiratory syncytial virus-induced activation of nuclear factor-kappaB in the lung involves alveolar macrophages and toll-like receptor 4-dependent pathways. *J Infect Dis* **186,** 1199-1206.

162. Peddi, S. R., Chattopadhyay, R., Naidu, C. V., and Izumi, T. (2006). The human apurinic/apyrimidinic endonuclease-1 suppresses activation of poly(adp-ribose) polymerase-1 induced by DNA single strand breaks. *Toxicology* **224,** 44-55.

163. Mustapha, O., Datta, R., Oumouna-Benachour, K., Suzuki, Y., Hans, C., Matthews, K., Fallon, K., and Boulares, H. (2006). Poly(ADP-ribose) polymerase-1 inhibition prevents eosinophil recruitment by modulating Th2 cytokines in a murine model of allergic airway inflammation: a potential specific effect on IL-5. *J Immunol* **177,** 6489-6496.

164. Gero, D. and Szabo, C. (2008). Poly(ADP-ribose) polymerase: a new therapeutic target? *Curr Opin Anaesthesiol* **21,** 111-121.

165. Boulares, A. H., Zoltoski, A. J., Sherif, Z. A., Jolly, P., Massaro, D., and Smulson, M. E. (2003). Gene knockout or pharmacological inhibition of poly(ADP-ribose) polymerase-1 prevents lung inflammation in a murine model of asthma. *Am J Respir Cell Mol Biol* **28,** 322-329.

166. Petrilli, V., Herceg, Z., Hassa, P. O., Patel, N. S., Di Paola, R., Cortes, U., Dugo, L., Filipe, H. M., Thiemermann, C., Hottiger, M. O., Cuzzocrea, S., and Wang, Z. Q. (2004). Noncleavable poly(ADP-ribose) polymerase-1 regulates the inflammation response in mice. *J Clin Invest* **114,** 1072-1081.

167. Szabo, A., Salzman, A. L., and Szabo, C. (1998). Poly (ADP-ribose) synthetase activation mediates pulmonary microvascular and intestinal mucosal dysfunction in endotoxin shock. *Life Sci* **63,** 2133-2139.

168. Falsey, A. R., Hennessey, P. A., Formica, M. A., Cox, C., and Walsh, E. E. (2005). Respiratory syncytial virus infection in elderly and high-risk adults. *N Engl J Med* **352,** 1749-1759.

169. Couch, R. B., Englund, J. A., and Whimbey, E. (1997). Respiratory viral infections in immunocompetent and immunocompromised persons. *Am J Med* **102,** 2-9.

170. Denny, F. W. and Clyde, W. A., Jr. (1986). Acute lower respiratory tract infections in nonhospitalized children. *J Pediatr* **108,** 635-646.

171. Hall, C. B., Hall, W. J., Gala, C. L., MaGill, F. B., and Leddy, J. P. (1984). Long-term prospective study in children after respiratory syncytial virus infection.*J Pediatr* **105,** 358-364.

172. Bauman, L. J., Wright, E., Leickly, F. E., Crain, E., Kruszon-Moran, D., Wade, S. L., and Visness, C. M. (2002). Relationship of adherence to pediatric asthma morbidity among inner-city children. *Pediatrics* **110,** e6.

173. Chilmonczyk, B. A., Salmun, L. M., Megathlin, K. N., Neveux, L. M., Palomaki, G. E., Knight, G. J., Pulkkinen, A. J., and Haddow, J. E. (1993). Association between exposure to environmental tobacco smoke and exacerbations of asthma in children. *N Engl J Med* **328,** 1665-1669.

174. Dietrich, M., Block, G., Benowitz, N. L., Morrow, J. D., Hudes, M., Jacob, P., III, Norkus, E. P., and Packer, L. (2003). Vitamin C supplementation decreases oxidative stress biomarker f2-isoprostanes in plasma of nonsmokers exposed to environmental tobacco smoke. *Nutr Cancer* **45,** 176-184.

175. Zlotnik, A. and Yoshie, O. (2000). Chemokines: a new classification system and their role in immunity. *Immunity* **12,** 121-127.

176. D'hulst, A. I., Vermaelen, K. Y., Brusselle, G. G., Joos, G. F., and Pauwels, R. A. (2005). Time course of cigarette smoke-induced pulmonary inflammation in mice. *Eur Respir J* **26,** 204-213.

177. Shen, Y., Rattan, V., Sultana, C., and Kalra, V. K. (1996). Cigarette smoke condensate-induced adhesion molecule expression and transendothelial migration of monocytes. *Am J Physiol* **270,** H1624-H1633.

178. Anto, R. J., Mukhopadhyay, A., Shishodia, S., Gairola, C. G., and Aggarwal, B. B. (2002). Cigarette smoke condensate activates nuclear transcription factor-kappaB through phosphorylation and degradation of IkappaB(alpha): correlation with induction of cyclooxygenase-2.*Carcinogenesis* **23,** 1511-1518.

179. Carpenter, L. R., Moy, J. N., and Roebuck, K. A. (2002). Respiratory syncytial virus and TNF alpha induction of chemokine gene expression involves differential activation of Rel A and NF-kappa B1. *BMC Infect Dis* **2,** 5.

180. Indukuri, H., Castro, S. M., Liao, S. M., Feeney, L. A., Dorsch, M., Coyle, A. J., Garofalo, R. P., Brasier, A. R., and Casola, A. (2006). Ikkepsilon regulates viral-induced interferon regulatory factor-3 activation via a redox-sensitive pathway. *Virology* **353,** 155-65.

181. Barnes, P. J. (1997). Nuclear factor-kappa B.*Int J Biochem Cell Biol* **29,** 867-870.

182. Phaybouth, V., Wang, S. Z., Hutt, J. A., McDonald, J. D., Harrod, K. S., and Barrett, E. G. (2006). Cigarette smoke suppresses Th1 cytokine production and increases RSV expression in a neonatal model.*Am J Physiol Lung Cell Mol Physiol* **290,** L222-L231.

183. Jamaluddin, M., Garofalo, R. P., Ogra, P. L., and Brasier, A. R. (1996). Transcriptional activation of the interleukin-8 gene by respiratory syncytial virus infection in alveolar epithelial cells: nuclear translocation of the RelA transcription factor as a mechanism producing airway mucosal inflammation. *J Virol* **70,** 1554-1563.

184. Noah, T. L., Henderson, F. W., Wortman, I. A., Devlin, R. B., Handy, J., Koren, H. S., and Becker, S. (1995). Nasal cytokine production in viral acute upper respiratory infection of childhood.*J Infect Dis* **171,** 584-592.

185. Hoffmann, D. and Wynder, E. L. (1986). Chemical constituents and bioactivity of tobacco smoke. *IARC SciPubl* 145-165.

186. Yamaoka, Y., Kudo, T., Lu, H., Casola, A., Brasier, A. R., and Graham, D. Y. (2004). Role of interferon-stimulated responsive element-like element in interleukin-8 promoter in Helicobacter pylori infection. *Gastroenterology* **126,** 1030-1043.

187. Wagoner, J., Austin, M., Green, J., Imaizumi, T., Casola, A., Brasier, A., Khabar, K. S., Wakita, T., Gale, M., Jr., and Polyak, S. J. (2007). Regulation of CXCL-8 (interleukin-8) induction by double-stranded RNA signaling pathways during hepatitis C virus infection. *J Virol* **81,** 309-318.

188. Kaushik, G., Kaushik, T., Khanduja, S., Pathak, C. M., and Khanduja, K. L. (2008). Cigarette smoke condensate promotes cell proliferation through disturbance in cellular redox homeostasis of transformed lung epithelial type-II cells. *Cancer Lett* epub ahead of print.

189. Vlahopoulos, S., Boldogh, I., Casola, A., and Brasier, A. R. (1999). Nuclear factor-kappaB-dependent induction of interleukin-8 gene expression by tumor necrosis factor alpha: evidence for an antioxidant sensitive activating pathway distinct from nuclear translocation. *Blood* **94,** 1878-1889.

190. Hull, J., Ackerman, H., Isles, K., Usen, S., Pinder, M., Thomson, A., and Kwiatkowski, D. (2001). Unusual haplotypic structure of IL8, a susceptibility locus for a common respiratory virus. *Am J Hum Genet* **69,** 413-419.

191. Puthothu, B., Krueger, M., Heinze, J., Forster, J., and Heinzmann, A. (2006). Impact of IL8 and IL8-receptor alpha polymorphisms on the genetics of bronchial asthma and severe RSV infections.*Clin Mol Allergy* **4,** 2.

192. Kaushik, G., Kaushik, T., Khanduja, S., Pathak, C. M., and Khanduja, K. L. (2008). *Cancer Lett* epub ahead of print.

193. Hosakote, Y, Tianshuang, L, Castro S. M., Garofalo R. P, and Casola A. (2008). Respiratory syncytial virus induces oxidative stress by modulating antioxidant enzymes.*Am J Respir Crit Care Med* (In Review).

VITA

Shawn Monique Castro was born on April 16, 1974 at St. Mary's Hospital in Galveston, Texas. Shawn attended St. Mary's University in San Antonio, Texas and received her Bachelor's of Science degree in Biology and Chemistry, in 1992. While an undergraduate she spent three summers gaining experience in biomedical research and presented her findings at numerous regional and national symposiums. Shawn matriculated to the University of California at Davis (UCD), and was a recipient of several fellowships from Center for Environmental Health Sciences and Department of Environmental Toxicology at UCD, the Howard Hughes Medical Institute and the National Institutes of Environmental Health Sciences (NIEHS) toxicology training grant. She graduated from UCD with a Masters in Science in Pharmacology and Toxicology and soon after in 2002 Shawn enrolled continued at the University of Texas Medical Branch to obtain her doctorate in Pharmacology and Toxicology.

While at UTMB, Shawn received several honors. Upon admittance she was funded on the NIEHS toxicology training grant at UTMB and in 2004, she was awarded the NIH Individual Predoctoral Ruth L. Kirschstein National Research Service Award. Shawn gained significant teaching experience while at the UTMB. She participated as a mentor in the Summer Undergraduate Research Program in 2003 and gave a lecture in environmental toxicology at Texas A&M University, in Galveston Texas. Community outreach served as a major impetus for Shawn throughout her graduate career and as such she judged regional high school science projects and served on several committees in support of higher education, particularly for minority students. As a member of the Society of Toxicology she has served as a peer mentor for undergraduates investigating careers in toxicology, and participated in "Paracelsus goes to school", an initiative to incorporate toxicological concepts and principles in K-12 education.

Shawn Monique Castro can be contacted through the Department of Pediatrics at Route 0366, Galveston, Texas 77555.

Education

B.S. in Biology and Chemistry, May 1992, St. Mary's University, San Antonio, TX
M.S. in Pharmacology and Toxicology, June 2001, University of California, Davis CA

Publications

Liu, T., **Castro, S.**, Brasier, A. R., Jamaluddin, M., Garofalo, R. P., and Casola, A. (2004). Reactive oxygen species mediate virus-induced STAT activation: role of tyrosine phosphatases. *J Biol Chem* **279,** 2461-2469.

Indukuri, H., **Castro, S. M.**, Liao, S. M., Feeney, L. A., Dorsch, M., Coyle, A. J., Garofalo, R. P., Brasier, A. R., and Casola, A. (2006). Ikkepsilon regulates viral-induced interferon regulatory factor-3 activation via a redox-sensitive pathway. *Virology* **353,** 155-165.

Castro, S. M., Guerrero-Plata, A., Suarez-Real, G., Adegboyega, P. A., Colasurdo, G. N., Khan, A. M., Garofalo, R. P., and Casola, A. (2006). Antioxidant treatment ameliorates respiratory syncytial virus-induced disease and lung inflammation. *Am J Respir Crit Care Med* **174,** 1361-1369.

Castro S. M., Kolli, D., Guerrero-Plata, A. Garofalo, R. P., Casola, A. (2008). Cigarette smoke condensate enhances respiratory syncytial virus-induced chemokine release by modulating NF-Kappa B and interferon regulatory activation. *Toxicol Sci* epub ahead of print.

Castro, S. M., Guerrero-Plata, A., Casola, A., Garofalo, R. P. (2008). Antiviral and Antioxidant Combination Therapy in RSV Induced Lung Injury. *J Infect Dis* (In Submission).

Castro, S. M., Tadahide, I., Casola, A., and Garofalo, **R.P.** (2008). A Role for Poly-(ADP-Ribose)-Polymerase (PARP) in Mediating RSV Induced Pulmonary Inflammation. *J Virol* (In Submission).

Hosakote YM, **Castro SM**, Zheng W, Haag A, Spratt H, Kurosky A, Garofalo RP and Casola A. Respiratory syncytial virus (RSV) induces cellular oxidative stress by down regulating the expression of antioxidant enzymes. *Am J of Respir Cell Mol Biol* (In Review).